MODELLING THE EFFECTS OF FOREST DISTURBANCES ON SNOW ACCUMULATION AND ABLATION IN THE OKANAGAN

REED DAVIS

B.Sc. Geography, University of Lethbridge, 2009

A Thesis
Submitted to the School of Graduate Studies
of the University of Lethbridge
in Partial Fulfillment of the
Requirements for the Degree

MASTER OF SCIENCE

Department of Geography
University of Lethbridge
LETHBRIDGE, ALBERTA, CANADA

For my father Gordon, my mother Diane, and my brother Lane

Abstract

Forest disturbances significantly affect snowmelt dominated watersheds. Given that snowmelt from mountain regions provides up to 80% of the annual streamflow in the North American west, disturbances in these watersheds will impact water availability for downstream users. This study used field data from stand-scale studies to represent forest disturbances in a hydrological model in order to quantify the potential snow hydrology response to varying spatial extent of disturbance. The sensitivity of snow accumulation and ablation response increased with disturbance severity and extent of disturbance. Results may provide water resource management with a greater understanding of the potential impact on post-disturbance snowmelt runoff.

Table of Contents

List of Tables

List of Figures

Chapter 1

Introduction

1.1 Introduction

Snow is an important component of both regional climate and hydrometeorology on most continents. The accumulation and extent of snow are major contributors to global climate while snowmelt is the dominant hydrologic event of the annual hydrograph for many watersheds worldwide (Elder et al., 1998). Snowmelt replenishes reservoirs for water storage, hydropower generation, irrigation and recreation, recharges soil moisture that is depleted throughout the previous summer and fall, and is used for urban consumption (Steppuhn, 1981; Black, 1996). It is estimated that approximately one billion people worldwide depend on melting snow and ice for their basic needs (Barnett et al., 2005; Stern, 2007), thus understanding the factors that influence the timing and volume of snowmelt runoff is a key objective in hydrology.

Snow processes, such as the timing and magnitude of snowmelt, are strongly affected by climate change. Studies in western North America show that a warmer climate has resulted in reduced winter snow accumulation and earlier spring snowmelt peaks, which has led to higher streamflow during the winter (December, January and February), an earlier flood season and lower flow during the summer months (June, July and August) (Cayan, 2001; Groisman and Davies, 2001; Leung, 2005; Stewart et al., 2005).

Forest cover is also an important factor determining the timing and volume of snowmelt runoff available not only for downstream human use, but for ecosystem services such as timing of aquatic species life stages, dispersal mechanisms, migration routes, and nutrition provision (Poff and Ward, 1989; Postel and Carpenter, 1997; Winkler, 2001; Chang, 2003; Murray and Buttle, 2003; Rutter et al., 2009; Birkinshaw et al., 2010). Snowmelt from forested mountainous regions provides up to 80% of the annual streamflow in the North American west (Cayan, 2001), while forests in general

provide nearly 65% of the clean water supply in the United States (Jones et al., 2009). On a global scale, forested headwaters that are hydrologically dominated by snowmelt produce 60% of the total runoff (Chang, 2003).

Given the importance of forests in streamflow, understanding the interaction between forests and hydrological processes is essential to the study of hydrology. The forest canopy intercepts snow that would otherwise reach the ground surface (Schmidt, 1991; Veatch et al., 2009). Forest canopy creates a platform for snow interception which increases the surface-area-to-mass ratio of intercepted snow, exposing more snow to wind (Schmidt, 1991) and increasing the amount of snow lost to the atmosphere by sublimation (López-Moreno et al., 2008). Sublimation of intercepted snow may be one of the most important processes contributing to snow water equivalent (SWE) loss in mid-latitude, continental climates because most seasonally snow-covered areas are forested (Schmidt, 1972). A forest canopy also reduces net radiation received at the snow surface, and acts to absorb and re-radiate both short-wave and long-wave radiation (Pomeroy and Granger, 1997; Link and Marks, 1999; Ellis et al., 2010). The canopy also reduces the turbulent energy transfers at the snow surface by increasing surface roughness (Gelfan et al., 2004). Areas without forest cover accumulate more snow and have greater net radiation and turbulent transfers at the snow surface relative to forested regions (Schmidt and Troendle, 1989; Winkler et al., 2009), resulting in increased volume of melt runoff and more rapid liberation of water from non-forested watersheds (Stednick and Troendle, 2004; Winkler et al., 2009).

Given the importance of forest cover to snow processes, both natural and anthropogenic forest disturbances significantly affect snow accumulation and melt. The forest disturbances can result from logging, wildfire, drought, insect infestation, and disease. Natural forest disturbance has increased with climate change, as a result of drier, warmer conditions that increase drought stress and make trees more susceptible to disease, insect infestation, and wildfire (Westerling et al., 2006; Littell et al.,

2009). Disturbances often result in forest canopy loss, altering the balance between incoming short-wave and outgoing long-wave radiation as the forest canopy opens (Link and Marks, 1999; Dale et al., 2001; Boon, 2009). Reductions in forest canopy increase ground snow accumulation by decreasing snow interception. A lower forest density can also enhance the snow ablation energy balance, increasing the timing and magnitude of melt production, affecting water yield, and increasing the potential for flooding (Gelfan et al., 2004; Winkler et al., 2004; Boon, 2009). The response of snow processes to clearcutting is well known as water managers have clearcut forests for decades to increase the amount of water produced from headwater watersheds (Hibbert, 1967; Bethlalmy, 1974; Ziemer et al., 1991; Wigmosta and Burges, 2001). However, the effects of disturbances such as mountain pine beetle (*Dendroctonus ponderosae* Hopkins, Coleoptera: Curculionidae, Scolytinae; MPB) infestation and wildfire have only recently been studied, thus our current understanding of these processes is limited (Winkler et al., 2009; Bewley et al., 2010; Pugh and Small, 2011; Schnorbus, 2011). Recent research suggests that MPB reduces the forest canopy sufficiently to enhance snow accumulation and increase melt, but the nature of incident snowfalls is a major driver of canopy interception even with a dead canopy (Boon, 2007, 2011). In terms of wildfire, reduction of the forest canopy by 75% of original leaf area index (LAI) can result in greater energy fluxes and up to 30% more energy available for snowmelt (Burles and Boon, 2011).

Freshwater supplies around the world have declined rapidly in the second half of the twentieth century and are expected to decline further (Shiklomanov, 2000). In southern Canada, average annual water yield declined at a rate of 3.52 km^3 y^{-1} between 1971 and 2004 (Bemrose et al., 2010). As climate change and associated forest disturbances continue, it is imperative to quantify the vulnerability of water resources to these changes through detailed understanding of physical processes that affect water resources (Dale et al., 2001). Our capacity to adapt to predicted changes

in our water supply is limited without a clear understanding of the effects of natural and anthropogenic disturbances on these water supplies (IPCC, 2007; Parry et al., 2008).

Assessing the response of snow-dominated hydrology to forest change requires an understanding of hydrological and ecological processes within a catchment and the interactions between them. Field studies are often conducted to quantify the dynamics of interrelated and often complex processes that govern water movement into, through and out of a watershed. These are conducted at a range of scales, including the sample-scale (e.g., sublimation of snow on a conifer branch), plot-scale (e.g., runoff generation from a hillslope), and watershed scale (e.g., snowmelt runoff generation following forest harvest) (Pomeroy et al., 1998a, 2012; Clark et al., 2009).

However, drawing conclusions regarding the effects of forest change on basin-scale hydrology from field data alone is challenging. First and foremost are issues of scale, as field data at the plot scale may not easily scale up to the watershed, while watershed scale data fail to tell us what processes are operating at smaller scales to drive total runoff. The second issue is one of transferability, in that field data may not be appropriate for field studies beyond the watershed in which they were collected due to specific hydrologic processes unique to that watershed. Finally, there are some hydrologic processes that may not be measured because of a meteorological station installation with few measurement instruments (Sidle, 2006).

To address these difficulties, paired watershed experiments are often used. This experimental approach is designed to assess pre- and post-disturbance hydrology at the watershed scale using high quality field-based observations of changing runoff patterns (Reid, 1993). However, this study design is limited by the lack of experimental replication across a full range of natural conditions (DeFries and Eshleman, 2004), and uncertainty regarding which internal processes are driving changes in observed outflow (e.g., peak flows and low flows) (Reid, 1993; DeFries and Eshleman, 2004).

Additionally, our ability to recreate natural disturbance effects on watershed hydrology in a field setting is limited given its difficulty, time requirement, and cost. As an alternative, hydrologic modelling allows hydrologists to test and understand interactions between hydrological processes and the factors that control them over time and space in a simulated environment (Dunne, 2001). The integration of field data from stand-scale studies with hydrological modelling is a highly effective process-based approach for quantifying and predicting snow hydrology response to forest disturbances (Ziemer et al., 1991; Beckers et al., 2009).

Models have previously been applied to quantify the impact of MPB and wildfire on snowmelt runoff response (van de Vosse, 2008; Bewley et al., 2010; Seibert et al., 2010). Generally, these studies agree that disturbance affects the timing and magnitude of snow accumulation and melt. However, these modelling studies either use simplified representations of forest cover (Carver et al., 2009), a significant driver of snow accumulation and melt, or analyze the effect of post-disturbance forest management via salvage logging, rather than focusing solely on the disturbance itself (Alila and Luo, 2007). Thus, the use of models to simulate snow accumulation and melt response to forest disturbance remains limited despite its importance of this information for sound forest and water management (Seidl et al., 2010).

1.2 Objectives

The goal of this thesis research is to quantify the effects of natural disturbance on snowmelt generated water supplies in a forested upland catchment. This research has two main objectives:

1. Initialize and validate a numerical watershed model for a highly instrumented, forested, and snowmelt-dominated catchment.

2. Quantify the sensitivity of snow accumulation and ablation at the catchment

scale to varying spatial extents of moderately severe wildfire and mountain pine beetle infestation.

This thesis has eight chapters, the first of which is this introduction chapter. Chapter 2 (Background), describes the biophysical and hydrological effects of forest disturbance on forest canopy and snow hydrology; outlines the basics of hydrologic modelling and simulation of watershed hydrology over varying temporal and spatial scales, and describes how to select a hydrologic model. Chapter 3 (Study Area), describes the research watershed selected for this project, including the biophysical and hydrological characteristics of this location, and the datasets used to parameterize and validate model runs. Chapter 4 (Methods), describes the methodology for sensitivity analyses and outlines the techniques used to initialize and validate the model, apply the forest disturbance scenarios, and quantifying hydrologic response to disturbance. Chapter 5 (Sensitivity Analyses and Model Performance), presents and discusses the results of the sensitivity analyses and model performance tests to assess potential model uncertainties. Chapter 6 (Snowcover Response to Forest Disturbance), quantifies differences in modelled snow accumulation and ablation after simulated forest disturbances. Chapter 7 (Discussion), explains response differences and identifies the driving processes, links to other research, and defines possible sources of error. Chapter 8 (Summary and Conclusions), summarizes the main research findings, and makes recommendations for future research.

Chapter 2

Background

2.1 Snow Accumulation and Melt in Forests

In forested, snow melt-dominated environments, snow hydrology is governed largely by the forest canopy given its effects on interception, sublimation, and snow melt runoff (Varhola et al., 2010) (Fig. 2.1).

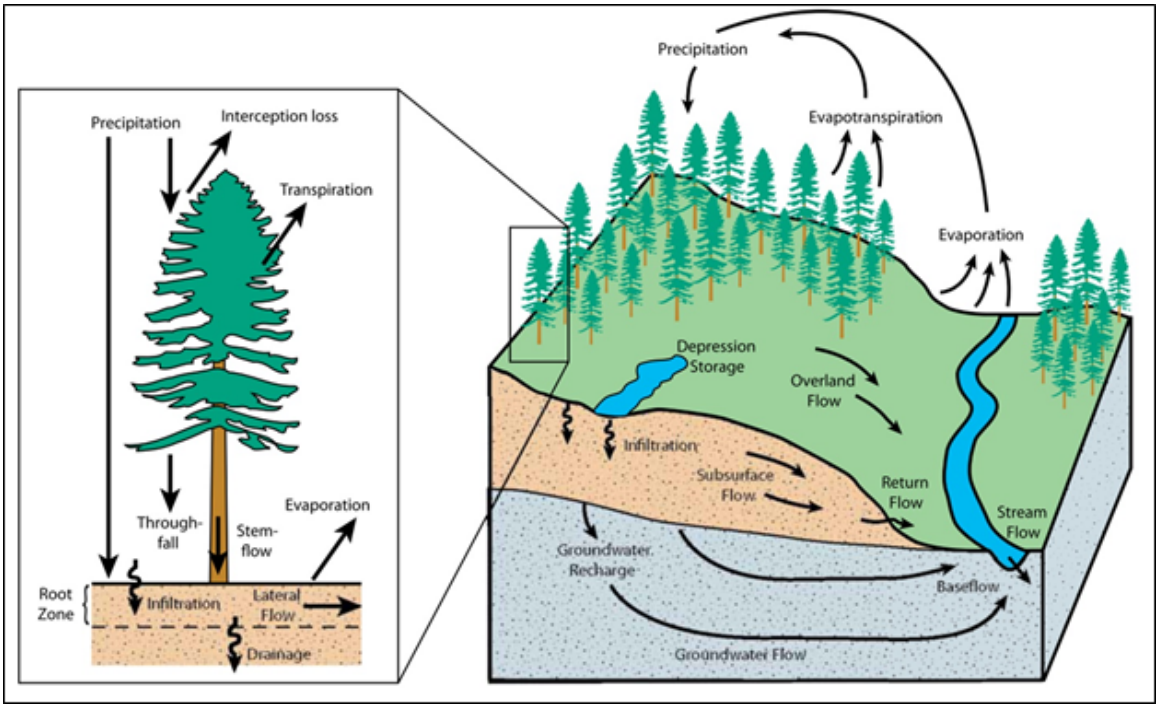

Figure 2.1: Conceptual representation of the hydrologic cycle for an individual tree and for a forest stand (from Smerdon and Redding, 2007).

2.1.1 Snow Accumulation

Coniferous canopies, which typically dominate mountain headwater basins, can intercept and store up to 60% of incoming snowfall (Fig. 2.2) (Pomeroy et al., 1998b). Thus sub-canopy accumulation is generally inversely proportional to canopy density. However, studies show that snowfall interception differences between stands also vary with the size and frequency of snowfall (Satterlund and Haupt, 1967; Satterlund,

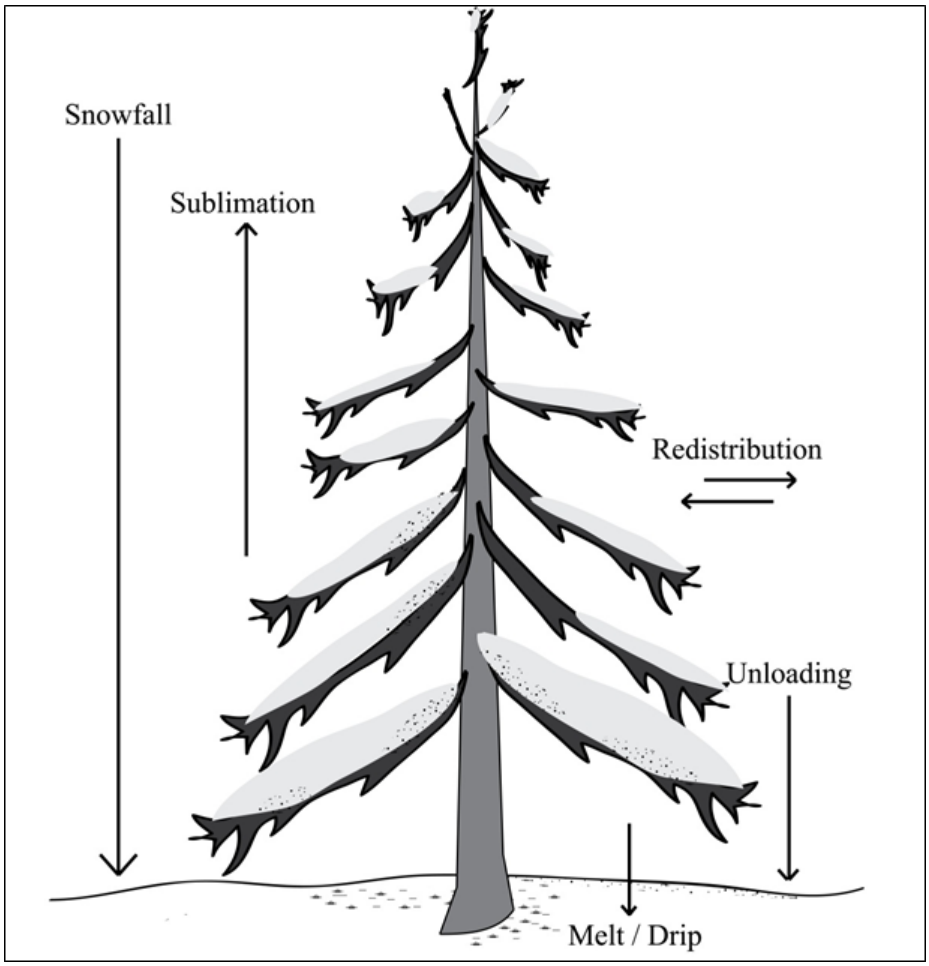

Figure 2.2: Conceptual representation of the process of snowfall interception in a coniferous forest canopy (reproduced from Pomeroy and Gray, 1995).

1970). Snow interception is a function of the leaf area index (LAI) and branch elasticity, which varies with air temperature, tree species and stand health (Schmidt and Pomeroy, 1990; Schmidt, 1991; Hedstrom and Pomeroy, 1998; Boon, 2011). During large snowfall events, snow accumulation in the canopy can quickly increase beyond the interception capacity, and snow is unloaded from the canopy. Small snowfall events, however, can accumulate snow within the canopy over longer timeframes, as more time is required to reach the interception capacity. Thus snowfall size and frequency may play a greater role in mediating snow transfer to the ground surface than total canopy interception capacity (Satterlund, 1970; Schmidt and Pomeroy, 1990; Schmidt, 1991; Varhola et al., 2010).

Loss of snow from the canopy occurs via unloading (as outlined above), melt, and sublimation. Schmidt (1991) suggested that melt of intercepted snow is relatively insignificant in North America, as it is more likely to unload than melt (Gubler and Rychetnik, 1991). Loss of intercepted snow is also governed by wind speed during snowfalls: high wind speeds (> 2 m s^{-1}) reduce interception and minimize differences in snow accumulation between forested and cleared sites (Miller, 1964; Wheeler, 1987; Schmidt and Troendle, 1989).

While snow is in the canopy, the ratio of snow surface area to mass is larger than for ground surface snow, increasing rates of turbulent transfer which can sublimate intercepted snow back to the atmosphere (Bailey et al., 1997). Measurements of boreal forest sublimation suggest that 10–40% of intercepted snow is sublimated (Hedstrom and Pomeroy, 1998), while studies in alpine regions suggest that 15–32% is sublimated (Hood et al., 1999; MacDonald et al., 2010). At wind-exposed alpine ridges devoid of forest cover, removal of snow due to sublimation may be between 10 and 90% (Strasser et al., 2007). High wind speeds at these locations have greater potential to suspend snow particles, exposing them to greater latent heat fluxes (Bailey et al., 1997; Pomeroy and Essery, 1999).

2.1.2 Snow Melt

Snow melt occurs via three phases (Dingman, 2002):

1. *Warming*: average snowpack temperature increases until reaching isothermality at 0 °C.

2. *Ripening*: melting occurs but meltwater is retained within the snowpack. The pack is ripe when it is saturated with liquid water and no more can be retained.

3. *Output*: continued inputs of energy produce water output from the pack.

Snowcover may accumulate and melt more than once during the accumulation and melt period so snowpack may go through the three phases of melt repeatedly (Male and Granger, 1981; Dingman, 2002). The net energy exchanges (S) that determine the progress of snow melt can be described by the following processes (all units in W m^{-2}) (Dingman, 2002):

$$S = K^* + L^* + Q_H + Q_E + Q_P + Q_G \tag{2.1}$$

where, K^* is net shortwave radiation, L^* is net longwave radiation, Q_H is turbulent exchange of sensible heat with the atmosphere, Q_E is turbulent exchange of latent heat with the atmosphere, Q_P is heat input by rain, and Q_G is conductive exchange of sensible heat with the ground. K^* and L^* are composed of incoming and outgoing fluxes:

$$K^* + L^* = L_{in} - K_{out} + L_{in} - K_{out} \tag{2.2}$$

Here, K^* is related to K_{in} through

$$K^* = K_{in} - K_{out} = (1 - \alpha_s) \tag{2.3}$$

where α_s is the snow albedo. Forest-cover has a limiting effect on radiation to snow by reducing incident shortwave radiation from reflection and absorption while increasing incident longwave radiation from vegetation thermal emissions (Link and Marks, 1999; Black et al., 1991; Reifsnyder and Lull, 1965). Shortwave radiation in forests is reduced as follows:

$$\tau = \frac{K_{in}}{K_{out}} \tag{2.4}$$

where τ is the forest shortwave transmittance. Reductions in incident shortwave radiation to the snow surface are often offset by canopy longwave emission, which is enhanced when snow albedo is high, and in high latitudes or altitudes where atmospheric longwave emissions are comparatively low (Sicart et al., 2004; Jeffrey, 1970).

In forested environments, the dominant component (60-90%) of the snowmelt energy balance is radiation, which has both short- (K) and longwave (L) components (Pomeroy and Gray, 1995). The percentage of diffuse and direct incident K and L at the snow surface is determined by cloudiness, day length, solar angle, sky-view factor (the degree to which sky-view is obstructed by terrain) and canopy transmission (McGaughey, 1984; Oke, 1987; Pomeroy and Dion, 1996; Bailey et al., 1997; Dingman, 2002). Diffuse K input ranges from 10% of net shortwave under clear-sky, up to 100% under overcast conditions or under dense canopies (Oke, 1987; Bailey et al., 1997; Lawler and Link, 2011). L is largely influenced by sky-view factor, atmosphere and canopy temperature, and atmosphere and forest emissivities (Essery et al., 2008; Lawler and Link, 2011). Turbulent heat fluxes (Q_H, Q_E) are reduced under forest canopies relative to non-forested surfaces, given that increased land surface roughness reduces wind speeds (Marks and Winstral, 2001; Boon, 2009). Q_P enhances snowmelt by transferring heat to the snowpack and Q_G is the conduction of heat between the snowpack and ground surface (Oke, 1987; Dingman, 2002). Given forest cover effects on radiative and turbulent fluxes, sub-canopy snow melt rates are lower than melt rates in open areas (Storck et al., 1999; Spittlehouse and Winkler, 2004), and are inversely proportional to canopy density given its control on radiation transmission to the snow surface (Molchanov, 1963; McKay and Adams, 1981). Changes to forest canopy structure will thus alter the energy available to melt snow.

2.2 Climate Change and Snow

Given the strong relationship between snow cover and climate, snow hydrology is highly sensitive to climate change. Global Circulation Model (GCM) predictions for North America indicate a range of air temperature and precipitation shifts in both the winter and summer seasons under standard climate change scenarios (Fig. 2.3) (IPCC, 2007).

Predictions for western North America indicate an increase in winter air temperature and an increase in the proportion of precipitation that falls as rain (IPCC, 2007) which has already been observed (Mote, 2006). Warming is expected to be greater at higher altitudes as a result of snow-albedo feedback effects: as snow covered area decreases and the snowpack duration declines, more dark land area is exposed to absorb and re-emit incoming radiation, with subsequent effects on warming the lower atmosphere (Beniston, 2003). Given the changing proportion of rain versus snow, SWE will be reduced and snow melt will peak earlier in the season. This has already led to higher flows during winter months, an earlier flood season and less flow during summer months (Stewart et al., 2005; Mote, 2006; IPCC, 2007).

2.3 Forest Disturbance

Forests are highly susceptible to natural disturbances driven by changing climate (Dale et al., 2001; Walther et al., 2002; Beniston, 2003; Carroll et al., 2006; Soja et al., 2007). The increase in average summer air temperature and decrease in summer precipitation has subjected forests to drought, leaving them increasingly susceptible to insect infestation, disease and wildfire (Mattson and Haack, 1987; Adams et al., 2009; Littell et al., 2009). A changing climate is thus likely to simultaneously affect snow cover and forest cover, with poorly understood impacts.

The two disturbances of particular importance in western North America are

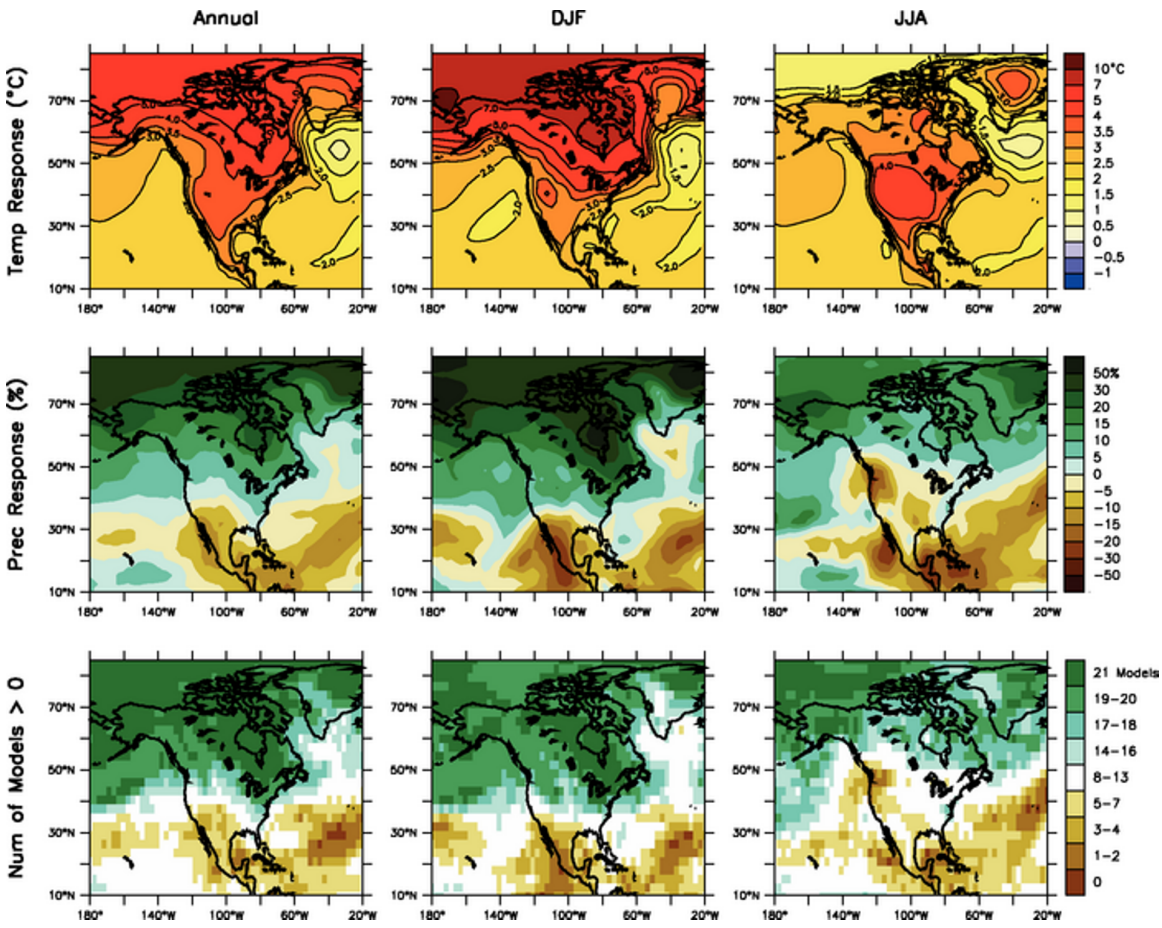

Figure 2.3: Temperature and precipitation changes over North America from GCM simulations. Top row: Annual mean, December January February and June July August temperature change between 1980 to 1999 and 2080 to 2099, averaged over 21 models. Middle row: same as top but for fractional change in precipitation. Bottom row: number of models out of 21 that project increases in precipitation (IPCC, 2007).

mountain pine beetle mountain pine beetle (*Dendroctonus ponderosae*; MPB) and wildfire. MPB has reached epidemic proportions in recent years as air temperatures at higher elevations and in more northerly latitudes have increased, expanding the insect's range into regions where cold winter air temperatures previously restricted establishment (Bentz et al., 1991; Shore and Safranyik, 1992; Carroll et al., 2006). Additionally, changes in snow-dominated hydrology as a result of climate change have increased wildfire severity, intensity and the length of wildfire season (Johnson and Larsen, 1991; Westerling et al., 2006). Studies show that forest canopy change due to disturbance (pine beetles, wildfire, harvesting) can alter both interception and the energy balance, altering ground snow processes (Koivusalo and Kokkonen, 2002; Boon, 2009; Burles and Boon, 2011).

2.3.1 Mountain Pine Beetle

Mountain pine beetle is endemic to forests in the Western Cordillera, but since 1996 has reached epidemic proportions. Infestation of mountain pine beetle occurs when there is an abundance of large, old ($>$ 80 years) lodgepole pine (*Pinus contorta*), which are most susceptible to infestation (Safranyik, 1978; Shore and Safranyik, 1992; Taylor and Barton, 2003; Safranyik and Carroll, 2006). Pine beetles pierce the bark of the tree to feed on the cambium, and then lay eggs in this layer. A blue stain fungus carried on the beetles mouthparts attacks the phloem, starving the tree of nutrients; within approximately two weeks, the tree dies (Ballard et al., 1984). Once the tree dies, the canopy begins to change colour; typically green needles turn bright red, fade to brown and eventually become grey as needles and small branches are lost (Mitchell and Preisler, 1998). The rate of change is dependent on weather in subsequent years: hot, dry weather withdraws any remaining moisture and results in more rapid colour change. Needles can remain in the canopy for 3-5 years after trees are killed, but as they are lost, the canopy opens and dense stands thin (Safranyik and Carroll, 2006).

Depending on the initial forest structure, beetle-killed stands may retain or release live understory vegetation which can in some cases offset the effects of overstory loss (Uunila et al., 2006).

The reduction in canopy density following MPB reduces interception, thus increasing snow reaching the ground. This snow then melts sooner as more radiation reaches the snowpack through the less-dense canopy (Boon, 2007, 2009; Bewley et al., 2010; Boon, 2011; Pugh and Small, 2011). Reduced canopy density also reduces surface roughness, increasing wind speeds and subsequent turbulent heat transfers. This increases the role of sensible and latent heat in snow melt (Koivusalo and Kokkonen, 2002; Boon, 2009). These changes can result in increased peak-flow magnitudes, which increases proportionally with disturbance severity (Schnorbus and Bennett, 2010). Additionally, soil moisture increases in beetle killed stands as a result of reduced canopy evapotranspiration and enhanced retention in accumulated litter can also increase the volume of overland flow (Clow et al., 2011; Penna et al., 2011).

2.3.2 Wildfire

Wildfire activity has increased and intensified due to increasing air temperatures and decreased summer precipitation (Flannigan et al., 2005; Shakesby and Doerr, 2006; Littell et al., 2009; Westerling et al., 2011). Depending on wildfire intensity, forest canopy is either largely or completely removed, with trunks and few branches remaining. The severity of wildfire is ranked by the amount and rate of heat release, which affects post-wildfire forest structure (Seidl et al., 2010).

While the effect of fire on snow-dominated hydrological systems is not well known, recent studies indicate that the loss of forest canopy reduces interception, thus more snow accumulates (Winkler, 2011). It also increases radiation reaching the snowpack and can decrease land surface roughness, consequently increasing wind speeds and sublimation (Burles and Boon, 2011). Longwave radiation incident on the snow surface

declines, but the reduction is balanced by the increase in shortwave radiation (Burles and Boon, 2011; Winkler, 2011). This results in greater peak flows: up to 120% greater after wildfire compared to pre-wildfire conditions (Stonesifer, 2007; Seibert et al., 2010).

2.3.3 Limitations of Previous Studies

Most of the post-disturbance studies outlined above have been conducted at the stand scale, thus the effects of MPB and wildfire at larger watershed scales is not well understood. The few previous watershed-scale MPB studies have focused largely on the cumulative effects of MPB and salvage harvesting, a management approach that involves complete removal of beetle killed stands (Alila and Luo, 2007; Alila et al., 2009; Schnorbus and Bennett, 2010; Schnorbus, 2011). Stonesifer (2007) and Seibert et al. (2010) looked at the watershed-scale effect of wildfire on streamflow; however, these studies either used undocumented parameters or simplistic representations (not physically based) of post-wildfire forest canopy.

Watershed-scale studies that assume complete disturbance of the entire watershed do not incorporate spatiotemporal variability in forest disturbances. The forest landscape is composed of a mosaic of stand types with varying structure due to interspecific competition and past disturbance effects (Halpern and Spies, 1995; Brown et al., 1999; Coulson et al., 1999). Current disturbances affect the forest landscape in varying ways: pine beetle is more likely to attack stands in close proximity, while wildfire effects are a function of fire intensity and topography (Amman and Baker, 1972; Nelson et al., 2003; Westerling et al., 2006; Aukema et al., 2008; de la Giroday, 2010). These varying patterns of disturbance will result in varying snow accumulation and melt responses which, when summed at the watershed scale, will have different effects depending on the disturbance distribution across the watershed.

Studies generally agree that the response of snow accumulation and melt in dis-

turbed forest stands is intermediate to these processes in undisturbed versus and cleared forests. Snow is intercepted less, accumulates more, and melts faster and sooner in beetle-killed and burned stands (Boon, 2007; Stonesifer, 2007; Boon, 2009, 2011; Burles and Boon, 2011; Pugh and Small, 2011; Winkler, 2011). However, given the rapid expansion of MPB-related forest disturbances and the episodic nature of wildfire, the traditional method of studying pre- and post-disturbance effects on hydrology has not been feasible for most studies (Winkler and Boon, 2010). Without sufficient pre-disturbance data, analyzing the impact of the difference between post-disturbance and undisturbed forest, and the transitional phase between them, is challenging.

Numerical modelling provides an alternative approach to conducting pre- and post- disturbance studies, as it allows us to digitally modify undisturbed forest stands based on field data. We can then represent a mosaic of these stands at the watershed scale, to test the sensitivity of snow accumulation and melt processes to post-disturbance forest change (Winkler, 2011). Data from undisturbed stands can be used as a baseline against which disturbance scenarios are compared, allowing for prediction of the hydrological impacts of forest disturbances in regions that have not yet been physically disturbed (Winkler and Boon, 2010; Pomeroy et al., 2011; Schnorbus, 2011). This is one of the first watershed-scale studies of beetle and wildfire disturbance in snowmelt dominated watersheds, and focuses on the snow accumulation and ablation processes that drive runoff given a mosaic of forest disturbance across a watershed.

2.4 Hydrological Modelling

Hydrologic models provide simplified, conceptual representations of the hydrologic cycle, and are used for both hydrologic prediction and to better understand hydrologic processes. Models range in complexity and functionality depending on their

application, and the research question to be answered.

2.4.1 Spatial Representation

Hydrologic models represent a watershed in model space in one of three ways (Fig. 2.4):

1. Lumped models represent watersheds by lumping the average spatial distribution of input/output variables and physical process parameters of the watershed into a single unit (Clarke, 1973). This single unit represents a generalization of the modelled extent, and thus has a low spatial resolution. These models are unable, for example, to account for water movement from steep mountainous terrain to slopes of lower relief (Carpenter and Georgakakos, 2006). The Water Resources Evaluation of Non-point Silvicultural Sources (WRENSS) model is an example of a lumped model. It calculates all hydrological processes for an entire watershed based on one input dataset and assumes the whole watershed responds uniformly (Swanson, 2004).

2. Semi-distributed models use physiographic basin properties such as soil type, vegetation cover and topography to divide a watershed into discrete, homogenous regions with common hydrologic properties (e.g., Hydrologic Response Unit; HRU) (Singh, 1989). It assumes that each HRU responds in a hydrologically similar fashion to external forcings. The Cold Regions Hydrological Model (CRHM) is an example of a semi-distributed model. It defines HRUs across the landscape and calculates the individual hydrologic response for each HRU, which is then aggregated into a basin-wide response.

3. Fully-distributed models explicitly account for the spatial variability of input variables, usually by partitioning the watershed into a network of equally sized grid cells (Kampf and Burges, 2007). The Distributed Hydrology Soil Vegeta-

tion Model (DHSVM) is an example of a fully-distributed hydrological model because it calculates all hydrological processes for each cell in a digital elevation model (DEM) grid that covers the entire watershed, and also calculates the interaction of hydrological processes between grid cells.

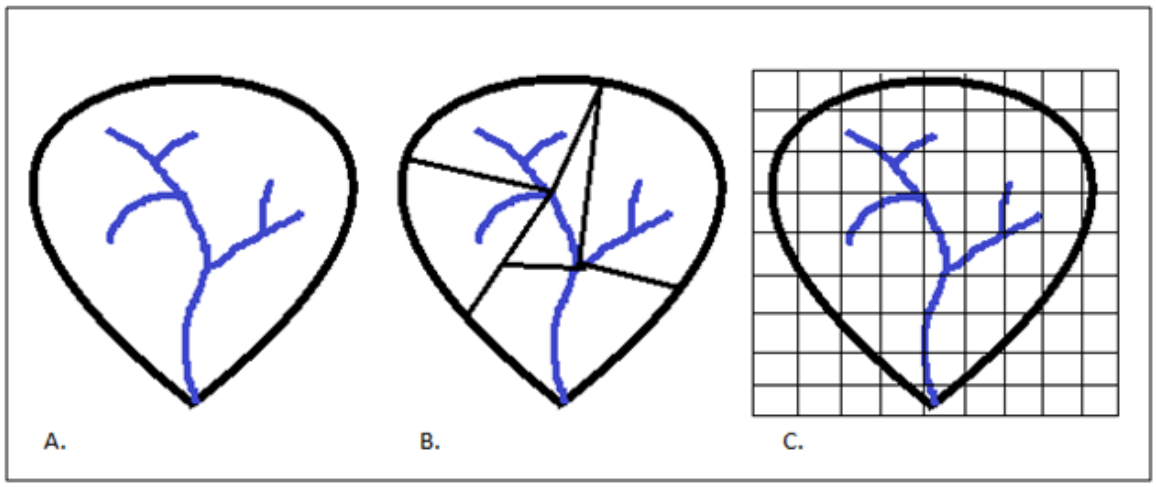

Figure 2.4: Simplified examples of spatial representation in hydrological modelling: (A) lumped model, (B) semi-distributed, and (C) fully-distributed.

Selecting a model with simple or complex spatial representation is usually dependant on data availability. A lumped model is generally selected for watersheds with limited hydrological and topographical data, while a fully-distributed model is applied to watersheds with greater data availability. In the past, basin size and computer processing speed may have driven model selection, but this is much less of an issue today.

2.4.2 Process Representations

Models typically incorporate one of three approaches when defining the numerical equations used to simulate hydrologic processes.

1. Empirical approaches are based on mathematical equations derived from evaluation of experimental observations (Refsgaard and Knudsen, 1996). For example,

the temperature index method of calculating snow melt assumes an empirical relationship between air temperature and melt rate (Hock, 2003):

$$\Delta w = (K + L)/(p_w \times \lambda_f) + M_r \times T_a \tag{2.5}$$

where, Δw is daily snow melt (cm day^{-1}), K is shortwave radiation input, L is longwave radiation exchange, p_w is liquid water content (1000 kg m^3), λ_f is latent heat of fusion (0.334 MJ kg^{-1}), M_r is restricted melt factor (2.0 mm day^{-1} °C), T_a is air temperature (°C).

2. Analytical models are run using a series of known functions that solve simplified mass and energy conservation equations used to describe change in hydrologic systems (Kampf and Burges, 2007). The Regional Hydro Ecological Simulation System (RHESSys), a GIS based watershed model that calculates snow melt from simulated daily shortwave radiation, is an example of analytical modelling (Coughlan and Running, 1997):

$$q_{melt} = \alpha_s(S_f/k) \tag{2.6}$$

where, q_{melt} is snow melt, α_s is snow surface albedo, S_f is amount of simulated daily shortwave radiation reaching forest floor (MJ m^{-2} day^{-1}), and k is latent heat of fusion (3.5 x 10^5 MJ mm^{-1} m^{-2})

3. Physically based models are built upon the conservation equations of mass, momentum and/or energy (Kavvas et al., 2004). For example, the Distributed Hydrology Soil Vegetation Model (DHSVM) uses a physically-based snowpack energy balance model to calculate snow melt from input variables measured

directly in the field (Anderson, 1968; Wigmosta et al., 1994):

$$c_s W \left(\frac{dT_s}{dt} \right) = R_n s + Q_s + Q_t + Q_p + Q_m + Q_g \tag{2.7}$$

where, c_s is standardized reference evapotranspiration rate from a vegetated surface (mm h^{-1}), W is net radiation at the vegetated surface (MJ m^{-2} h^{-1}), T_s is temperature of the snowpack (°C), t is time (h), $R_n s$ is energy exchange at the snow-air surface (MJ m^{-2} h^{-1}), Q_s is sensible heat transfer by turbulent convection (MJ m^{-2} h^{-1}), Q_t is energy lost to evaporation and sublimation or energy gained through release of latent heat during condensation (MJ m^{-2} h^{-1}), Q_p is heat advected to the pack by rainfall (MJ m^{-2} h^{-1}), Q_m is internal latent heat lost by melting, or heat gained by refreezing liquid water (MJ m^{-2} h^{-1}), Q_g is heat transfer by conduction from the snow-ground interface (MJ m^{-2} h^{-1}).

Selecting the appropriate process representation in a hydrologic model depends largely on data type and availability. Empirical models can run simulations with minimal and easy to acquire data, such as simulating snow melt from air temperature. Analytical models allow for simulation of snow melt but first require a GIS to simulate the incoming solar radiation on a particular slope. Physically-based models typically require extensive field datasets at an hourly time step.

Regardless of the model representation (empirical, analytical, or physical), hydrological processes can be calculated either at a point or over an area. In order to simulate hydrological processes over space, however, the results of each calculation must be routed from one model region to another. Individual hydrological processes are thus interconnected between HRUs or grid cells. In CRHM, once a threshold condition is exceeded, snow is moved from one HRU to another, and is subject to processes in this HRU. For example, once wind speed is sufficient to enable suspension and transport, snow may blow from a clearcut and be deposited in a forest. Once

deposited in the forest, the forest canopy acts upon the newly deposited snow whereas in the clearcut HRU there was no snow-vegetation interaction.

2.4.3 Models Used in Forest Hydrology

While there are many hydrologic models in existence, several key models are regularly used by the forest hydrology community. RHESSyS is a semi-distributed, analytically-based GIS-modelling framework that has been used to quantify land use change impacts on runoff generation (Whitaker et al., 2003; Tague and Band, 2004). DHSVM is a fully-distributed, physically-based forest hydrology model developed to simulate the effects of vegetation, soil and topography on the energy and water balance and has been applied to many forest hydrology scenarios in Canada and the United States, including land use change and the hydrologic effects of logging and wildfire (Wigmosta et al., 1994; Storck et al., 1998; Alila and Beckers, 2001; Stonesifer, 2007). Hydrologiska Byrns Vattenbalansavdelning (HBV) is a semi-distributed, empirically-based hydrologic model that has been applied globally. Examples of applications of HBV include modelling the effects of both land use change and future climate scenarios on runoff generation (Bergstrom, 1995; Lindstrom et al., 1997; Liden and Harlin, 2000; Andreasson et al., 2004; Jasper et al., 2004). Topography based hydrological model (TOPMODEL) is commonly used for overland and subsurface flow in the United States and Europe, and has strong groundwater and water table components (Beven and Kirkby, 1979; Lamb et al., 1998; Cameron et al., 1999; Gunter et al., 1999). Finally, the University of British Columbia Watershed Model (UBCWM) is a semi-distributed, empirically-based watershed model that has previously been used to model the effects of MPB on streamflow characteristics (Quick and Pipes, 1977; Alila and Luo, 2007).

When selecting a model to examine the effect of forest disturbances on snow processes, the model must be able to represent the forest canopy, as well as the

processes that govern sub-canopy snow accumulation and ablation. The canopy must be able to be modified by adjusting key model parameters. Additionally, given the complex spatial distributions of soil types, land cover, and meteorological conditions particular to the study site, the model selected must be able to incorporate spatial complexity.

RHESSyS has previously been applied to land use change scenarios, but these studies were of simple forest cover change (e.g. clearcutting) as the model does not have a strong interception module (Tague and Band, 2001). DHSVM is a useful model for simulating the impact of forest cover change on snowmelt hydrology, given that forest disturbance studies have successfully been completed previously, and it allows for complex representations of spatially distributed physical processes. However, DHSVM is highly parameterized, requiring parameter values well beyond the scope of data available at the study site. While it has been applied to the study site in the past (Alila and Beckers, 2001), this study application focused largely on the effect of logging roads on streamflow. As a semi-distributed model, HBV has good representation of spatial complexity in soils, topography and climate. However, because this model uses empirical representations of watershed processes and forest canopy, its ability to represent forest disturbances is limited.

2.5 The Cold Regions Hydrological Model

2.5.1 Model Description

This study applies the Cold Regions Hydrological Model (CRHM), a physically based , semi-distributed modular software platform for building hydrological models (Pomeroy et al., 2007) that uses a Microsoft Windows interface and is written in the C++ programming language. Users select modules from a process module library that CRHM links to physical measurement data to simulate basin hydrology. As a semi-distributed model (capable of lumped modelling by using one HRU), CRHM can represent spa-

tially complex basins (Pomeroy et al., 2007), and uses a range of empirical, analytical and process-based algorithms that the user can select based on the type and range of available input data. Each process module uses parameters and state variables to simulate hydrologic response for each homogeneous HRU. Additionally, CRHM can process interactions between HRUs to simulate intra-basin hydrological processes such as flow and runoff between HRUs, and runoff out of a basin and can be run with minimal calibration (Abbot et al., 1986; Beven, 1989; Grayson et al., 1992).

2.5.2 Model Selection Justification

Selection of an appropriate hydrologic model is based on the particular watershed characteristics, research questions, and time, data, expertise and funding constraints of a given project (Beckers et al., 2009). The study watershed is small (< 5 km^2), relatively uniform in aspect and slope, and has largely homogeneous forest density (see Chapter 3); therefore, a semi-distributed model is appropriate for representing spatial variability in watershed physiographic characteristics (Beckers et al., 2009).

Given that the study watershed is affected by snow processes, a model that can accurately simulate these processes is required. CRHM is capable of representing most hydrologic processes in a watershed that are critical for forest disturbance simulation (Fig. 2.5) and was found to be one of the most capable models for simulating forest management scenarios that require manipulation of forested and clearcut environments (Beckers et al., 2009). An extensive dataset from the study site allows for use of a physically-based modelling approach and the ability of CRHM to modify internal algorithms based on available data is highly useful. The model is moderately parameterized, and field data are available to assist in selecting parameter values.

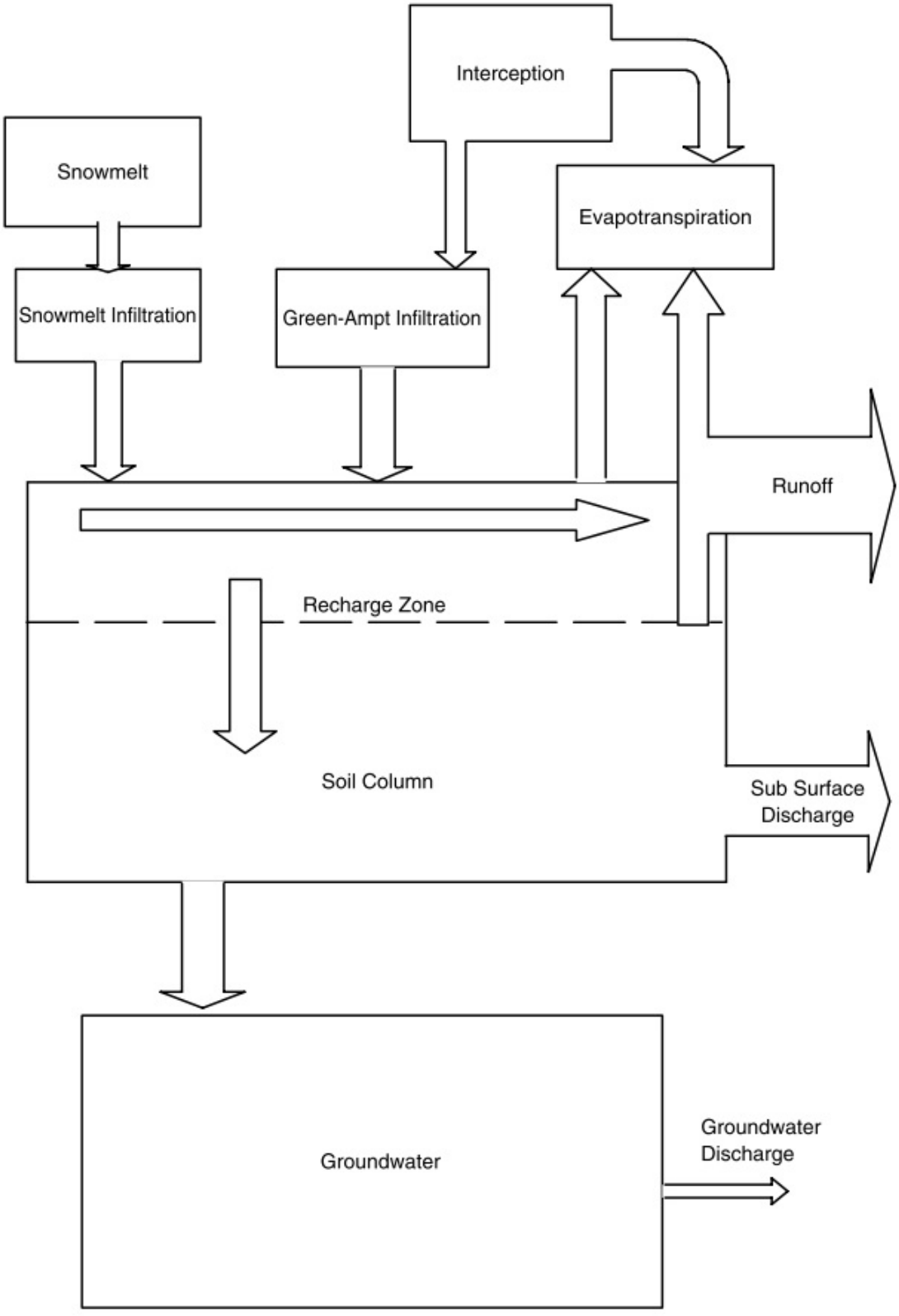

Figure 2.5: Conceptual diagram of individual modules and interactions between them in CRHM (from Pomeroy et al., 2007). The Green-Ampt Infiltration module determines the surface infiltration rate.

2.5.3 Previous CRHM Applications

CRHM is primarily a prairie/tundra model with a strong focus on cold regions hydrology (i.e. blowing snow, frozen soils) (Pomeroy et al., 2007). As such, it has largely been applied outside of the western Cordillera. However, CRHM was able to successfully simulate both snow melt runoff from a small alpine basin in the Front Ranges of the Canadian Rocky Mountains (DeBeer and Pomeroy, 2010), and to simulate snow accumulation and melt in coniferous forest environments (Ellis et al., 2010). This indicates that it is a useful analytical and/or predictive tool to quantify the mass and energy balance of snow in forests and clearings. A recent model inter-comparison found that CRHM simulated snow accumulation and melt well in both clearcut and forested sites relative to 33 other snowpack models (Rutter et al., 2009). While this study did not directly compare individual model performance, CRHM was reported to have a low normalized root mean square error (RMSE) and no outliers when simulating SWE in both site types (Fig. 2.6) (Rutter et al., 2009).

Ellis (2011) found that CRHM was able to capture the timing and magnitude of snow accumulation and melt both under forest canopy and in forest clearings. The poorest simulations of SWE occurred when accumulation was significantly lower in forest sites relative to other sites, which may be expected given that shallower snowpacks are highly sensitive to model errors in energy and mass balance. Modelled SWE was good at the beginning and peak of winter accumulation but poorer towards the melt period, suggesting a melt rate lag. Substantial late season snowfall may result in particularly large lags in snow melt, likely due to an overestimation of the additional energy deficit to the snowpack (Ellis, 2011). Thus changing the snow energetic algorithms within CRHM during large snowfalls may improve snow melt timing. Representation of daily and cumulative mass loss to sublimation was satisfactory; however, sensitivity analysis has shown that sublimation estimates within the model are highly responsive to errors in canopy interception. This may be indicative

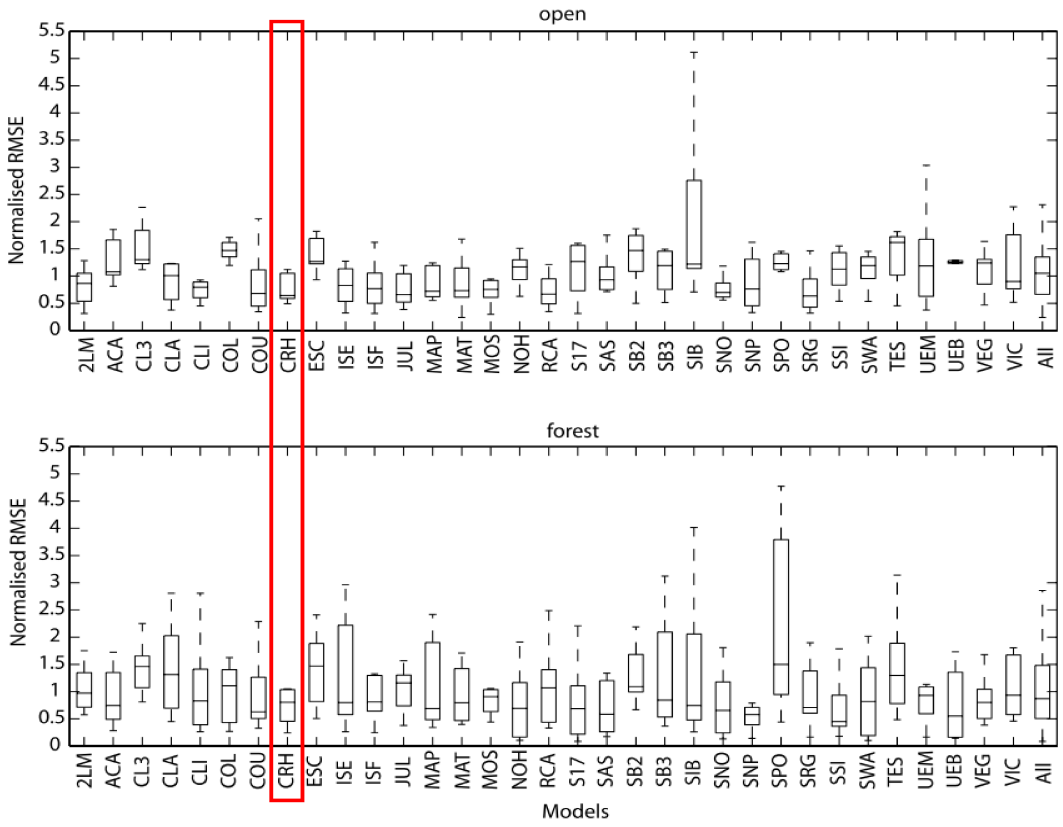

Figure 2.6: Box plot summaries illustrating the performance of individual models for all years at open and forested sites, from the SnowMIP2 model comparison study. CRHM is represented by CRH in this figure and a box is drawn around both open and forest model performance. Solid horizontal lines on each box are lower and upper quartile, and median values. Dashed vertical lines extend from box ends to 1.5 times the interquartile range; outliers beyond the dashed lines are omitted (from Rutter et al., 2009).

of CRHM's rigorous method of representing snow unloading from forest canopy. At a single paired clearing-forest site, CRHM was able to accurately represent the energy balance in both an open and sub-canopy snow surface (Ellis, 2011). Errors in estimating short and longwave radiation were small but generally increased under forest canopy, likely due to the increasing number of combined energy terms. Collective errors in simulating the sum of energy available for snow melt were small and likely due to miscalculations from individual energy terms cancelling each other out (Ellis, 2011).

2.5.4 Model Limitations

CRHM is able to simulate complex hydrological processes for watersheds of different scales and across varying time scales; however, complexity is not without difficulty (Beckers et al., 2009). As model complexity increases, the number of qualified users with model experience and expertise decreases. Fewer qualified modellers increase the resources and time required for model initialization and validation. Additionally, few studies have applied CRHM to forest disturbance scenarios (Pomeroy et al., 2012); therefore, the supporting literature is limited. Physically based models also require significant discussions with field personnel and other researchers to define appropriate parameter values and determine internal processes specific to the watershed, and extensive field data to run and validate the model. However, this study was able to capitalize on a long record of snow, meteorological and streamflow data that were readily available for this study site. Additionally, the site has been under study for 20 years, so field personnel were able to provide detailed information on watershed-specific processes, data collection and field observations that are often not be available in other watershed modelling projects.

2.6 Summary

Snow processes are strongly influenced by the presence of a forest canopy at the stand and watershed scale. Forest disturbances open the canopy, increasing snow accumulation and changing the rate and timing of snowmelt compared to undisturbed stands. To date, stand scale studies of forest disturbances have improved our understanding of snow accumulation and ablation below disturbed forest canopy; however, studies of forest disturbances, and a mosaic of forest disturbances at the watershed scale are deficient and require further examination.

Chapter 3

Study Area

3.1 Introduction

Research for this thesis was conducted at the Upper Penticton Creek watershed (UPCr) in the Okanagan Basin, British Columbia (BC), Canada. This chapter outlines the UPCr watershed experiment, then describes the hydrologic significance of the study area within the Okanagan Basin, defines its biogeoclimatic characteristics and outlines the meteorological, snow and hydrological research program underway as part of the UPCr experiment.

3.2 Okanagan Basin

The Okanagan Basin is located in south-central BC with a small southern portion located in northeast Washington (WA), USA (Fig. 3.1). The basin is approximately 160 km in length, ($8,200$ km^2), and feeds water south to the Columbia River. The elevation range of the landscape surrounding the Basin is approximately 1,100 m, with valley bottom elevation at approximately 340 m asl (Toews and Allen, 2007). The basin lies largely within the Thompson Plateau region which consists of volcanic, sedimentary and metamorphic rocks that were uplifted and subsequently eroded by glacial and fluvial processes (Roed and Greenough, 2004).

Due to the rain-shadow effect of the Coast and Cascade Mountain Ranges, the Okanagan has a dry continental climate. Average annual air temperatures at Okanagan Lake level are approximately 6 °C, while winter (December, January and February) air temperatures average -3.5 °C and summer (June, July and August) air temperature average 15 °C (Cohen and Kulkarni, 2001). Annual precipitation averages approximately 600 mm y^{-1} and varies with elevation and location within the basin (Brewer et al., 2001; Toews and Allen, 2007). According to the National Climate

Figure 3.1: Location of the Okanagan Basin. Dot represents location of Upper Penticton Creek.

Data Archives, the proportion of precipitation that falls as snow is approximately 25% (2011). Between April and mid-July, high elevation snowpacks above 1,200 m melt to produce peak flows, of which approximately 120 mm of water reaches Okanagan Lake (Neilson-Welch and Allen, 2007). Approximately 85% of precipitation is lost through evapotranspiration and evaporation from lakes (Cohen and Kulkarni, 2001). Mean annual groundwater recharge rates are estimated to be (22 mm y^{-1}) and (40 mm y^{-1}) in the valley bottom and upland areas, respectively (Summit Environmental Consultants Ltd, 2005).

The dominant land uses in the Okanagan Basin are agriculture and urban/rural residential uses; this region is home to most of the orchards and vineyards in the province (Cohen and Kulkarni, 2001). Agriculture in this semi-arid region relies on irrigation, thus freshwater supply is essential for sustaining the local agricultural economy (Cohen and Kulkarni, 2001). The urban population will be affected by changing water supply, which may be a challenge for water management planners given that population in the Basin was 310,000 in 2001, and is predicted to reach 450,000 by 2031 (Cohen and Kulkarni, 2001; Demographics Analysis Section: BC Stats, 2009).

Predicted climate change will substantially affect water supply and demand in the Okanagan Basin (Taylor and Barton, 2003). Global circulation models (GCM) predict warmer and wetter winters relative to the 1961-1990 climate normal; scenarios suggest that by the 2050s there will be an increase in winter air temperature of approximately 0.5–2.5 °C, a 10% increase in early winter precipitation and a 0–5% decrease in mid-winter to early spring precipitation (Spittlehouse, 2006). In summer, drought-like conditions are likely to increase as the scenarios suggest an increase in summer air temperatures of 2–4 °C, and a decrease in precipitation of 0–35%. These changes will likely increase the susceptibility of forested areas in the region to natural disturbances (Overpeck et al., 1990; Westerling et al., 2006; Hicke and Jenkins, 2008; Littell et al., 2009).

3.3 Upper Penticton Creek

The study is focused on the Upper Penticton Creek (UPCr) watershed, located 26 km northeast of Penticton, British Columbia (Fig. 3.2). UPCr consists of two headwater tributaries: 240 Creek and 241 Creek, which feed Penticton Creek. The 240 Creek and 241 Creek watersheds flow south; each is approximately (5 km^2) in size, with gentle slopes that range in elevation from 1,600 to 2,000 m (Winkler et al., 2004). Mean annual air temperature is 1.9 °C, mean minimum temperature is −7.2 °C and mean maximum temperature is 12.6 °C. Mean annual precipitation is 690 mm, about 50% of which falls as snow with peak snowpacks 1-1.5 m deep (Winkler et al., 2008). Total annual flow from each watershed ranges from (0.8–3 million km^3), totaling approximately 30–60% of annual precipitation (Winkler et al., 2004). The watersheds are forested with lodgepole pine (*Pinus contorta*), Engelmann spruce (*Picea engelmannii*) and subalpine fir (*Abies lasiocarpa*). In the lodgepole pine stands, tree spacing is fairly homogeneous, while the spruce and fir stands have a more clumped tree distribution (Winkler et al., 2008). Trees are > 100 years old, up to 26 m tall, with canopy density ranging from 35–50% depending on location in the watershed. Forest floor soils are thin (< 4 cm) and well drained, as all soil horizons are low in clay and high in coarse fragments. Past glacial activity is evidenced by coarse-grained granitic rocks that are covered by glacial till and glacio-fluvial sand and gravel (Winkler et al., 2008).

The Upper Penticton Creek Watershed Experiment was established in 1982 to monitor the long-term effects of natural and anthropogenic forest disturbances on hydrologic processes in the semi-arid Okanagan basin. This experiment follows a paired watershed design, for which pre- and post-logging measurements were collected in the logged and unlogged (control) watersheds. One watershed served as a control while the other was clearcut in increments up to 50% over an eight year period (Winkler et al., 2008). Investigations of stand-scale and site-specific hydrologic processes

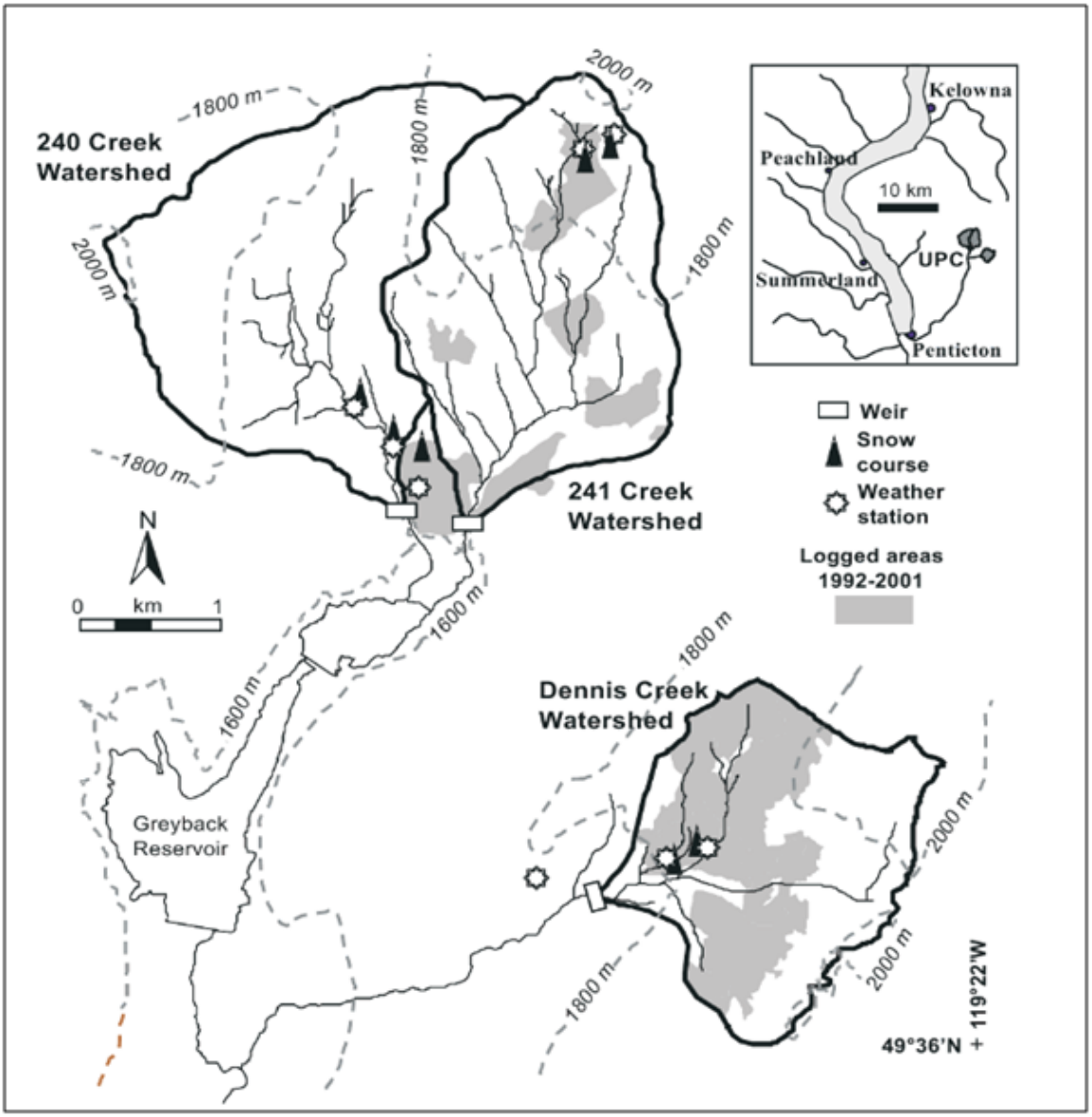

Figure 3.2: Stream network, monitoring stations, and harvested regions in the Upper Penticton Creek watershed; including 240 Creek, 241 Creek and Dennis Creek watersheds (from Winkler et al., 2004). This study focuses on 241 Creek watershed.

include measurements of net precipitation, interception, evaporation, transpiration, soil moisture and ground water at six meteorological stations and six snow courses. Streamflow is measured at a Water Survey of Canada gauge site at the outlet of each watershed. The long-term dataset at UPCr also includes measurements from specific experiments, including: watershed delineation, soil and vegetation classification, snow surveys, water quality, channel surveys and climate stations with hourly measurements of wind speed and direction, relative humidity, air temperature, solar radiation and precipitation. This study uses data from two meteorological stations in 241 Creek where hourly meteorological data (solar radiation, air temperature and humidity, wind speed, soil and snow temperature) were collected between 1999 and 2009 (Table 3.1). Measurements of snow depth and precipitation were collected over 11 snow accumulation and melt periods (1997-2008) in the 241 Creek catchment.

Table 3.1: Input data, including duration of record for data collected at UPCr and applied to CRHM

Dataset	Duration of record
Solar radiation (W m^{-2})	10 Oct 1999–1 Aug 2009 (Hourly)
Air temperature (°C)	10 Oct 1999–1 Aug 2009 (Hourly)
Relative humidity (%)	10 Oct 1999–1 Aug 2009 (Hourly)
Wind (m s^{-1})	10 Oct 1999–1 Aug 2009 (Hourly)
Precipitation (mm)	10 Oct 1999–1 Aug 2009 (Hourly)
SWE (mm)	Feb–May 2000–2009 (Bi-weekly surveys during snowmelt)

Extensive meteorological and topographic measurements of the watershed have allowed for an understanding of how the watershed responds hydrologically pre- and post-harvesting. The data from UPCr can be used to parameterize a hydrological model for current forest conditions (mature forest and clearcut), and by applying known or theoretical parameters from forest disturbances (i.e. mountain pine beetle and wildfire), Upper Penticton Creek can be used as an experiment for modelling forest disturbances in the Okanagan region.

Chapter 4

Methods

4.1 Introduction

This chapter outlines the methods used to model the response of snow accumulation and ablation to forest disturbances in 241 Creek (241Cr) (a sub-basin of the Upper Penticton Creek (UPCr) watershed) using the Cold Regions Hydrological Model (CRHM). The specific objectives of this chapter are to: 1) describe the field data used for this study, and the pre-processing of this data for model runs; 2) define the equations used by CRHM, the parameters and variables required to run the equations, and the assumptions implicit within CRHM; 3) define the methods for validation of model output using (1); and 4) outline forest disturbance scenario development and application, and analysis of model output.

4.2 Field Data

Meteorological data used in this study were collected at the lower meteorological station at 241Cr (P1; Fig. 4.1), using a Campbell Scientific CR1000 data-logger and the instruments listed in Table 4.1. Average hourly data was recorded based on 60 second measurements of incoming solar radiation, air temperature, relative humidity, wind speed, and precipitation (Table 4.1, Table 4.2). While this station is not located within the watershed, conditions are similar to those at the lowest elevations of 241Cr.

Snow survey data have been collected annually at 241Cr since 1999 in two forested and clearcut site pairs. The lower elevation pair is out of the watershed but represents within-watershed conditions (Fig. 4.1, Table 4.2). Snow surveys were conducted weekly or bi-weekly from February or early March until late May or early June, depending on snow accumulation conditions and funding availability. Snow water equivalent (SWE) was measured using the Standard Federal snow sampler and weighed

on a spring scale that provides direct values of SWE (Goodison et al., 1981). The following values were calculated annually from the field dataset: April 1 SWE, maximum SWE, date of 0 SWE, average melt rate, day of year of maximum SWE, day of year when continuous melt started, SWE at onset of continuous melt, day of year of onset of maximum melt, and maximum melt rate. Average melt rate was calculated as the average SWE lost per day between peak SWE and snow disappearance. The maximum melt rate was defined as the maximum melt rate of SWE loss between peak SWE and snow disappearance.

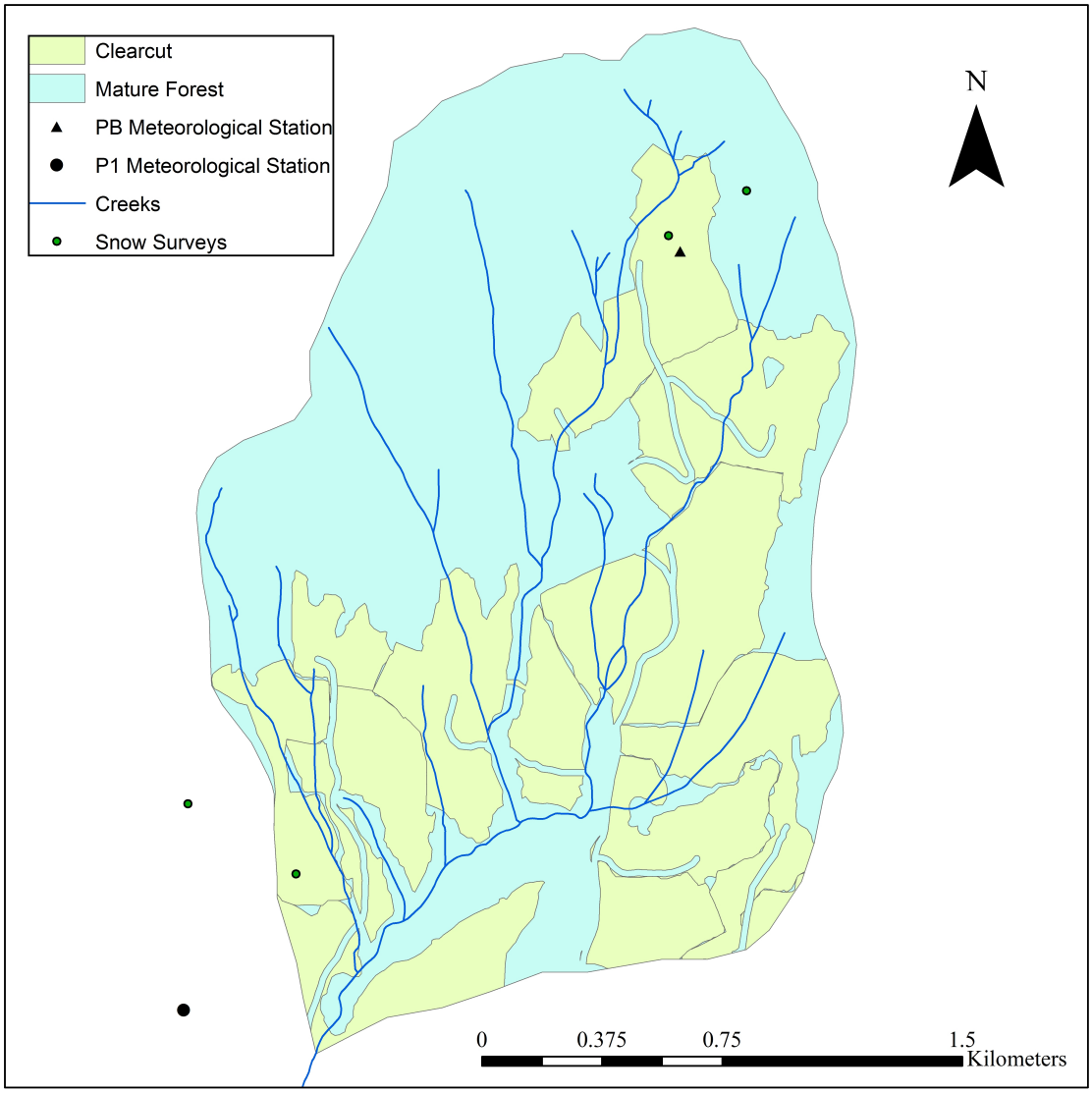

Figure 4.1: 241Cr meteorological stations and snow survey locations.

Table 4.1: Instruments and measurement height

Variable	Instrument model	Instrument accuracy	Height above ground (m)
Incoming solar radiation (W m^{-2})	LiCor LI200 pyranometer	± 5%	3
Air temperature, relative humidity (°C)	Campbell Scientific HMP35C; in multi-plate radiation shield	±0.4 °C, ± 3%	2.5
Wind speed (m s^{-1})	MetOne 013 wind speed sensor	± 2%	4
Precipitation (rain; mm)	Texas Electronic TR525i tipping bucket	± 1%	0.5
Snow depth	Campbell Scientific UDG01 ultrasonic depth gauge	± 1 cm	2

Table 4.2: Meteorological and snow survey collected at 241Cr and used in this study

Dataset	Duration of record
Solar radiation (W m^{-2})	10 Oct 1999–1 Aug 2009 (hourly)
Air temperature (°C)	10 Oct 1999–1 Aug 2009 (hourly)
Relative humidity (%)	10 Oct 1999–1 Aug 2009 (hourly)
Wind speed (m s^{-1})	10 Oct 1999–1 Aug 2009 (hourly)
Precipitation (mm)	10 Oct 1999–1 Aug 2009 (hourly)
Snow surveys	Weekly and bi-weekly in 1995–2008 (survey grids in both clearcut and mature forest)

4.3 GIS Data

To characterize the vegetation and topographic properties of 241Cr, spatial input data were obtained from the British Columbia Ministry of Forests, Lands, and Natural Resource Operations (Fig. 4.2). These data were part of the Terrain Resource Information Management (TRIM) program to catalogue vegetation and elevation data (Government of British Columbia, 2010). Vegetation data, including leaf area index (LAI), canopy cover (area of the ground covered by a vertical projection of the canopy (%)), vegetation distribution, species, age and stem density shape files were created through a combination of aerial photo and satellite imagery analyses, and

ground sampling. A 25 m digital elevation model (DEM) was created by the TRIM program using aerial photography and stereoscopic air photo interpretation. Using Raster Calculator and Spatial Analyst in ArcGIS 9.3.1, watershed boundaries, slope, aspect and elevation ranges were derived from the DEM.

4.4 Structure and Application of CRHM

CRHM functions through interaction between observations, parameters, and modules. Observations are measured meteorological data used to drive the model at each timestep (hourly for this study). The data in Table 4.3 are required at each timestep.

Table 4.3: Input variables

Input variable
Incident solar radiation (Q_{si}, in W m^{-2})
Air temperature (T_a^*, in °C)
Relative humidity (RH, in %)
Wind speed (u, in m s^{-1})
Precipitation (P, in mm)

The model uses meteorological data from a single station and extrapolates it across the watershed for distributed modelling. T_a, RH, and P were distributed across the watershed using a lapse rate calculated from measured meteorological data (-2.87 °C km^{-1}): the lapse rate was calculated as the average (1999–2008) change in air temperature with elevation between the low and high elevation meteorological stations (P1 and PB, respectively) (Fig. 4.2). The low lapse rate value relative to the mean adiabatic lapse rate of -6 °C km^{-1} is noted, and may be affected by local influences at one or both stations. Incident shortwave radiation is corrected for slope and aspect across the basin based on Granier and Ohmura (1970).

Two sets of parameters were defined based on a combination of measured field data and values from the literature. First, parameters were defined for topography and hydrological response units (HRUs) which serve to represent the physiographic

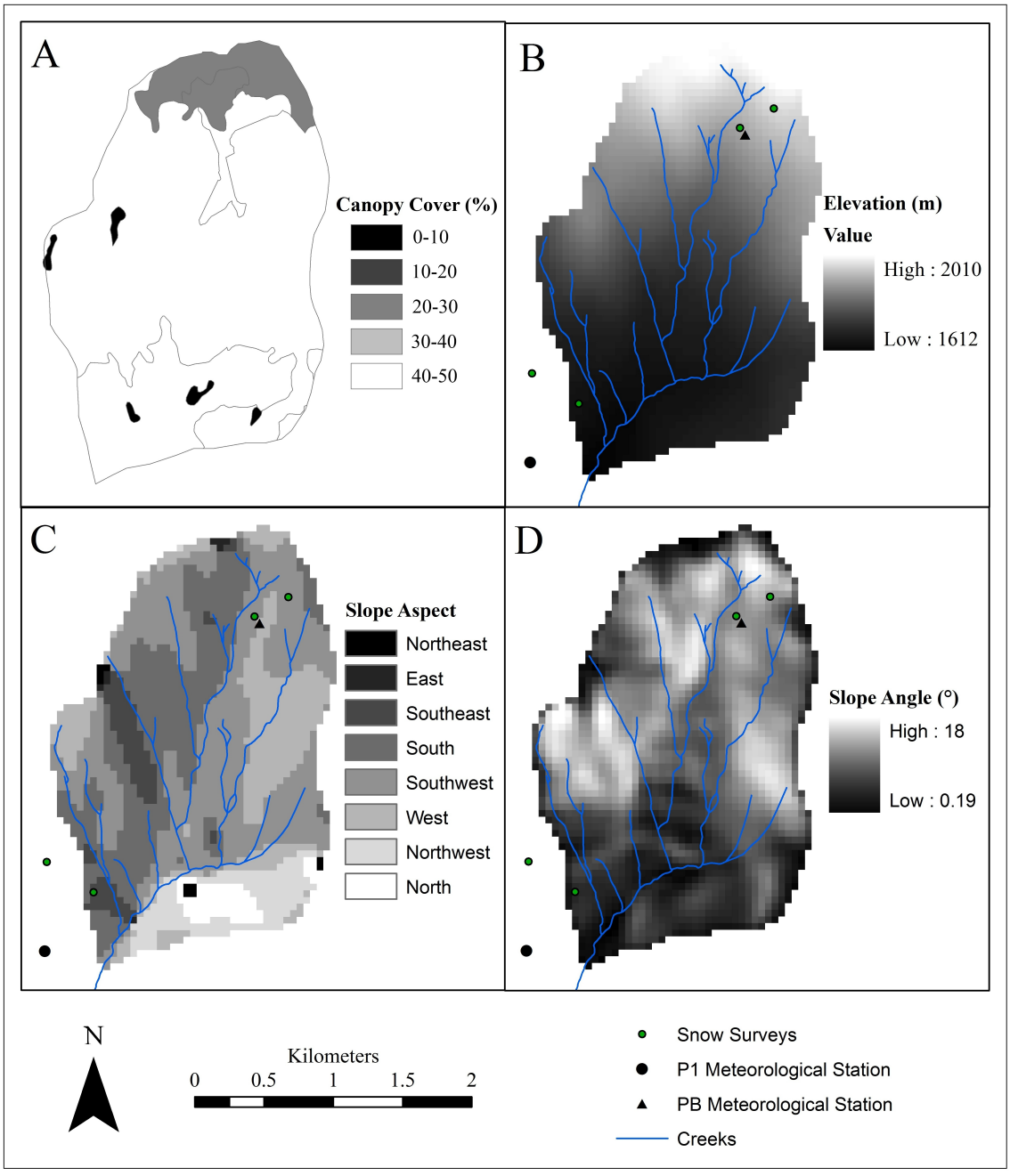

Figure 4.2: Forest cover and topographic characteristics of 241Cr: canopy cover (A), elevation (B), slope aspect (C), and slope angle (D).

characteristics of the watershed. HRUs divide the watershed into discrete units of homogeneous elevation, slope, aspect, and *LAI*, each of which is assumed to have a homogenous hydrological response (Table 4.4) (Winkler, 2001). Parameters were also defined for calculation of specific hydrological processes at each timestep. The user determines the initial model setup by selecting individual modules and specific algorithms within each module based on data availability, quality, and the purpose of the modelling exercise (Fig. 4.3).

Table 4.4: User defined parameters

User defined parameter
HRU area (km^2)
HRU aspect (^{o})
Elevation (m)
Ground slope ($^\circ$)
HRU latitude ($^\circ$)
Maximum snow load per branch area (*Sbar*, in kg m^{-2})
Leaf area index (*LAI*, m^2 m^{-2})
Snow surface albedo (α_s, dimensionless)
Fresh snow adjustable albedo (α_f, dimensionless)
Adjustable albedo decay time constant for melting snow (τ, in s)

LAI is defined as the needle area per ground unit area, and is often used as a canopy interception parameter in forest studies. However, this term does not include the total surface area available to collect snowfall. Values for *LAI* in this study were measured by the LI-COR LAI-2000 Plant Canopy Analyzer (Gower and Norman, 1991). The LAI-2000 measures the effective leaf area index (*LAI'*), which includes the total horizontal area of stems, needles and leaves per unit of ground, and is calculated by $LAI(\Omega)$, where Ω is the stand clumping index. Disregard for clumping may result in an underestimation of *LAI* by up to 62%, and subsequent decrease in amount of snow retained in the canopy. Therefore, *LAI'* is more applicable for snow interception studies than the physical leaf area of the canopy (Hedstrom and Pomeroy, 1998) because all surfaces of the canopy are incorporated in its calculation. While

more accurately defined as LAI', LAI is the parameter label for canopy calculations in CRHM, and will be referred to as such throughout this document.

Modelling snow accumulation and ablation in a forest must incorporate two important factors: 1) the interception of snow by the canopy, and 2) the transmission of radiation through the canopy. CRHM uses LAI to define the canopy closure, defined as the amount of canopy covering the ground surface, which then provides a surface for snow interception. Transmission of radiation through the forest canopy is a function of forest-cover density, which is quantified using the forest sky view factor (v). In this study, v is the amount of sky visible from the ground through gaps in the canopy. The value may be specified explicitly, or as in this study is estimated by CRHM from LAI.

In CRHM, forest-cover density is estimated by the optical depth of the forest (L') and the forest sky view factor (v):

$$\tau_f = e^{-L'} \tag{4.1}$$

where L' is produced as the negative logarithm of the vertical radiation transmittance (τ_f) through the forest layer. L' may be alternately specified as the radiation extinction coefficient of the forest layer (m^{-1}). Subsequently, L' relates only to the canopy vegetation influencing radiation transfer through the forest layer, and exempts vegetation that is self-shaded (Chen and Black, 1992). The forest sky view factor (v) may be evaluated by integrating Eq. 4.1 as follows:

$$v = 2\int_0^{\frac{\pi}{2}} e^{-\frac{L'}{sin\Theta}} cos\theta sin\theta \cdot \delta\theta = 2\int_0^{\frac{\pi}{2}} \tau_f(\theta) cos\theta sin\theta \cdot \delta\theta \tag{4.2}$$

where Θ is the solar elevation angle above the horizon (radians). Accordingly, the overlying hemisphere not occupied by v is covered by forest (canopy-closure; 1-v), which neglects radiation transmittance. As a result, the equation permits for an

overlying hemisphere with two components, one of which transmits radiation, while the other is non-transmitting, in magnitudes defined by v and (1-v), respectively (Ellis, 2011).

Model output includes hourly calculated values of: snow albedo, incoming short- and long-wave radiation, incident short- and long-wave radiation at snow surface, sensible and latent heat transfer, and daily snow ablation (Fig. 4.3). Model output is exported to Microsoft Excel for analysis.

4.4.1 Snow Mass Balance

The snow mass balance module of CRHM represents mass fluxes at the snow surface. In non-forested environments (i.e. clearcut), mass balance is calculated as:

$$SWE = SWE_o + (P_s + P_r + H_{in} + H_{out} - S - M)t \tag{4.3}$$

where SWE_o is the antecedent SWE; P_s is the rate of snowfall; P_r is the rate of rainfall; H_{in} and H_{out} are the incoming and outgoing horizontal and lateral snow transport rates, respectively; S is the rate of sublimation loss; M is the melt loss rate (all units in kg m^{-2} h^{-1}); and t is the model calculation timestep (all rates calculated at this timestep).

In forested environments we must consider the role of the canopy in trapping and retaining snow until it is either sublimated or unloaded. Thus, the mass balance is expressed as:

$$SWE = SWE_o + (P_s - (I_s - U_l) + P_r - (I_r - R_d) - M)t \tag{4.4}$$

where I_s and U_l are the canopy snow interception and unloading rate, respectively; I_r is the canopy rainfall interception rate; and R_d is the canopy rain drip rate (all units kg m^{-2} h^{-1}). Rain is considered negligible in Equations 4.1 and 4.2, as observations

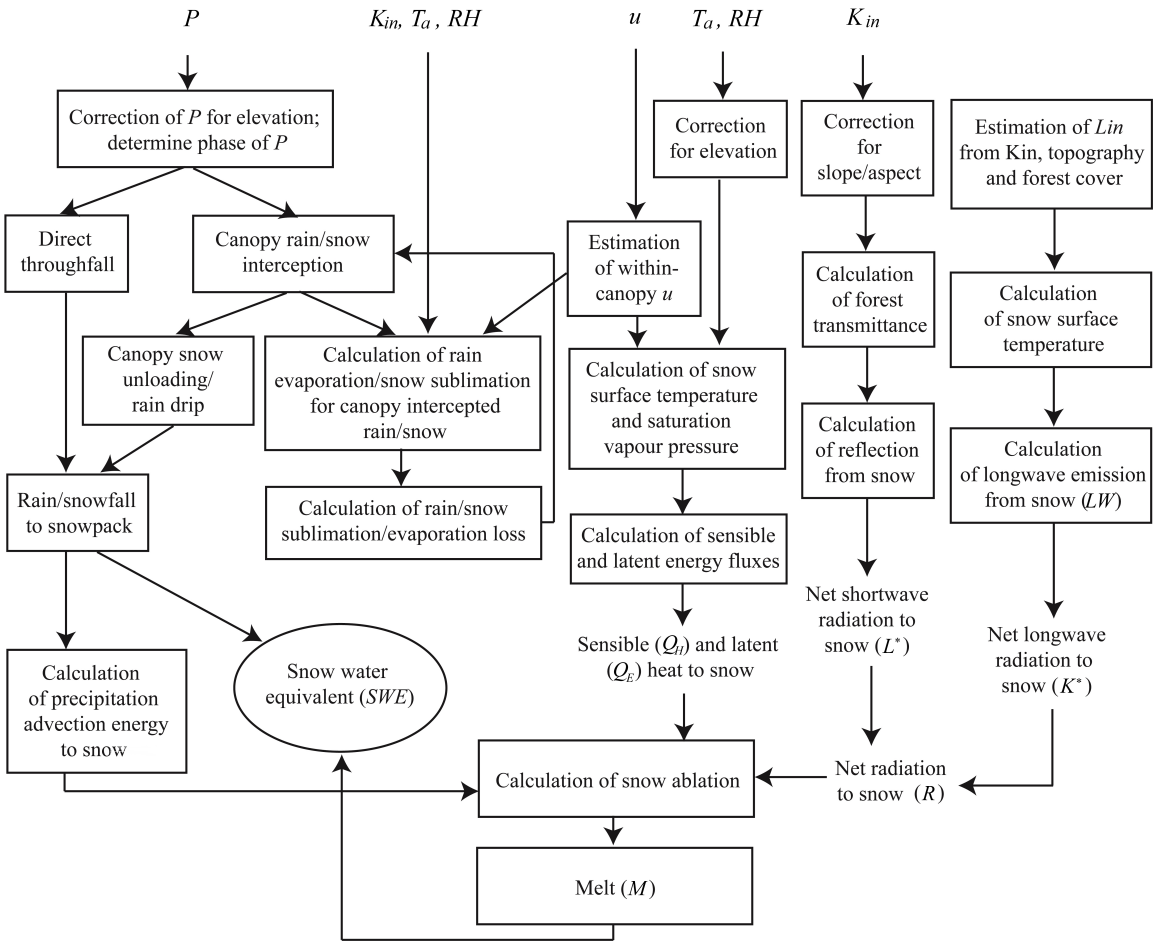

Figure 4.3: Diagram of the mass and energy balance calculations and interactions in CRHM (reproduced from Ellis, 2011).

indicate rain is insignificant in this region during the winter and spring period (R. Winkler, unpub. data).

Interception and unloading processes for a single tree are modelled following Hedstrom and Pomeroy (1998):

$$I = P - P_{FC} = \sum L\uparrow - \sum L\downarrow \tag{4.5}$$

where I is the canopy interception (mm); P is the clearing snowfall (mm); P_{FC} is the sub-canopy snowfall (mm); $\sum L\uparrow$ is the sum of increases in canopy load; and $\sum L\downarrow$ is the sum of unloading to the ground (all units in mm of SWE per unit area for the model timestep).

The maximum snow canopy load (L_s, kg m^{-2}), is calculated from the leaf area index (*LAI)* and the maximum snow load per unit branch area (*Sbar,* kg m^{-2}):

$$L_s = Sbar \times LAI \tag{4.6}$$

Sbar is defined based on Schmidt and Gluns (1991) using a mean value based on tree species that fluctuates with snow density:

$$Sbar = \overline{Sbar}\left(0.27\frac{46}{p_s}\right) \tag{4.7}$$

where $\overline{Sbar}$ is the mean snow load for the tree species; and p_s (kg m^{-3}) is the density of fresh snow.

The initial snow canopy load, L_0 (kg m^{-2}), is calculated by Hedstrom and Pomeroy (1998) using:

$$L_0 = N \times M_t \tag{4.8}$$

where N is the ratio of increased canopy intercepted load to increased tree intercepted load (mm kg^{-1} m^{-2}); and M_t is snow weight (kg) on the tree. The weight of snow on

a single tree is upscaled to the entire canopy using a scaling parameter, N, defined as:

$$N = \frac{\sum L \uparrow}{\sum M_t \uparrow} \tag{4.9}$$

where N is the ratio of increased canopy intercepted load to increased tree intercepted load (mm kg^{-1} m^{-2}); and $\sum M_t \uparrow$ is the cumulative increase in snow weight (M_t, kg) on the tree. Therefore, tree canopy interception is related to the increase in canopy load and the increase in snow weight. Snow that is intercepted in the canopy can be sublimated to the atmosphere. The rate of unloading intercepted snow from the canopy (dI/dt) is calculated as:

$$\frac{dI}{dt} = -UI \tag{4.10}$$

where U (s^{-1}) is the unloading rate coefficient. To calculate an exponential decay in unloading over time, t, Hedstrom and Pomeroy (1998) use:

$$I = I_1 e^{-Ut} \tag{4.11}$$

where I_1 is the intercepted canopy load at the start of unloading, and t is the timestep.

Sublimation of intercepted snow is calculated from Pomeroy (1998c) as:

$$q_e = V_i I_s \tag{4.12}$$

where q_e is the canopy sublimation flux (kg m^{-2} s^{-1}); and V_i is the sublimation rate coefficient for intercepted snow (s^{-1}), expressed as:

$$V_i = V_s C_e \tag{4.13}$$

where V_s is the adjusted sublimation flux for a 500 m radius ice sphere (s^{-1}) (assumes snow is uniform radius sphere); and C_e is the intercepted snow exposure coefficient

(dimensionless) which is calculated as:

$$C_e = k\left(\frac{I_s}{I_s^*}\right)^{-0.4} \tag{4.14}$$

where I_s^* is the maximum intercepted load for the conifer (6.6 kg for mature forest), k is a coefficient indexing the age/structure of snow on the conifer ($k = 0.0001099$ and 0.0000545 for fresh and aged snow, respectively) (Pomeroy and Schmidt, 1993).

4.4.2 Snow Ablation Energy Balance

The snow ablatation energy balance is calculated in CRHM as the sum of radiative, advective, conductive, and turbulent energy fluxes at the snow-ground and snow-atmosphere interfaces (all in W m^{-2}):

$$Q^* = K^* + L^* + Q_H + Q_E + Q_P + Q_G = \frac{dU}{dt} + Q_M \tag{4.15}$$

where Q^* is the total energy input to the snow; K^* and L^* are net shortwave and longwave radiation, respectively; Q_H and Q_E are the sensible and latent heat fluxes, respectively; Q_G is the net ground heat flux; Q_P is the energy advected from rainfall; $\frac{dU}{dt}$ is the change in internal (stored) energy of the snow pack; and Q_M is the energy available for snowmelt. Positive and negative values represent energy gains and losses in energy to snow, respectively.

Calculation of net all-wave radiation to snow (R^*) requires the sum of K^* and L^*, each made up of incoming and outgoing fluxes:

$$R^* = \ K^* + L^* = K_{in} - K_{out} + L_{in} - L_{out} \tag{4.16}$$

Net shortwave radiation to the snow surface (K^*) is calculated as the amount of radiation transmitted through the forest canopy less the amount reflected by the

snow surface:

$$K^* = K_o\ \tau(1 - \alpha_s) \tag{4.17}$$

where K_o is the incident above-canopy shortwave radiation; τ is shortwave radiation transmittance through the canopy; and α_s is the snow surface albedo. τ is estimated using Pomeroy (2009), expressed here as:

$$\tau = e^{-\frac{0.081\theta cos(\theta) LAI}{\sin(\theta)}} \tag{4.18}$$

where θ is the solar angle above the horizon (radians). Thus radiation transmittance is a function of both canopy structure (LAI) and incident shortwave radiation (sun angle).

Incoming longwave radiation to sub-canopy snow (L_{in}) can be greater than incoming longwave radiation in a clearcut (L_o) given the thermal energy emitted from the canopy (Link and Marks, 1999; Sicart et al., 2004; Pomeroy et al., 2009), and is calculated as:

$$L_{in} = vL_o + (1 - v)\varepsilon_f \sigma T_f^4 \tag{4.19}$$

where v is the forest sky view factor; ε_f is the forest thermal emissivity; σ is the Stefan-Boltzmann constant (5.67×10^{-8} W m^{-2} K^{-4}); and T_f is the forest canopy temperature (K). Outgoing longwave radiation from the snow surface (L_{out}) is calculated as:

$$L_{out} = \varepsilon_s \sigma T_s^4 \tag{4.20}$$

where ε_s is the thermal emissivity of snow (0.98) (Oke, 1987) and T_s is the snow surface temperature (K).

Fresh snow is given an adjustable albedo α_f, that decays exponentially to a minimum value = 0.5. For each model time step, albedo is updated using Essery (Essery

et al., 2001):

$$\alpha_s \rightarrow (\alpha_s - 0.5)\, e^{-\frac{\triangle t}{\tau}} + 0.5 \tag{4.21}$$

where Δt is the model timestep (h) and τ (s) is the adjustable albedo decay time constant for melting snow (parameter value set by user). When snow is falling, albedo is increased by:

$$\alpha_s \rightarrow \alpha_s + (\alpha_f - \alpha_s)\, \frac{Ps \triangle t}{10} \tag{4.22}$$

where Ps is the snowfall rate (h). In this case, 10 mm of snowfall depth resets albedo to α_f.

Sensible (Q_H) and latent (Q_E) heat fluxes (both in MJ m^{-2}) are calculated from a method adapted by Marks and Dozier (1992) from Brutsaert (1982) using a sequence of nonlinear equations to solve for the Minin-Obukhov stability length scale L (m), the friction velocity (u^*; m s^{-1}), Q_H, and the mass flux of sublimation (condensation) from (or to) the snow surface (E; kg m^{-2} s^{-1}):

$$L = \frac{u^{*3}\rho}{kg(\frac{Q_H}{T_a C_p} + 0.61E)} \tag{4.23}$$

$$u^* = \frac{uk}{ln(\frac{z_u - d_0}{z_0}) - \Psi_{sm}(\frac{z_u}{L})} \tag{4.24}$$

$$Q_H = \frac{(T_a - T_{s,0}) a_H k u^* \rho C_p}{ln(\frac{z_u - d_0}{z_0}) - \Psi_{sh}(\frac{z_T}{L})} \tag{4.25}$$

$$E = \frac{(q - q_{s,0}) a_E k u^* p}{ln(\frac{z_u - d_0}{z_0}) - \Psi_{sv}(\frac{z_q}{L})} \tag{4.26}$$

where ρ is the density of air (1.225 kg m^{-3} at sea level); k is the dimensionless von Kármán constant ($\sim$0.40); g is the acceleration due to gravity (9.81 m s^{-2}); T_a is the air temperature (K); C_p is the specific heat of dry air at constant pressure

(1005 J kg^{-1} K^{-1}); u is the wind speed (m s^{-1}); z_u, z_T, and z_q are the measurement heights (m) for wind, temperature and humidity, respectively; and d_0 is the zero-plane displacement height (m; (2/3) 7.35 (where z_0 is the roughness length in m)). In each of Equations 4.21-4.24, Ψ_{sm}, Ψ_{sh} and Ψ_{sv} are the stability functions for mass, heat and water vapour, respectively (positive, negative and zero for stable, unstable and neutral stability); $T_{s,0}$ is the snow surface layer temperature (K); a_H and a_E are the ratio of eddy diffusivity for heat and water vapour to eddy viscocity, respectively (both set to 1.0); and q is the specific humidity (g kg^{-1}) (Marks et al., 2008).

Q_E is calculated as $L_v E$ where L_v is the latent heat of vapourization or sublimation (J kg^{-1}) which varies with temperature and the state of water (liquid or solid) from 2.501 x 10^6 J kg^{-1} for liquid water at 0°C (vapourization) to 2.834–2.839 x 10^6 J kg^{-1} for ice between 0 and -30°C (sublimation) (Marks et al., 2008).

When rain falls on melting snow, the energy transfer from rainfall advection to the snowpack, Qp (MJ m^{-2} h^{-1}) is calculated as suggested by Gray and Landine (1988):

$$Q_P = 4.2 \times 10^{-3} \ (P_r - I_t)T_r \tag{4.27}$$

where T_r is the rainfall temperature (°C), which is approximated by T_a at the time of rainfall.

The amount of melt (M) is calculated from:

$$M = \frac{Q_M}{p_W B h_f} \tag{4.28}$$

where p_W is the density of water (1000 kg m^{-3}); B is the fraction of ice in wet snow (∼0.95–0.97); and h_f is the latent heat of fusion for ice (333.5 kJ kg^{-1}).

4.4.3 Blowing Snow

Removal of snow is not limited to canopy sublimation or melt. Blowing snow can occur if sufficient wind speed occurs, lifting snow particles from the ground and transporting them within or out of the basin. In CRHM, blowing snow is handled via the blowing snow module and is useful for snow ablation calculations. However, based on field measurements and observations, these processes are not prevalent in the 241Cr basin and thus this module was not used for SWE calculations.

4.5 Model Sensitivity

Sensitivity tests were conducted to determine which of the key parameters used to calculate snow accumulation and ablation had the greatest effect on model output (Table 4.5). The parameter values selected for this study were chosen to represent a range of potential over- or under-estimations. Results were plotted as the iterative change in each parameter value versus the average accumulation and average ablation rates. Average accumulation rate was calculated as the average daily amount of snow accumulation between the first day of continuous snow accumulation and the date of peak SWE. The average ablation rate was calculated as the average amount of snow ablation between the date of peak SWE and the first date when snow was completely melted. This information was used when parameterizing module variables, as sensitive parameters require highly accurate values given their effect on model output. The year 2001 was selected for the sensitivity test because early model runs suggested CRHM was able to represent snow accumulation and ablation well during this year. 2001 has the lowest peak SWE compared with years in the range of 2000–2008.

Table 4.5: Range, number of iterations, and iterative change used for sensitivity analysis of each parameter during the 2001 snow accumulation and snowmelt period (1 October to 1 July) in the mature and clearcut stand. NOTE: Maximum intercepted canopy snow load, and leaf area index are not included for clearcut sensitivity tests.

Parameter	Range	Number of iterations (Iterative change)
Albedo decay time constant for cold snow ($a1$; s)	9 x 10^2 to 9 x 10^7 1 x 10^4 to 1 x 10^7*	6 (1 x 10^1) 7 (1.5 x 10^1)*
Albedo decay time constant for melting snow ($a2$; s)	10 x 10^2 to 10 x 10^7 5 x 10^2 to 1.5 x 10^3*	6 (1 x 10^1) 10 (1 x 10^2)*
Maximum albedo for fresh snow (a_{max})	0.5 to 0.95	10 (0.05)
Minimum albedo for aged snow (a_{min})	0.3 to 0.8 0.2 to 0.7*	6 (0.01) 6 (0.01)*
Maximum intercepted canopy snow load ($Sbar$; kg m^{-2})	1 to 8	8 (1)
Leaf Area Index (LAI; m^2 m^{-2})	0.25 to 3.0	12 (0.25)

* = Denotes sensitivity test values used only in the clearcut.

4.6 Baseline Run

Before disturbance modelling was conducted, a baseline run was completed to ensure that CRHM was accurately representing observed conditions in both mature forest and clearcut stands. Parameter values to represent mature and clearcut forests at 241Cr were derived from both field data and the literature, and were kept constant throughout a nine year simulation period (1 October 1999 to 1 July 2008) (Table 4.6). The snow accumulation period is defined from 1 October to peak SWE (early April), while the snowmelt period is defined from peak SWE to the complete removal of snowpack (late June to early July). Model runs were labelled according to the year in which they end; for example, the 2001 model run refers to 1 October 2000–1 July 2001. The model was set up for the baseline with two HRUs: one to represent 241Cr as completely clearcut and the other to represent 241Cr as completely mature forest. Each HRU had the same topographic characteristics (average elevation, slope angle, aspect).

Table 4.6: Baseline parameter values for mature and clearcut forests.

Parameter	Mature forest	Clearcut	Reference
Area (km^2)*ˆ	4.82	4.82	
Elevation (m)*ˆ	1753	1753	
Slope (°)*ˆ	10	10	
Aspect (°)*ˆ	180	180	
Latitude (°)*ˆ	49.39	49.39	
Albedo decay time constant for cold snow ($a1$; s)	9 x 10^5	1 x 10^8	(D. Spittlehouse, unpub. data)
Albedo decay time constant for melting snow ($a2$; s)	1 x 10^3	1 x 10^6	(D. Spittlehouse, unpub. data)
Initial albedo for bare ground (a_{bare})	0.17	0.17	(D. Spittlehouse, unpub. data)
Initial albedo for snow cover (a_{snow})	0.9	0.9	(Gray and Prowse, 1993)
Maximum albedo for fresh snow (a_{max})	0.84	0.84	(Wiscombe and Warren, 1980)
Minimum albedo for aged snow (a_{min})	0.36	0.72	(D. Spittlehouse, unpub. data)
Minimum snowfall to refresh snow albedo (s_{min}; mm h^{-1})	10	10	(D. Spittlehouse, unpub. data)
Leaf Area Index (LAI; m^2 m^{-2})	2.2	n/a	(R. Winkler, unpub. data)
Maximum intercepted canopy snow load ($Sbar$; kg m^{-2})	6.6	n/a	(Schmidt and Gluns, 1991)

* = Derived from field data (Government of British Columbia, 2010)
ˆ = HRU definition
n/a = Not applicable

Four statistical metrics were used to assess model performance. Each compared daily average observed SWE with the daily average of hourly simulated SWE: root mean squared error ($RMSE$), mean absolute error (MAE), coefficient of determination (R^2), and linear regression. These metrics were calculated for each individual year in the 9-year dataset, as well as for the dataset as a whole.

$RMSE$ is a widely used metric of model accuracy that is calculated in the same units as the dataset. As errors are squared before being averaged, the $RMSE$ gives

more weight to large errors (Legates and McCabe Jr., 1999). RMSE is calculated as:

$$RMSE = \frac{1}{n}\sqrt{\sum_{i=1}^{n}(X_{si} - X_{oi})^2} \tag{4.29}$$

where n is the number of samples; X_s are the simulated values; and X_o are the observed values. Lower RMSE values indicate better model performance.

Mean absolute error (MAE) measures the proximity of predicted to measured values using an average of the absolute errors (Zar, 1999), thus all the individual differences are weighted equally in the average. MAE is calculated as:

$$MAE = \frac{1}{n}\sum_{i=1}^{n}|X_{si} - X_{oi}| \tag{4.30}$$

The coefficient of determination (R^2), is the proportion of variance explained by the regression model (Nagelkerke, 1991). This metric is useful to determine the goodness of fit between measured and modelled data, and to calculate ouliers and residuals. R^2 is expressed as:

$$R^2 = \left(\frac{\sum_{i=1}^{n}\left(X_o - \overline{X_o}\right)\left(X_s - \overline{X_s}\right)}{\sqrt{\sum_{i=1}^{n}\left(X_o - \overline{X_o}\right)}\sqrt{\sum_{i=1}^{n}\left(X_s - \overline{X_s}\right)^2}}\right)^2 \tag{4.31}$$

The relationship between the independent and dependent variables was defined by fitting a linear regression to the observed data:

$$y = ax + b \tag{4.32}$$

where y is the dependent variable, a is the slope of the line, x is the independent variable, and b is the y-intercept. A positive or negative y-intercept suggests that simulated data is of higher or lower magnitude than measured data. The slope of a

line refers to the rate at which y increases proportionately to x. A steep slope (> 1) suggests that y values increase at a greater rate than x values, while shallow slopes (< 1) suggest that the x values increase at a greater rate than y values.

The outcomes of these statistical tests were used to select years for which disturbance scenarios were run. As the mature forest was modified for the forest disturbance scenarios, it was most important to select years with the best goodness of fit in the mature forest. Two years were selected for forest disturbance scenarios, based first on model performance in the mature forest, and second on the clearcut performance of the baseline runs. It was also important to select years with different snow conditions to assess a potential disturbance response.

4.7 Forest Disturbance Scenarios

HRUs were created in ArcGIS 9.3.1 by selecting homogeneous units from the 20 m DEM with similar slope, aspect, and elevation (Fig. 4.4). The average of each variable was then applied as a single value in each HRU (Table 4.7). Average *LAI* show minimal change across the watershed, thus the same parameter value was used in each HRU to describe vegetation. HRUs were labelled 1 to 4 from low to high average elevation, respectively.

Table 4.7: Topographic parameter values for HRUs.

Variable	HRU 1 (Low Elevation)	HRU 2 (Mid-Low Elevation)	HRU 3 (Mid-High Elevation)	HRU 4 (High Elevation)
Area (km^2)	1.16	1.05	2.09	0.52
Elevation (m)	1637	1682	1825	1950
Slope (°)	5	8	12	14
Aspect (°)	231	193	195	192
Latitude (°)	49.39	49.39	49.39	49.39

Two disturbance scenarios were represented: 1) mountain pine beetle (MPB) at the red-attack stage, and 2) immediately following moderately severe wildfire (WF).

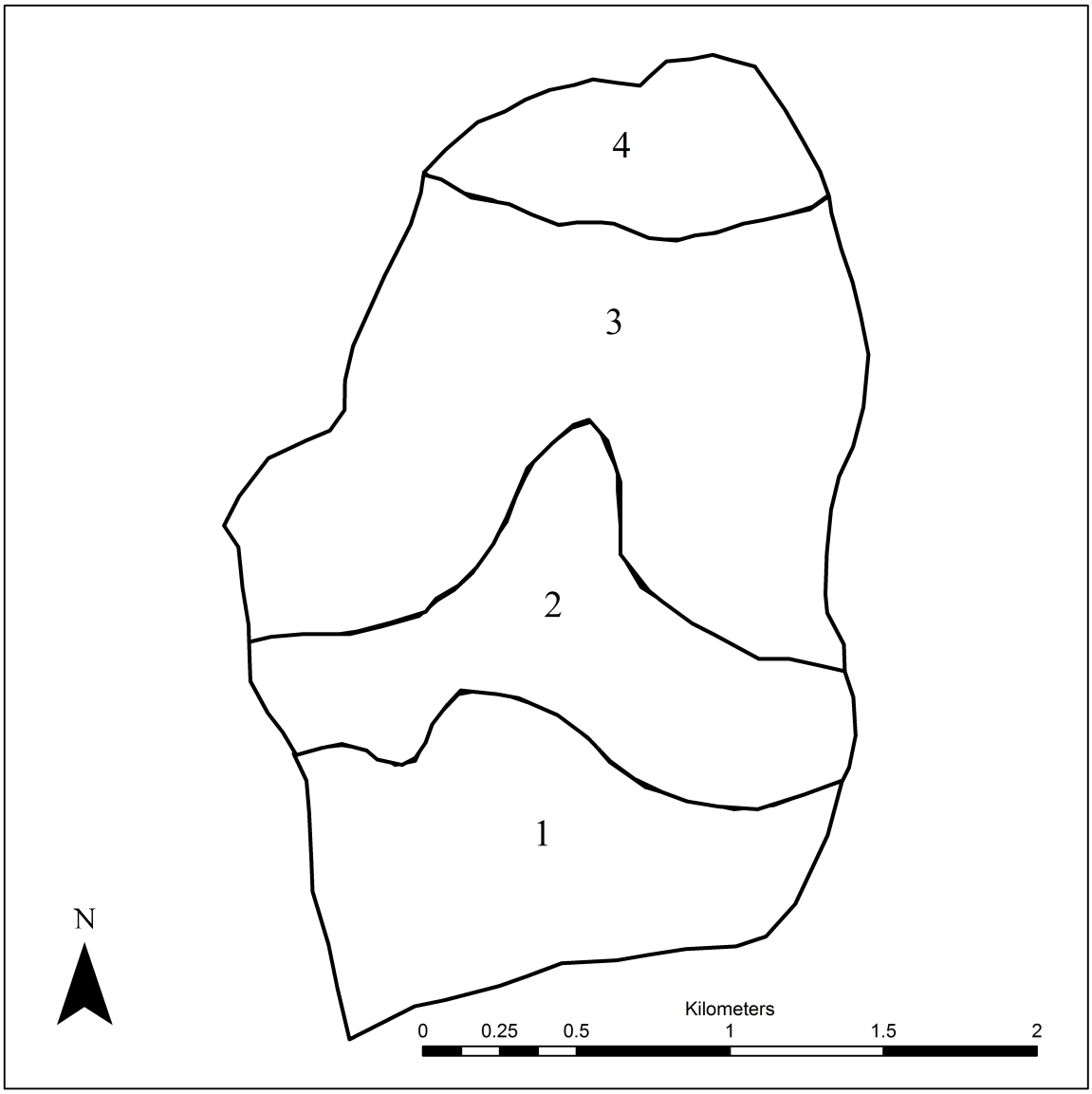

Figure 4.4: Hydrologic response units (HRUs) for 241Cr derived from average slope, aspect, elevation and forest cover characteristics (1 is the lowest elevation while 4 is the highest).

These particular scenarios represent the key disturbances currently affecting forests in western North America (Dale et al., 2001). By comparing the snow accumulation and ablation response of these disturbance types with mature forest and clearcut snow processes, we were able to analyze the hydrological response of increasing disturbance severity: mature forest to MPB to WF and to clearcut.

Given that each disturbance type has a range of severities, the simulated disturbance was selected to represent the most common current disturbance severity. For example, MPB killed trees go through three stages of decline (green, red, grey-attack). Green and red-attack trees have all or most needles remaining in the canopy, whereas grey attack trees have the least LAI as most or all needles have been shed (Winkler et al., in review). Of the three stages, current literature is mostly limited to red-attack.

Wildfire severity can range from minimal, where undergrowth is damaged or removed, to severe, where the undergrowth and canopy are completely removed (Keeley, 2009). This rapid forest disturbance requires many years to regenerate, so hydrological processes are modified for many years. Moderately severe wildfires were selected for this study because the existing literature on post-wildfire forest structure is limited to this severity type.

For each of the two years selected from the baseline run, 241Cr meteorological data were used to parameterize and run CRHM for mature and clearcut forests, as well as for MPB and WF disturbances (Tables 4.8, 4.9). To parameterize CRHM for MPB disturbance, parameters values were drawn from the literature and/or calculated from field data collected at other sites (Table 4.9). As discussed in Section 4.4, all measured values for LAI were collected by the LI-COR LAI-2000 Plant Canopy Analyzer (Gower and Norman, 1991). LAI decreases when forest canopy is disturbed by MPB (R. Winkler, unpub. data), therefore parameter values were set as a percent change to baseline LAI values at 241Cr based on the difference between undisturbed and

beetle-killed canopy at Mayson Lake, British Columbia (R. Winkler, unpub. data), and may not represent actual MPB conditions at 241Cr. However, Mayson Lake is an established study site, is relatively close (approximately 200 km northwest) and has similar forest structure to 241Cr (R. Winkler, unpub. data). No values of *Sbar* exist for disturbed canopies so disturbed values used in this study were calculated as a percent change of disturbed *LAI–Sbar* relative to mature forest*LAI–Sbar*; mature forest LAI was 2.5 and *Sbar* was 6.6, so the post MPB LAI was reduced by 40%, thus *Sbar* was also reduced by 40%). Confidence in derived post-MPB LAI value were high given the close proximity and similar forest structure of Mayson Lake to 241Cr, but confidence in the *Sbar* value is lower as there were no measured values in the literature, and the mass of snow held in the canopy may change in MPB disturbed stands. Litter from MPB killed forests can strongly affect snow surface albedo relative to that in a mature forest or clearcut (Winkler et al., 2010; Boon et al., in review). Winkler et al. (2010) provided values of post-MPB snow albedo, a_{max} and a_{min}; these values were lower than mature forest because of observed litter in the MPB-killed sub-canopy snowpack. Maximum and minimum snow albedo values were adjusted based on the literature to represent these values. Albedo decay time constants for cold (*a1*) and melting (*a2*) snow are not available in the literature. Values defined by Spittlehouse (unpub. data) were used as initial starting points, after which these parameters were used to tune the model and improve model fit while remaining within a reasonable range of values (+/- 1000 s).

Table 4.8: Parameters used for mature and clearcut forest at 241Cr.

Parameter	Mature forest	Clearcut	Referenced in literature or calculated
LAI	2.2		(R. Winkler, unpub. data)
Sbar (kg m^{-2})	6.6		(Schmidt and Gluns, 1991)
a1 (s)	9×10^6	9×10^6	(D. Spittlehouse, unpub. data)
a2 (s)	100,000	1,000	(D. Spittlehouse, unpub. data)
α_{max}	0.84	0.84	(D. Spittlehouse, unpub. data)
α_{min}	0.36	0.72	(D. Spittlehouse, unpub. data)

Table 4.9: Parameters used for mountain pine beetle and wildfire killed forest at 241Cr.

Parameter	Mountain pine beetle	Wildfire	Referenced in literature or calculated
LAI	1.8	0.4	(Burles, 2010; R. Winkler, unpub. data)
Sbar (kg m^{-2})	5.8	2.0	Calculated from (Schmidt and Gluns, 1991)
a1 (s)	9×10^6	9×10^6	(D. Spittlehouse, unpub. data)
a2 (s)	100,000	1,000	(D. Spittlehouse, unpub. data)
α_{max}	0.80	0.84	(Wiscombe and Warren, 1980; Conway et al., 1996; Winkler et al., 2010)
α_{min}	0.35	0.50	(Wiscombe and Warren, 1980; Conway et al., 1996; Winkler et al., 2010; Burles and Boon, 2011)

Wildfire parameter values were also drawn from the literature and/or calculated from field data collected at other sites (Table 4.9). Forest canopy removal following a moderately severe wildfire was represented by modifying *LAI* values based on the measured percent difference in canopy between a mature and burned forest canopy in the Crowsnest Pass, Alberta (Burles, 2010). There is less confidence in the wildfire *LAI* given the distance between study sites (approximately 350 km), and the value is based on fewer measurements and different pre-disturbance forest structure. As with MPB, *Sbar* was set as a percent change of disturbed *LAI*–*Sbar* relative to mature

forest *LAI–Sbar*, assuming that disturbed canopy *Sbar* declines proportionally with *LAI*. Again, similar to MPB, the *Sbar* value may not transfer between study sites, and should be quantified in field studies, so confidence in the value is reduced. Soot from burned forests can also strongly affect snow surface albedo relative to that in a mature forest or clearcut (Rouse, 2009). Minimal data on post-wildfire snow albedo are available, with the exception of anecdotal evidence. Values were therefore calculated from Conway et al. (1996) and Wiscombe and Warren (1980) who found that carbon can reduce snow albedo by up to 30% relative to fresh snow to represent this changed caused by soot. This study assumes uniform reduction of snow albedo throughout the simulation period, but may be subject to temporal and spatial variation. Therefore, confidence in these values is low, thus the amount and timing of soot that falls from the trees should be measured in future field studies.

Based on the baseline run results, two years were selected for this study: 2002 and 2007. These years had the best model fit for mature forest, which is the most important given we adjusted mature forest to represent forest disturbances. Selecting years based on model fit in clearcut conditions was less important because the model represented clearcut conditions well in all years.

For each year, four disturbance types were simulated: 1) mature undisturbed, 2) red attack mountain pine beetle, 3) moderately severe wildfire, and 4) clearcut. For each year and each disturbance type, the watershed was incrementally disturbed from the least to greatest elevational extent (lowest elevation HRU (1) to the highest (4)) (Table 4.7). Thus for the first run, the lowest elevation HRU was represented as a disturbed forest while the three higher HRUs remained undisturbed mature forest. Next, the lowest and mid-low HRUs were disturbed while the mid-high and high HRUs remained undisturbed mature forest. Then the low, mid-low and mid-high HRUs (1 to 3) were disturbed while the highest remained a mature undisturbed forest, and finally all HRUs were simulated as disturbed. By incrementally disturbing

the watershed from low to high HRUs, there may be a threshold at which disturbance greatly changes SWE. Additionally, dividing the watershed into HRUs allows us to test the hydrologic response of individual HRUs to forest disturbance.

4.8 Analysis of Model Output

The following variables were calculated from the ouput from each scenario in each year: maximum amount of SWE (mm), date of maximum SWE (days since January 1), date of 0 SWE (date of complete snowpack removal; days since 1 January), average ablation rate (mm d^{-1}), and duration of ablation period (number of days between date of maximum SWE and date of 0 SWE). To quantify differences between scenarios, the following metrics were calculated: percent change in maximum SWE, differences in timing of maximum SWE and total SWE removal, average rates of SWE accumulation and ablation, and ratio of scenario to clearcut SWE. The accumulation of SWE in clearcuts is the theoretical maximum of SWE, thus the ratio of scenario to clearcut SWE to forested SWE allows for comparison of scenarios to the porportion of snow lost to interception and/or sublimation. In most cases, the disturbance response was compared to the undisturbed forest baseline. However, some standard metrics are used in the literature that compare forested with clearcut sites, so these metrics were used to allow for comparison with these other studies. To determine the total amount of SWE at the watershed scale in response to forest forest disturbance, the peak SWE for each combination of elevational extent forest disturbance was multiplied by the percent of total watershed area, and summed.

Chapter 5

Sensitivity Analyses and Model Performance

5.1 Introduction

This chapter presents and discusses the results of the sensitivity analyses and model performance tests to assess potential model uncertainties. The objectives of this chapter are to: 1) define and discuss model sensitivity to parameters outlined in Chapter 4; and 2) quantify model performance in the two forest types for which field data are available at the 241 Creek, and discuss the results.

5.2 Sensitivity Analysis

Sensitivity tests were conducted from 1 October 2000 to 1 July 2001. Results from the following sensitivity analyses were compared to the length of the measured accumulation and ablation periods, and peak snow water equivalent (SWE) for mature forest (MF) and clearcut (CC) in 2001: accumulation period of 160 days for both MF and CC; 75 and 45 ablation days for MF and CC, respectively; and 217 mm and 284 mm of peak SWE for MF and CC, respectively.

5.2.1 Albedo Decay Time Constant for Cold Snow

SWE accumulation rates under mature forest conditions were relatively insensitive to changes in albedo decay time constant for cold snow (*a1*) (Fig. 5.1). The accumulation rate increased by only 0.2 mm d^{-1} from the lowest to the highest rate across the range of *a1* values. A change in 0.2 mm d^{-1} was equivalent to 25.6 mm over the entire accumulation period, or 11.8% of peak SWE. The ablation rate was slightly more sensitive with a decrease of 0.8 mm d^{-1}, but only beyond a threshold value of $a1 > 9.0 \times 10^6$ s. An ablation rate change of 0.8 mm d^{-1} was equivalent to 60.0 mm (27.6% of peak SWE) over the entire ablation period. The increase in ablation rate is likely due to the importance of albedo in snow ablation, and its limited effect on

snow accumulation (Wiscombe and Warren, 1980; Veatch et al., 2009; Winkler et al., in review).

The SWE accumulation rate under clearcut conditions was relatively insensitive to changes in *a1*, as the rate increased by only 0.2 mm d^{-1} when *a1* was changed from 1.0×10^7 to 1.0×10^8 s (Fig. 5.1). This was equivalent to 32.0 mm over the accumulation period, or 11.2% of peak SWE. The SWE ablation rate was more sensitive, with a decrease of 1.5 mm d^{-1} with $a1 = 1.0\times10^7 - 1.0\times10^8$ s (Fig. 5.1). This was equivalent to 67.5 mm over the entire ablation period, or 23.8% of peak SWE. The ablation rate was greater at higher values of *a1* due to the concurrent increase in accumulation rate, which resulted in a later date of peak SWE, and subsequently shorter ablation period.

5.2.2 Albedo Decay Time Constant for Melting Snow

SWE accumulation rates under mature forest conditions were relatively insensitive to changes in albedo decay time constant for melting snow (*a2*), as the rate decreased by only 0.3 mm d^{-1} between $a2 = 1.0 \times 10^6$ and 1.0×10^7 s (Fig. 5.2). This was equivalent to 48 mm over the entire accumulation period, or 22.1% of peak SWE. The rate decreased because the date of peak SWE occurred 25 days later than in the first five iterations. SWE ablation rate was more sensitive to *a2*, particularly at $a2 = 1.0 \times 10^7$ s, where it increased from 6.5 mm d^{-1} to a maximum of 11.0 mm d^{-1} (Fig. 5.2). This 4.5 mm d^{-1} change was equivalent to 337.5 mm over the entire ablation period, or 155.5% of peak SWE. The ablation rate was greater at higher values of *a2* because the decreased rate of accumulation resulted in a later date of peak SWE, and subsequently shorter ablation period. Compared with *a1*, higher values of *a2* had more effect on snow ablation rate because the snow was likely warm during the ablation period, so a change in *a1* only affected time periods when snow is not melting. Thus *a2* applies over a longer time period that incorporated the entire melt season.

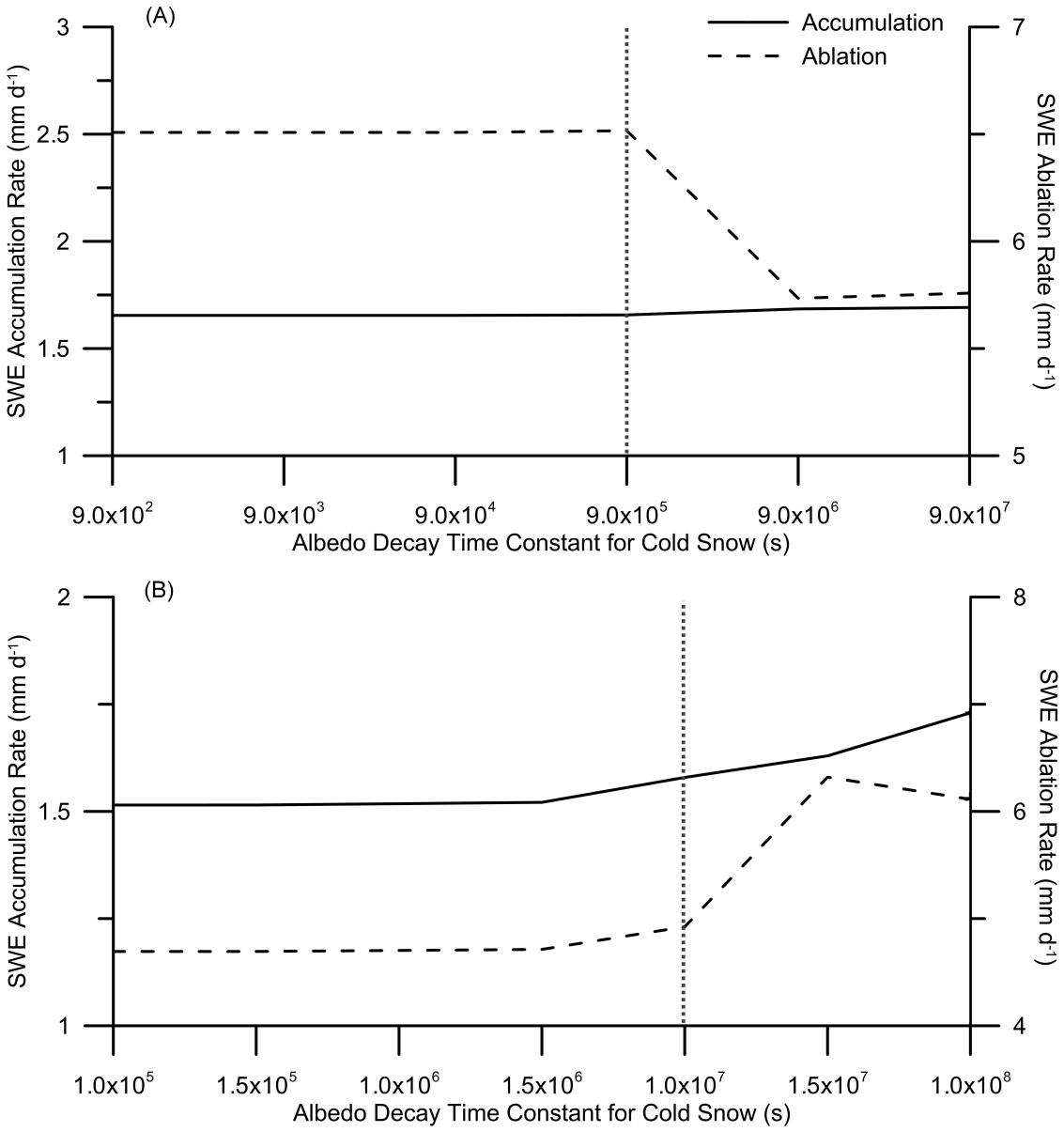

Figure 5.1: Sensitivity results for albedo decay time constant for cold snow (s) with (A) mature forest and (B) clearcut conditions. The solid line represents snow water equivalent (SWE) accumulation rate (mm d^{-1}), the dashed line represents snow ablation rate (mm d^{-1}), and the dotted vertical line represents the value used for simulations. Note that the figure axes are not standardized.

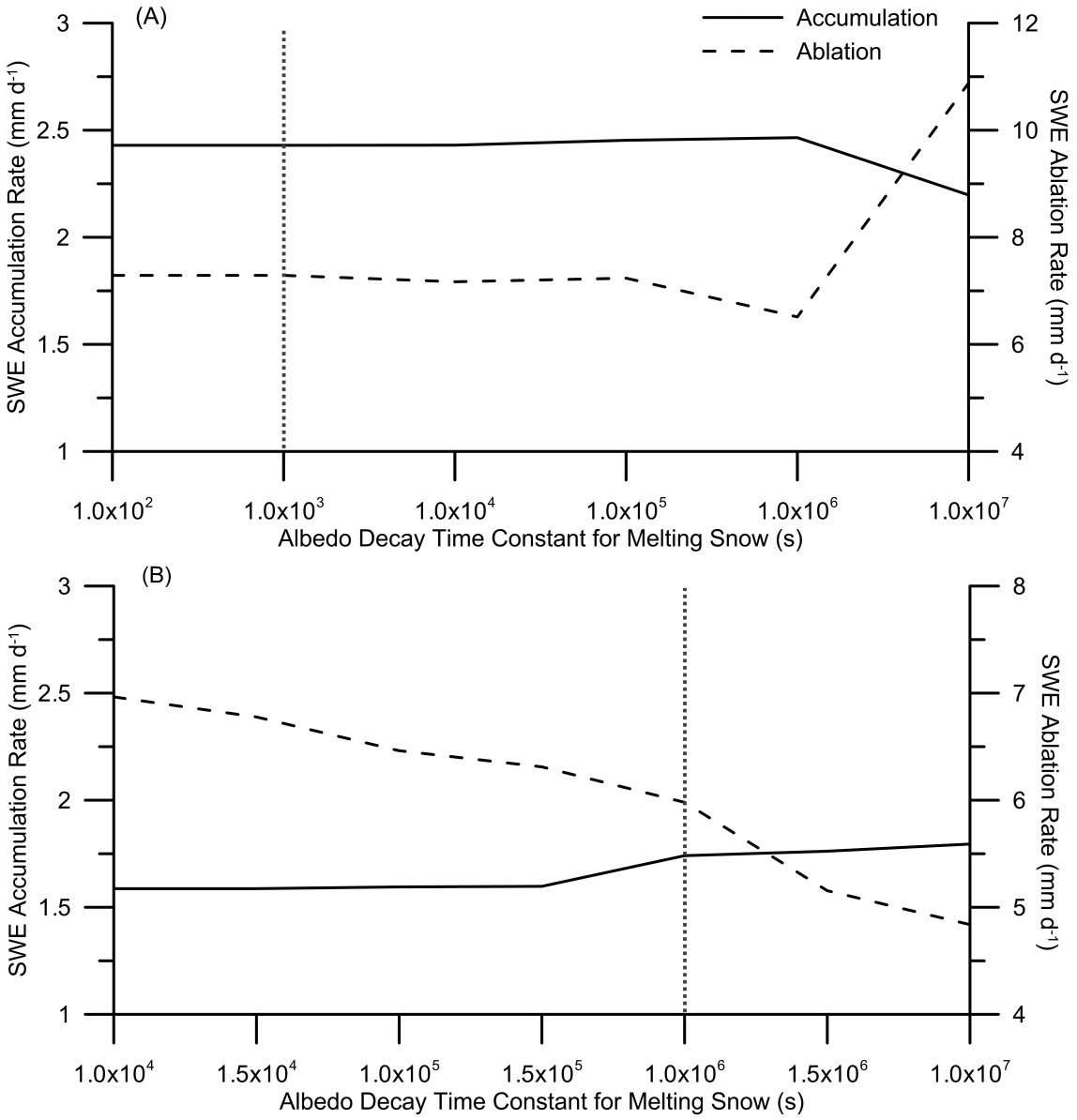

Figure 5.2: Sensitivity results for albedo decay time constant for melting snow (s) with (A) mature forest and (B) clearcut conditions. The solid line represents snow water equivalent (SWE) accumulation rate (mm d^{-1}), the dashed line represents snow ablation rate (mm d^{-1}), and the dotted vertical line represents the value used for simulations. Note that the figure axes are not standardized.

SWE accumulation rates were also relatively insensitive to *a2* in clearcut conditions as there was only a difference of 0.3 mm d^{-1} between the lowest to highest rate across the range of *a2* values (Fig. 5.2). This change was 48.0 mm over the accumulation period, or 16.9% of peak SWE. The SWE ablation rate was more sensitive throughout the entire range of *a2* values, where the greatest increase in ablation rate (2.2 mm d^{-1}) occurred within the range of $a2 = 1.0 \times 10^6$ – 1.0×10^7 s (Fig. 5.2). A change in 2.2 mm d^{-1} represents 99.0 mm over the entire ablation period, or 34.9% of peak SWE. Snow albedo decays at an exponential rate during the ablation period, so increasing *a2* subsequently reduced the ablation rate. Results were similar to studies that indicate ablation rates were more sensitive to snow albedo in areas without canopy cover than in sub-canopy snowpacks (Wiscombe and Warren, 1980; Colbeck, 1988; Blöschl et al., 1991).

5.2.3 Maximum Albedo for Fresh Snow

SWE accumulation and ablation rates in the mature forest were insensitive to iterative change in the values for maximum albedo for fresh snow (a_{max}) used in this test (Fig. 5.3). In theory, the accumulation rate should show little response to change in a_{max} because albedo is less important for snow accumulation than for snow ablation. Therefore, the ablation rate would be more likely to change with a_{max}: as a_{max} increases, the ablation rate should decrease. As expected, the accumulation rate was not affected by a_{max}; however, the ablation rate was also not affected. This was likely due to the speed at which fresh snow albedo decays. During the ablation season, precipitation events do not fully reset the albedo to a_{max}, and since the decay rate was exponential during the ablation period, new snow is rapidly converted to old snow (US Army Corps of Engineers, 1956).

SWE accumulation rates under clearcut conditions were much more sensitive to changes in a_{max} than in the mature forest (Fig. 5.2). Across the range of a_{max} values

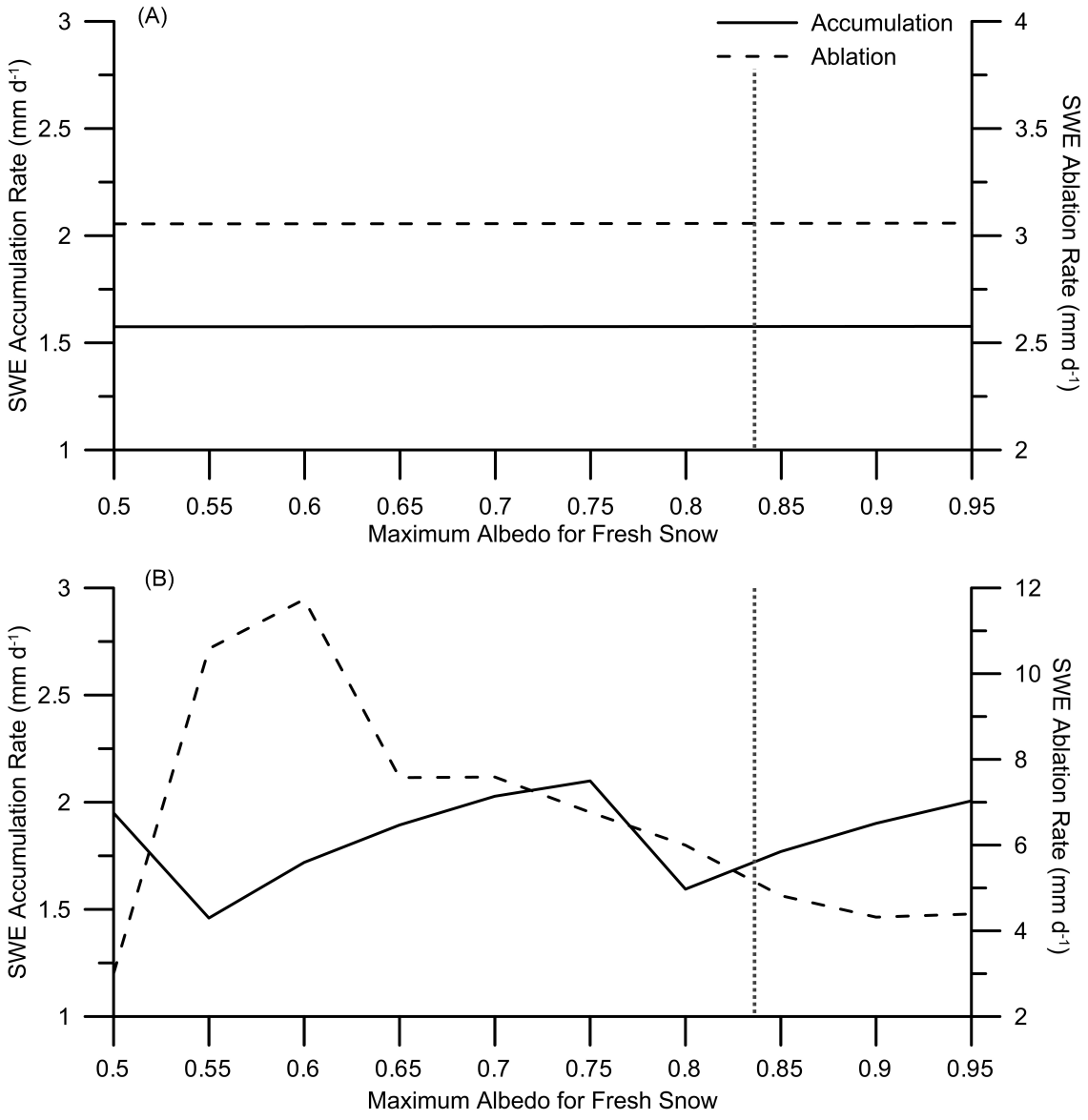

Figure 5.3: Sensitivity results for maximum albedo for fresh snow with (A) mature forest and (B) clearcut conditions. The solid line represents snow water equivalent (SWE) accumulation rate (mm d^{-1}), the dashed line represents snow ablation rate (mm d^{-1}), and the dotted vertical line represents the value used for simulations. Note that the figure axes are not standardized.

between 0.5 – 0.95, the accumulation rate increased by approximately 0.8 mm d^{-1} (Fig. 5.3). This was equivalent to 128.0 mm over the entire accumulation period, or 45.1% of peak SWE. At $a_{max} > 0.8$, the rate of accumulation declined and then increased relative toa_{max} values between 0.55 – 0.75. Ablation rates were very sensitive to changes in a_{max} as evidenced by a decrease of 9.0 mm d^{-1} from the lowest to highest rate across the range of a_{max} values (Fig. 5.3). This was equivalent to approximately 405.0 mm over the entire accumulation period, or 142.6% of peak SWE. The rate of snow ablation was faster in the lower values of a_{max} because the date of peak SWE and date of complete snowpack removal occurred earlier than highest a_{max} values. The lower a_{max} values also permit more radiation to be absorbed by the snow pack, therefore increasing the rate of ablation.

5.2.4 Minimum Albedo for Aged Snow

SWE accumulation rates under mature forest conditions were relatively insensitive to incremental change to the minimum albedo for aged snow (a_{min}), with a decrease of only 0.3 mm d^{-1} at the highest a_{min} value (Fig. 5.4). This was equivalent to 48.0 mm over the entire accumulation period, or 22.1% of peak SWE. SWE ablation rate was more sensitive (increase of 4.5 mm d^{-1}) but only beyond a threshold value (a_{min} = 0.7) (Fig. 5.4). A 4.5 mm d^{-1} change was equivalent to 337.5 mm over the entire ablation period or 155.5% of peak SWE. Since peak SWE occurred later in the year at the highest value of a_{min}, but the date of 0 SWE remained constant, the ablation rate increased.

Under clearcut conditions, SWE accumulation rates were sensitive to a_{min} as there was an increase of 0.7 mm d^{-1} but only beyond the threshold value of $a_{min} = 0.4$ (Fig. 5.4). A change of 0.7 mm d^{-1} was equivalent to 112.0 mm over the entire accumulation period or 0.39% of peak SWE. The decrease in accumulation rate was the result of a peak SWE threshold: at $\alpha_{min} = 0.5$, both peak SWE and the date of

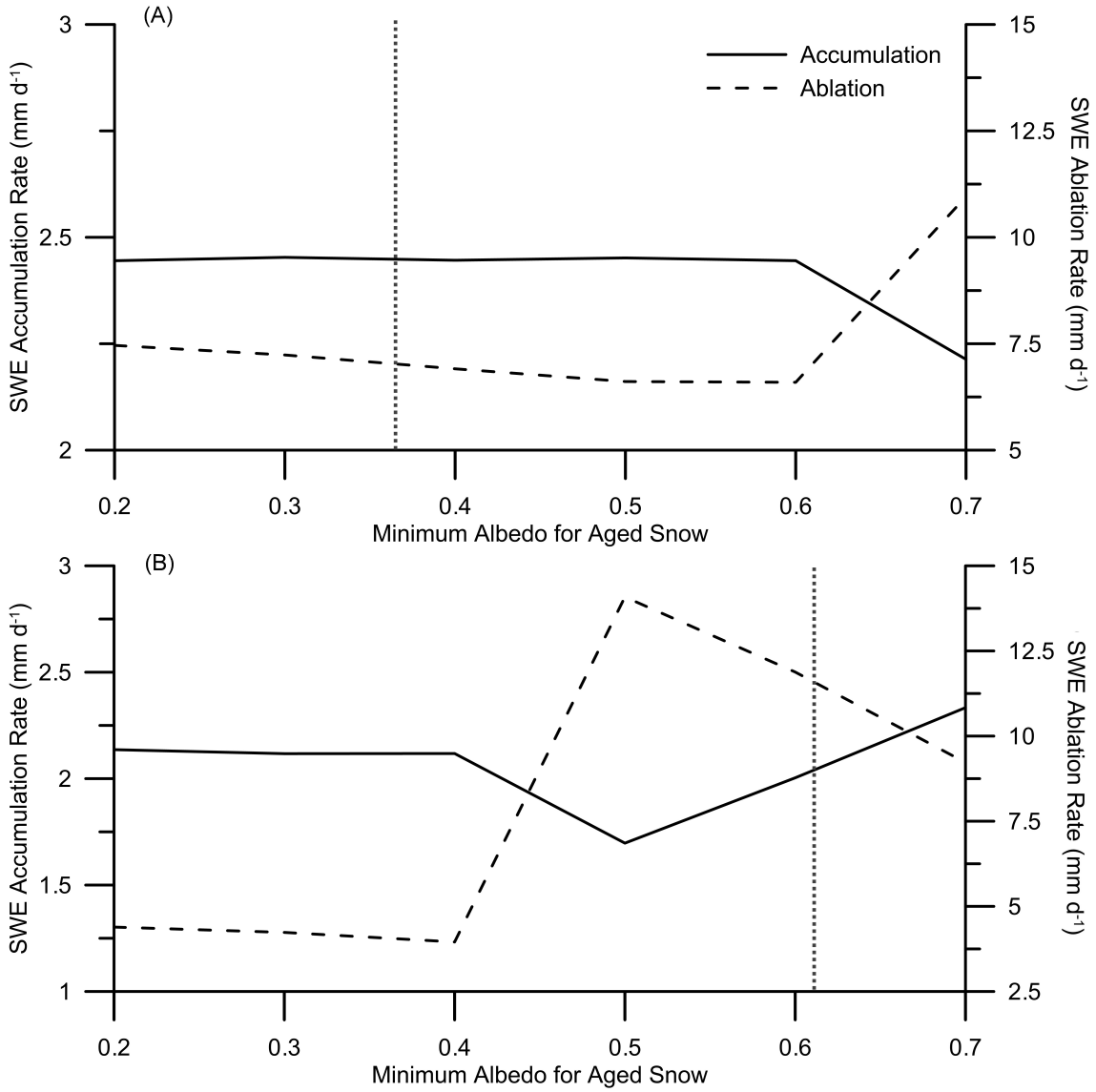

Figure 5.4: Sensitivity results for minimum albedo for aged snow with (A) mature forest and (B) clearcut conditions. The solid line represents snow water equivalent (SWE) accumulation rate (mm d^{-1}), the dashed line represents snow ablation rate (mm d^{-1}), and the dotted vertical line represents the value used for simulations. Note that the figure axes are not standardized.

peak SWE increased, thus the rate of accumulation decreased. Peak SWE increased between $a_{min} = 0.5 - 0.7$, subsequently the rate of accumulation also increased. The SWE ablation rate were much more sensitive where the greatest increase (almost 9.0 mm d^{-1}) occurred at $a_{min} = 0.5$ (Fig. 5.4). This was equivalent to 405.0 mm over the entire ablation period or 142.6% of peak SWE. At $a_{min} = 0.5$, a threshold exists where peak SWE occurred later in the year, which decreases the rate of accumulation and increases the rate of melt.

5.2.5 Maximum Intercepted Canopy Snow Load

SWE accumulation rates were moderately sensitive to changes in the maximum intercepted snow load (*Sbar*) as there was a decrease of only 0.5 mm d^{-1} from the lowest to highest rate across the range of *Sbar* values (Fig. 5.5). This was equivalent to ∼80.0 mm over the entire accumulation period, or 36.9% of peak SWE. This decrease was caused by an increase in the mass of snow held within the canopy so less snow was able to accumulate on the ground. SWE ablation rates were relatively insensitive to changes in *Sbar* as the rate decreased only 0.5 mm d^{-1} throughout the range of values for *Sbar* = 1 – 4 kg m^{-2}. A change of 0.5 mm d^{-1} was equivalent to 37.5 mm over the entire ablation period, or 17.3% of peak SWE. The snow ablation rate decreased throughout the first four iterations of *Sbar* because less snow reached the ground and the date on which snowpack was completely removed remained constant. At *Sbar* values = 4 kg m^{-2}, ablation rates remain relatively unchanged. Sensitivity analyses were run during a low snow year, thus the mass of snow in the canopy was lower than the maximum retained by increasing *Sbar* values.

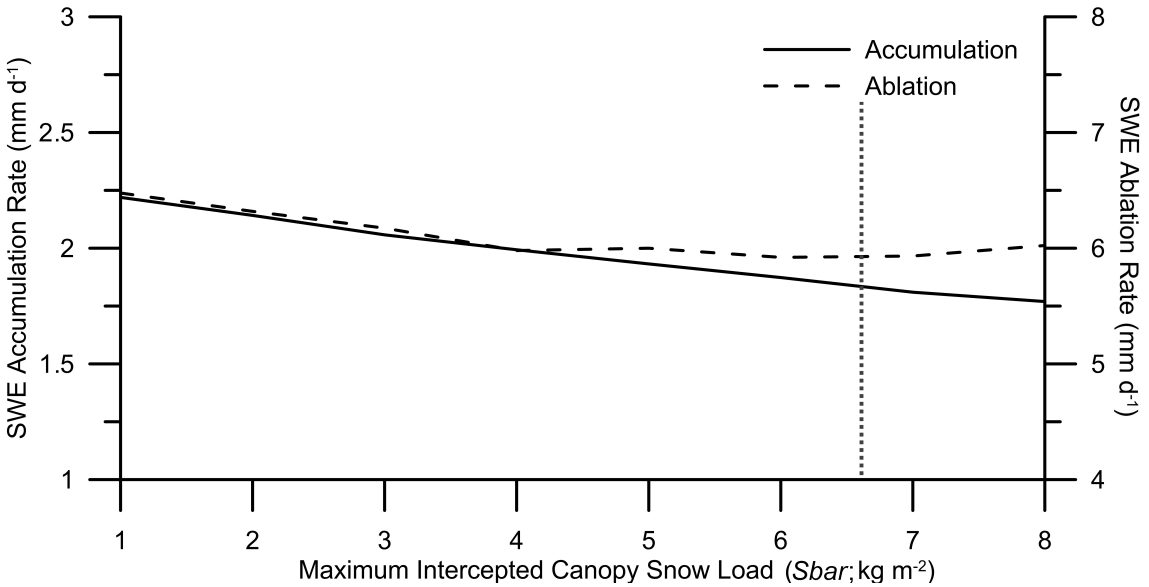

Figure 5.5: Sensitivity results for maximum intercepted canopy snow load (kg m^{-2}) with mature forest conditions. The solid line represents SWE accumulation rate (mm d^{-1}), the dashed line represents snow ablation rate (mm d^{-1}), and the dotted vertical line represents the value used for simulations.

5.2.6 Leaf Area Index

SWE accumulation rates were very sensitive to changes in the leaf area index (LAI), with a decrease of 1.3 mm d^{-1} from the lowest to highest rate across the range of LAI values used in the test (Fig. 5.6). This represents a cumulative effect of 208.0 mm over the entire accumulation period, or 95.9% of peak SWE. The increase in SWE accumulation rate between $LAI = 0.25$ – 1 occurred because peak SWE occurred up to two months earlier than peak SWE simulated at $LAI > 1.25$; therefore, there were fewer days between the first day of continuous snow cover and peak SWE. In theory, the rate of accumulation should decrease with an increase in LAI because ground snow accumulation occurred more rapidly and reaches higher peaks with reduced forest cover (Stanton, 1966; Toews and Gluns, 1986). The increase in accumulation from $LAI = 0.25$ – 1 suggests that mass and energy balance equations within CRHM were overly sensitive to low LAI input values. The stepped response in accumulation rate at higher LAI values (1.5 – 2) resulted from a slight increase in the amount

of peak SWE relative to lower LAI values and consequently increased the rate of accumulation.

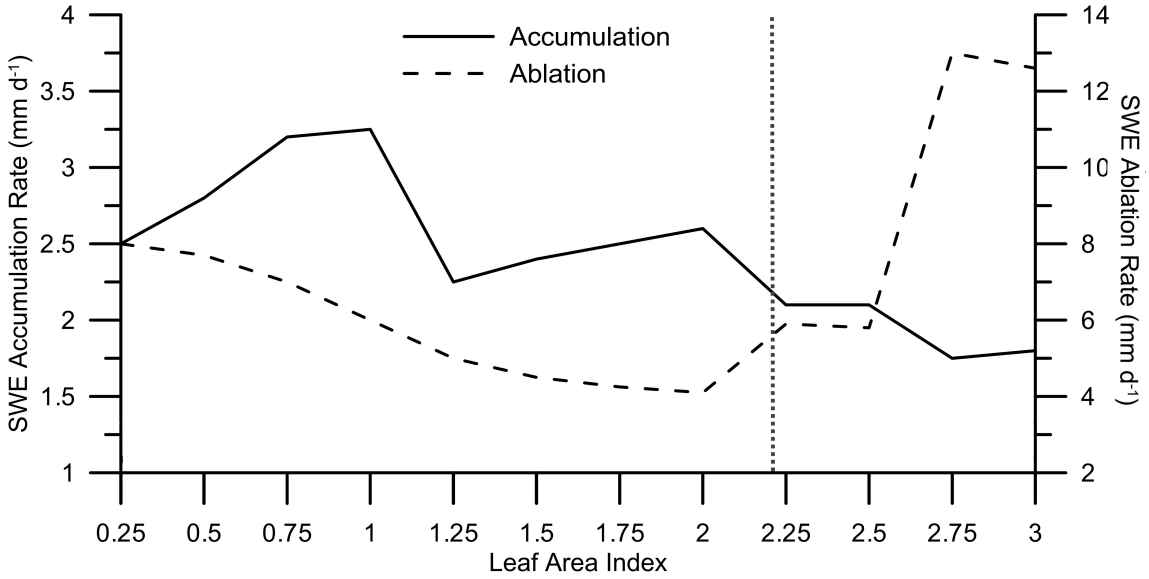

Figure 5.6: Sensitivity results for leaf area index (LAI) with mature forest conditions. The solid line represents SWE accumulation rate (mm d^{-1}), the dashed line represents snow ablation rate (mm d^{-1}), and the dotted vertical line represents the value used for simulations.

SWE ablation rates were also very sensitive to changes in LAI as evidenced by the increase of nearly 9.0 mm d^{-1} from the lowest to highest rate across the range of LAI values (Fig. 5.6). This was equivalent to 675.0 mm over the entire ablation period, or 311.1% of peak SWE. In the $LAI = 0.25 - 2$ range, the snow ablation rate decreased steadily: as LAI increased, less incoming shortwave radiation was able to penetrate the canopy, thus less energy was available for ablation. At LAI in the 2 – 3 range, however, the snow ablation rate response was most sensitive, which suggests that there may be an error internal to the model. It is likely that the increase in LAI in this range reduced both sub-canopy accumulation and radiation transmission to the snow surface. Subsequently, the thin snowpack was likely protected by the canopy until a threshold was passed where a slight increase in radiation and/or air temperature late in the melt season was able to remove the thin snowpack.

5.2.7 Discussion

Under mature forest conditions, modelled accumulation rates were most sensitive to *Sbar* and *LAI*, and least sensitive to *a1*, *a2*, and a_{max}. Ablation rates were most sensitive to *a1*, *a2*, *amin*, and *LAI*, and least sensitive to a_{max}, and *Sbar*. Under clearcut conditions, accumulation rates were most sensitive to *a1*, a_{max}, and a_{min}, and least sensitive to *a2*. Ablation rates were sensitive to *a1*, *a2*, a_{max}, and a_{min}.

Given the variable response to parameter values in both forest types, it was important to carefully select parameter sets for each forest condition. Accurate values of *LAI* are fundamental for simulating accumulation and melt given the importance of canopy for interception and radiation transmission, so measured and/or literature-derived values were used to ensure they were appropriate. Values for a_{max} and a_{min} were also initially selected from 241Cr field data, then modified within the range of measured values to improve model fit (Spittlehouse, unpub. data). Values for the disturbance types were selected from Mayson Lake field data and the literature (Winkler, unpub. data).

Values of a_{max} and a_{min}, and *LAI* were based on field measurements so confidence in their selection was high. The value of *Sbar* for the MF was derived from experimental measurements collected by Schmidt and Gluns (1991) who calculated a value of 6.6 kg m^{-2} for mature pine trees with an *LAI* of 2.5. No values of *Sbar* exist for disturbed canopies, thus disturbed values used in this study were calculated as a percent change of the disturbed *LAI-Sbar* ratio relative to the mature forest *LAI-Sbar* ratio. While this not scale directly with reduction in forest canopy following disturbance, it represents a first approximation of shifts in *Sbar* in relation to post-disturbance canopy change (Schmidt and Pomeroy, 1990; Schmidt, 1991; Pomeroy and Schmidt, 1993; Pomeroy et al., 1998b). No specific values of *a1* and *a2* exist in the literature, so values were used as tuning parameters.

The large increase in SWE ablation rate under the three highest *LAI* values was

most likely the result of reduced radiation penetration through the canopy, which extended snowcover period until later in the year when high solar angle and air temperatures rapidly ablated the snow. The model may have been developed for a certain range of values and produces erroneous output past a threshold; however, the *LAI* values selected for this study were not within the range that resulted in rapid SWE ablation.

The reduction in *LAI* permitted an increase in both the amount of sub-canopy accumulation, because there was less canopy available for interception of snow, and the amount of incoming radiation as a result of greater sky view factor due to reduced forest density.

SWE accumulation and ablation rates were sensitive to iterative changes in *LAI* parameter values. This parameter was a key factor in representing the forest canopy in this study, and together with *Sbar*, is the most altered between the CC and MF. Results from the baseline indicate that without forest canopy representation, the model was able to simulate measured values well, but presence of canopy as represented by *LAI* and *Sbar* parameter values decreased goodness of fit. The selected values were kept constant throughout model runs, so this indicates that there may be an internal model issue decreasing the ability of the model to simulate measured values. CRHM is known to oversimulate the energy available for ablation when snowfall is both above and below average, but the energy available for ablation is not the only factor changing the amount of SWE. For example, since the storage and unloading of snow in and from the canopy can play an important role in the amount of accumulation and the timing of ablation, the model incorporates these considerations.

LAI includes the trunks, branches, stems, needles, and any other surface that may retain snow. While the stems are more rigid than the needles, they are spaced far apart from each other so there is less opportunity for bridging. This bridging of snow is essential for development of snow clumps. The density of snowfall will

also govern the development of snow clumping in the forest canopy, and is more likely to develop into clumps with greater snow density. Given the methodology and results from the sensitivity test, where iterative change to one parameter value likely also requires a change in another parameter in order to maintain the appropriate representaiton of physical processes (e.g., *LAI* and *Sbar*). In such cases, the model output may be affected by the failure to change additional values, which then has cascading effects throughout the simulation. One example could include interception and unloading occurring too often or not frequently enough. Another possibility is that the interception surface for snow is not properly defined when values of *LAI* are low (0 – 1.5), which may result in miscalculation of intercepted and throughfall snow. Further investigation of the relationship between *LAI* and *Sbar* within the model should be considered in future studies. Also, while model sensitivity analyses indicated potential sources of uncertainty and model errors, future studies may benefit from applying sensitivity tests to multiple years to better understand model response to a range of meteorological conditions.

The year 2001 was selected for these tests as it was a dry year with the lowest average SWE (25.3% lower), and should be most sensitive to parameter value changes. Further studies may find it useful to perform sensitivity tests on all years to analyze the response to a range of conditions, and average selected values for model runs.

5.3 Model Performance

The selected model fit methods are used commonly in the literature and provide robust analysis of model fit (Rutter et al., 2009). The highest emphasis was placed on R^2 and RMSE when selecting the best fit years because these are commonly used methods in snow modelling studies (Pomeroy et al., 2012; Singh and Woolhiser, 2002).

Model fit over the nine year period was moderate under mature forest conditions. From 1 October 1999 – 1 July 2008, mean hourly SWE was over-simulated (Fig. 5.7;

Table 5.1). High RMSE and mean error values indicated a large predictive error. The average coefficient of determination for all years shows that the simulation explained 29.0% of the variance in the measured data, while a positive y-intercept suggests that simulated SWE was higher than measured SWE for most years. A low slope value suggested modelled values increased at a slower rate than observed values.

The clearcut simulation showed excellent fit over the nine year simulation period, given the absence of complicating factors from forest canopy (Fig. 5.7; Table 5.1). Mean hourly SWE was slightly under-simulated, while RMSE and mean error values indicated a small predictive error. The average coefficient of determination for all clearcut years shows that the simulation explained over 79.0% of the variance in the measured data. A low y-intercept value suggested a slight oversimulation of SWE for most years, while a slope value of close to unity indicated that modelled values increased at a very similar rate to observed values.

High inter-annual variability of model fit in mature forest conditions was an indicator of difficulties associated with modelling snow processes in forests, as evidenced by the low inter-annual variability in model fit under clearcut conditions. Simulation under mature forest conditions add complexity due to the interaction between canopy and incoming precipitation, and the role of the canopy in attenuating meteorological conditions. In this study, parameters were kept constant throughout the baseline runs but the inputs changed annually. The model should be able to generate acceptable model fit in all years regardless of interannual variability in meteorological changes. Results from the MF baseline suggest that model limitations in the representation of canopy, interception and radiation transmission properties are unable to account for inter-annual differences in the magnitude and timing of precipitation events, precipitation phase, and meteorological conditions. Thus, model fit under mature forest conditions may be improved through annual adjustment of model parameters.

Regeneration of trees in the clearcut may reduce the model fit between measured

Table 5.1: Comparison of goodness of fit statistics for observed (Upper Penticton Creek snow surveys; 2000-2008) versus simulated snow water equivalent (SWE) in a clearcut and mature forest.

	Clearcut	Mature forest
No. of values	66	66
Mean of observed SWE (mm)	182.4	198.8
Mean of simulated SWE (mm)	182.3	252.8
% difference between observed and simulated mean SWE	-1%	27%
Standard deviation of observed SWE (mm)	115.4	77.0
Standard deviation of simulated SWE (mm)	119.3	57.3
RMSE (mm)	55.7	85.1
Mean error (mm)	0.1	-53.2
Coefficient of determination (R^2)	0.79	0.29
Regression coefficient (slope)	0.9	0.4
Regression intercept (mm)	15.3	173.2

and modelled SWE, but there was no consistent decline in fit from the beginning to the end of the model period, which suggests that regeneration has no effect.

Evaluation of model performance for individual years in both MF and CC indicated that the model fit was poorest in 2001 and 2006 (Fig. 5.8). In MF, 2001 had a high RMSE (130.8 mm), a large negative mean error (-124.4 mm), and low R^2 value (0.5), while 2006 had a moderate mean error (61.7 mm), low R^2 value (0.5), low slope of the regression line (0.4), and a high y-intercept (215.2). In CC, 2001 had a high RMSE (109.0 mm), a large negative mean error (-106.3 mm), while 2006 had a moderate mean error (18.1 mm), and the slope of the regression line was close to unity (1.01).

The poor model fit in 2001 was partially a function of the annual snowfall amount. Average SWE for 2001 was 25.3% lower than average annual (2000-2008) SWE. A previous CRHM study found that the poorest model fit occurred at sites where accumulation was substantially lower than other sites, and was likely the result of shallower snowpack increasing the sensitivity of simulation to errors in mass and energy balance calculations (Ellis, 2011). The poor model fit in 2006 was likely a function of late-

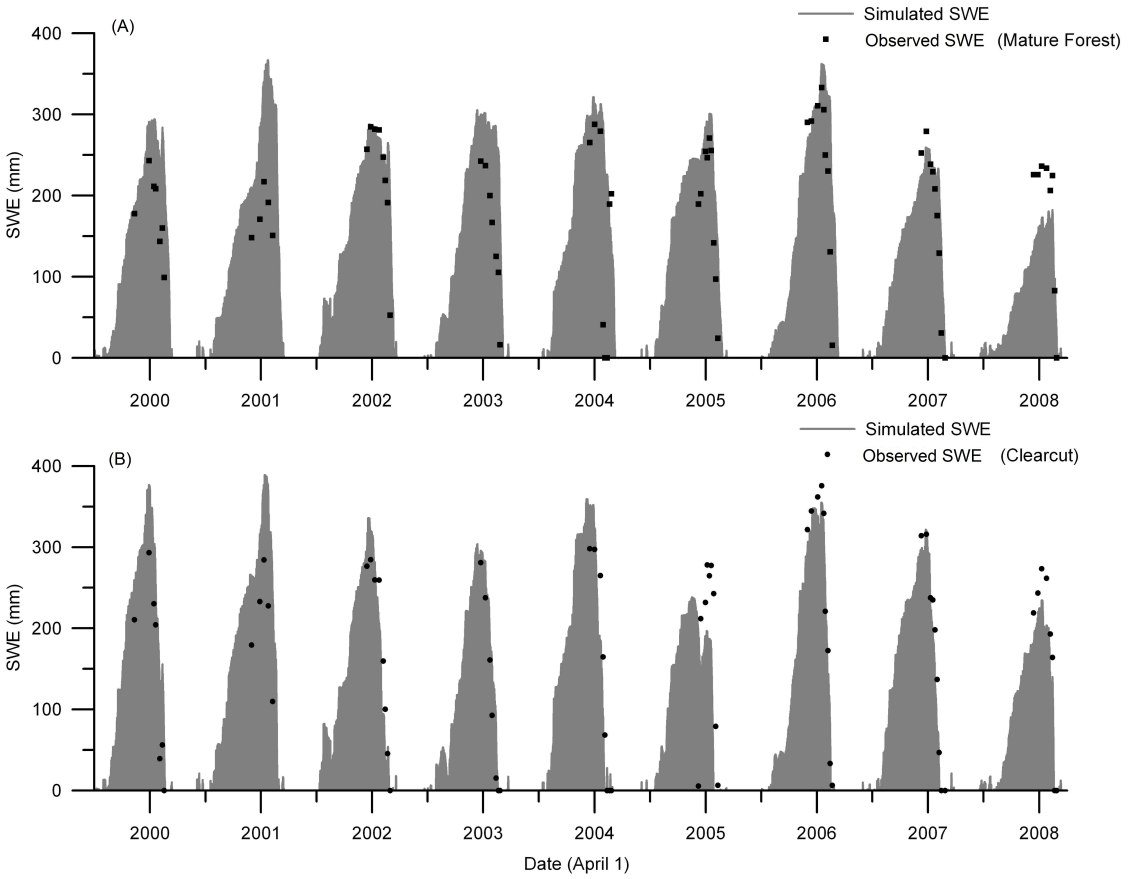

Figure 5.7: Modelled hourly snow water equivalent (SWE; mm) and measured average daily SWE from 1 October 1999 to 1 July 2008 under (A) mature forest and (B) clearcut conditions.

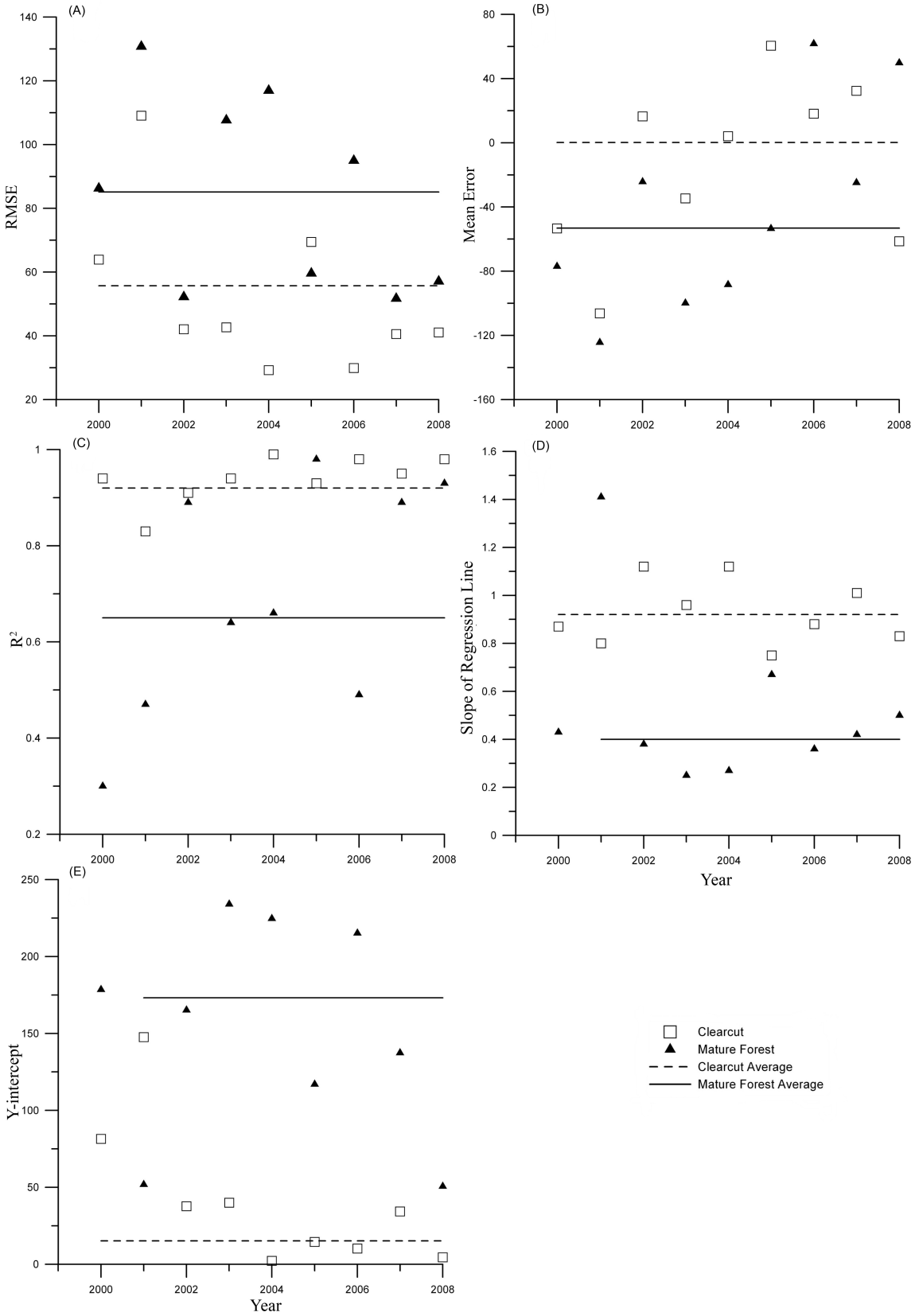

Figure 5.8: Yearly and average (A) RMSE, (B) mean error, (C) R^2, (D) y-intercept, and (E) slope of regression line for mature forest and clearcut conditions.

season snowfalls. Another CRHM study suggested that late-season SWE simulations are poor and likely result in a lag in simulated melt rates (Ellis et al., 2010). In 2006, late snowfalls pushed the date of complete snowpack removal to late May, approximately two weeks later than the average (2000-2008) date; this may have resulted in overestimation of energy available to melt the snowpack (Ellis, 2011).

Model fit was best in 2002 and 2007 (Fig. 5.8), as the baseline parameter values did a good job of representing MF. For 2002, the good model fit was evidenced by low RMSE (52.2 mm) and mean error (-24.3 mm), and high R^2 values (0.9). For 2002 under CC, model fit was good as indicated by low RMSE (42.1 mm) and mean error (16.4 mm), and high R^2 values (0.9). For 2007, MF model fit was good according to low RMSE (51.7 mm) and mean error (-24.8 mm), and high R^2 value (0.9). The 2007 CC model fit was also good: low RMSE (40.6 mm) and mean error (32.3 mm), and high R^2 value (0.9).

Since this study focused on modifying forest canopy parameters to represent forest disturbance, simulation years were selected primarily on the best model fit for MF. While good model fit was also required for clearcut conditions, fit was much less variable between years than in MF, and the model well represented snow in most years. Thus 2002 and 2007 represent the best model fit for both MF and CC.

5.4 Conclusion

Results from sensitivity analyses of model parameter values emphasize the importance of parameter selection to represent mature forest and clearcut conditions. Additionally, this chapter highlights model performance in mature forest and clearcut conditions, and underscores the challenges inherent in modelling different forest canopy types and years. Although the model was unable to simulate mature forest and clearcut conditions well in all years of the baseline run, overall CRHM was able to represent these conditions well in multiple individual years.

Chapter 6

Snowcover Response to Forest Disturbance

6.1 Meteorological Conditions

Of the precipitation that fell between 1 October and 1 July during 2002 and 2007 (480 and 551 mm), rain accounted for a small percentage (18% and 25%, respectively) (Table 6.1) of the total precipitation so the remainder of this chapter will focus on snowfall events. Snowfall events were on average larger and more frequent in 2007 than 2002. In 2007, large snowfall events (>10 mm) occurred in late November, mid-December, late May and throughout June. However, the largest individual snowfall event occurred in 2002 (28.0 mm), even though 2002 snowfall events were on average smaller than in 2007. A slightly higher standard deviation of precipitation event size in 2007 indicates greater variability in event size than in 2002.

Measured maximum snow water equivalent (SWE) was greater in the clearcut (CC) (284 and 316 mm) than mature forest (MF) (284 and 279) in both 2002 and 2007 (Table 6.2). More snow fell in 2007 than 2002, but maximum SWE was 5 mm higher under the mature forest in 2002 than 2007. The date of maximum SWE occurred on the same day of year (DOY 87) in CC and MF in both years, while the date of 0 SWE occurred 12-14 days later in 2002 than 2007 for both stands. The average ablation

Table 6.1: Characteristics of precipitation events (1 October to 1 July) in 2002 and 2007.

	2002	2007
Total # of events	59	75
# of rainfall events	8	12
# of snowfall events	51	63
Maximum snowfall event size (mm)	28.0	18.6
Minimum snowfall event size (mm)	0.3	0.3
Average snowfall event size (mm)	3.6	5.2
Standard deviation of snowfall event size	0.6	0.9

rate in CC was slightly lower in 2002 than 2007, but in MF was higher in 2002 than 2007. In both years, the average ablation rate was higher in CC than MF by ∼30%.

Table 6.2: Measured maximum snow water equivalent (SWE) timing and magnitude, and ablation duration and rate, at Upper Penticton Creek (UPCr) in a clearcut and mature forest during 2002 and 2007.

	Clearcut		Mature forest	
	2002	2007	2002	2007
Maximum SWE (mm)	304	320	284	279
Date of maximum SWE (DOY)	87	87	87	87
Date of 0 SWE (DOY)	147	133	154	142
Average ablation rate (mm d^{-1})	6.9	7.0	5.1	4.7

Hourly air temperatures had a slightly greater range in 2007 than 2002 (53.6°C versus 50.9°C, respectively), but averages and standard deviations were similar between years (Table 6.3). Average incoming solar radiation was also similar between years, as was relative humidity. The main difference in meteorological variables was wind speed. The maximum, average, and standard deviation of wind speed were higher in 2002 than 2007 by an average of 38%.

Table 6.3: Hourly meteorological conditions (1 October to 1 July) in 2002 and 2007.

	Minimum		Maximum		Average		Standard deviation	
	2002	2007	2002	2007	2002	2007	2002	2007
Temperature (°C)	-24.2	-28.8	26.7	24.8	-1.6	-1.3	7.4	7.7
Wind speed (m s^{-1})	0.0	0.0	8.8	6.4	2.0	1.5	1.3	0.9
Incoming solar radiation (W m^{-2})	0.0	0.0	1130.0	1039.0	116.8	118.1	203.3	206.0
Relative humidity (%)	19.3	15.3	100.0	100.0	82.0	76.4	18.4	19.9

6.2 Modelled Snow Response to Forest Disturbance

6.2.1 Seasonal Cycle of Snow Accumulation and Ablation

In 2002, modelled snowpack for all disturbance scenarios accumulated from mid-October until maximum in the last week of March, and complete snowpack removal occurred between the third week of April and first week of June (Fig. 6.1). SWE ablated in late October, with complete removal of snowpack under all disturbances at low and mid-low elevational extents that lasted for approximately one week. SWE then accumulated until a small ablation event ($<$ 5 mm of SWE) in the last week of December, then accumulated until peak during the third week of March.

In 2007, modelled snowpack began to accumulate in mid-October as in 2002, but peaked in the first week of March, with complete snowpack removal occurring in the same period as 2002 (third week of April and first week of June) (Fig. 6.2). In mid-February, an ablation event decreased SWE under the wildfire (WF) disturbance, and under the most severe disturbance (CC) at the low and mid-low elevational extents. SWE accumulation resumed after this ablation event until peak SWE in the first week of March.

In 2002 and 2007, both the accumulation and ablation seasons were affected by disturbance severity and extent of disturbance. Although there was a small increase in accumulation with disturbance severity and extent, the increase was greatest at the lowest elevational extent. This change was greatest in 2002 ($\sim$90 mm), while in 2007 there was less difference in accumulation between disturbance extents ($\sim$50 mm). Effects on ablation were greatest under the greatest extent of the most severe disturbances, as melt rates were higher than those at the lowest elevational extents. This effect on ablation rates increased with disturbance extent in 2002, but showed minimal extent gradient in 2007.

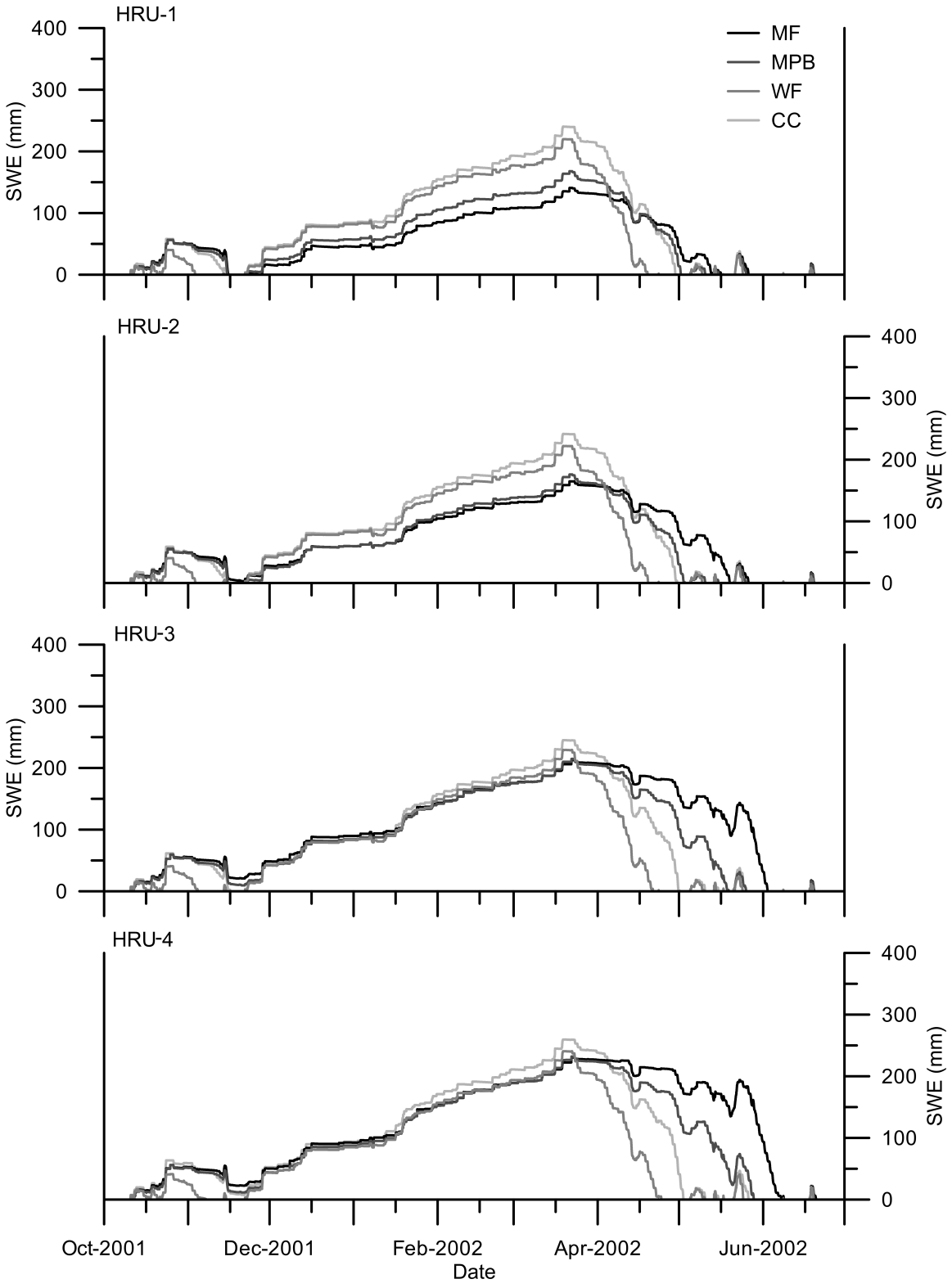

Figure 6.1: Simulated 2002 snow water equivalent (SWE) for all disturbance scenarios under all elevations (HRUs 1-4 (lowest to highest)). Disturbance scenarios: mature forest (MF), mountain pine beetle (MPB), wildfire (WF) and clearcut (CC).

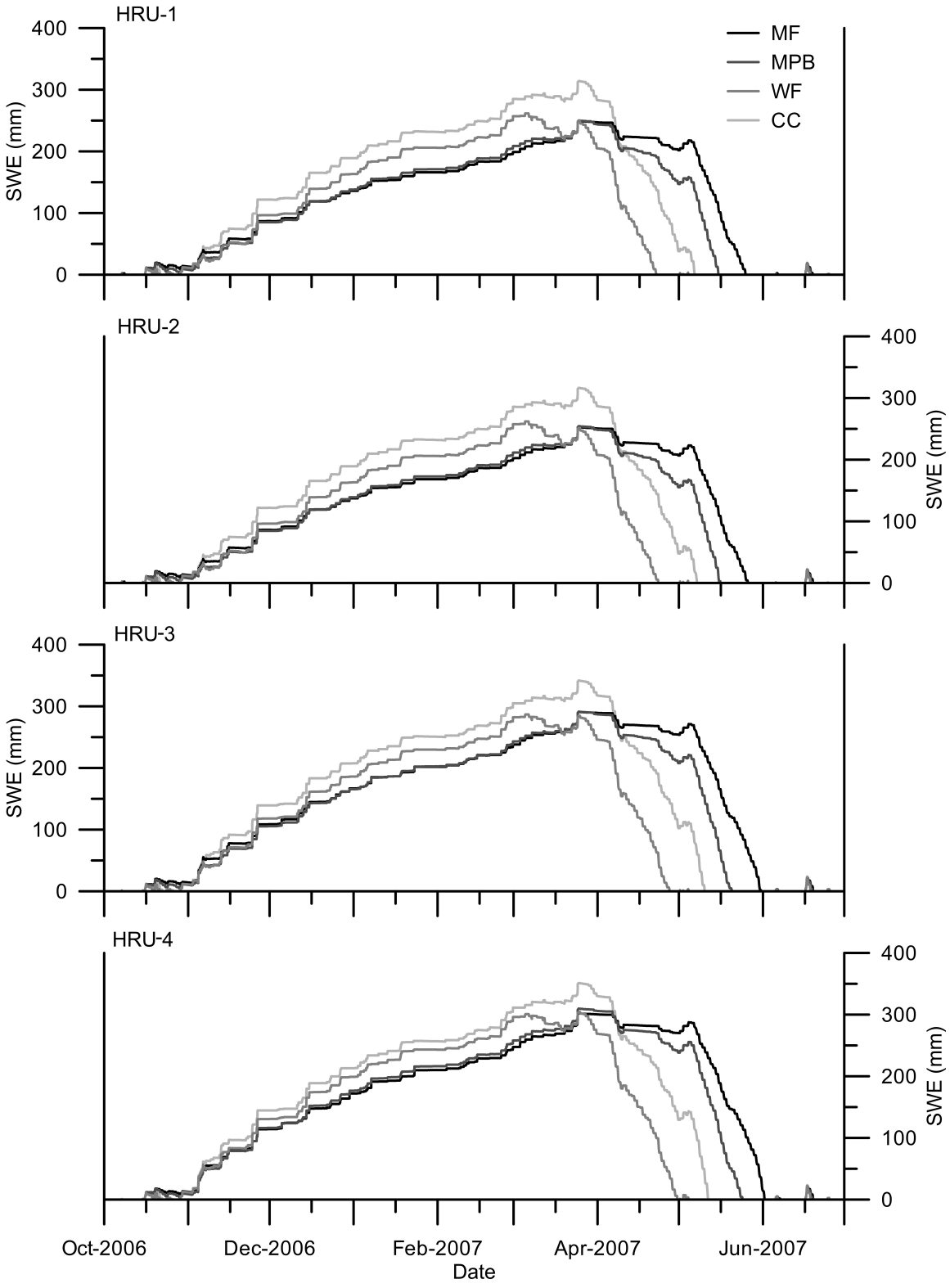

Figure 6.2: Simulated 2007 snow water equivalent (SWE) for all disturbance scenarios under all elevations (HRUs 1-4 (lowest to highest)). Disturbance scenarios: mature forest (MF), mountain pine beetle (MPB), wildfire (WF) and clearcut (CC).

6.2.2 Snow Response to Forest Disturbance

6.2.2.1 Maximum SWE

Maximum SWE increased with the severity and extent of forest disturbance in both years and was of lower magnitude under all forest disturbance scenarios and extents in 2002 (260 mm) compared with 2007 (351 mm) (Fig. 6.3). In 2002, the greatest difference in maximum SWE occurred under the MF scenario at all elevations, followed by the MPB scenario (28–39% change in maximum SWE), with the least difference between the WF and CC scenarios (7–9% maximum SWE). In 2007, maximum SWE overall increased with disturbance severity, and was greatest under the CC scenario at up to 350 mm. The greatest difference in maximum SWE between disturbance scenarios and extents occurred under the MF and MPB scenarios (up to 75 mm), and the least difference occurred under the WF and CC scenarios (up to 50 mm).

6.2.2.2 Date of Maximum SWE

The date of peak SWE was overall earlier in 2002 than 2007 by approximately three to five days (Fig. 6.3). In 2002, maximum SWE occurred two to three days earlier with increasing forest disturbance, but only at the greatest extents under the most severe disturbance scenarios (WF and CC). In 2007, the date of maximum SWE remained constant under all disturbance scenarios and extents, except at the three lowest extents under the WF scenario, where the date of maximum SWE occurred 18 days earlier.

6.2.2.3 Percent Change in Maximum SWE

Overall, the percent change in maximum SWE of individual disturbance scenarios relative to maximum SWE in the clearcut was more variable in 2002 than 2007 (Fig. 6.4). The percent change in maximum SWE in 2002 decreased both with increasing

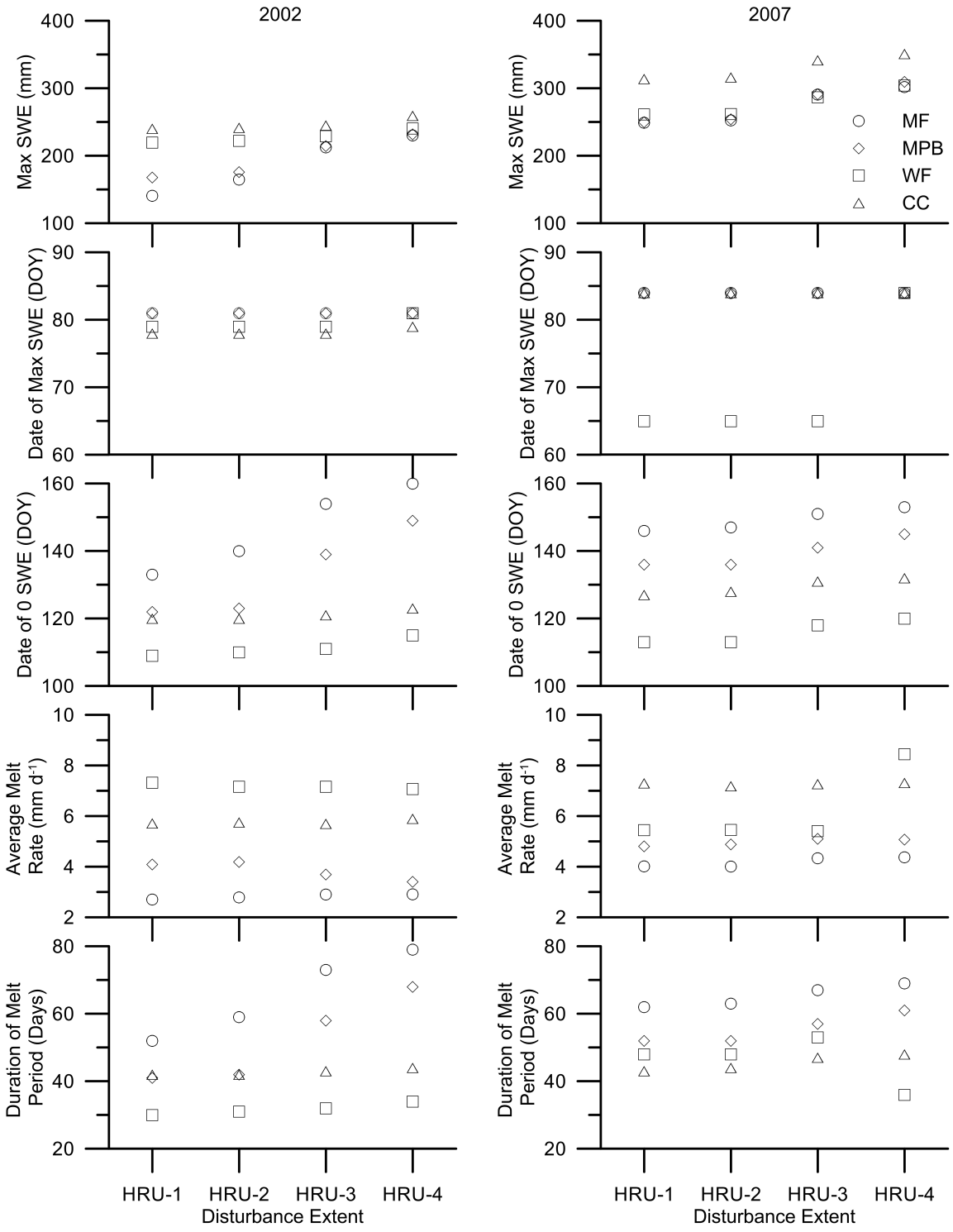

Figure 6.3: Simulated snow accumulation and ablation metrics for 2002 (left) and 2007 (right), for forest disturbance scenarios (mature forest (MF), mountain pine beetle (MPB), wildfire (WF) and clearcut (CC)) and disturbance extents (lowest to highest elevation (HRU 1-4)): maximum snow water equivalent (SWE) (mm), date of maximum SWE, date of 0 SWE, average ablation rate (mm d^{-1}), and duration of ablation period (days).

severity of forest disturbance (MF to MPB to WF) and extent of disturbance. It was greatest under the MF, followed by MPB and WF (average change of 28%) at the lowest extent. The least percent change occurred at the highest extent, where maximum SWE decreased with forest disturbance severity from MF to MPB and to WF (average change of 10%). In 2007, the percent change in maximum SWE also decreased with increasing extent of all disturbances. While the percent change in maximum SWE at low and mid-low extents decreased overall with increasing forest disturbance severity, the two highest extents had a different response. At these elevations, the percent change in maximum SWE either decreased or remained relatively similar between the MF and MPB scenarios, but increased under the WF scenario.

6.2.2.4 Ratio of Scenario to Clearcut Peak SWE

The calculation of ratio of peak SWE in the clearcut to peak SWE under MF, MPB, and WF scenarios allows for comparison with other studies that use this method. Overall the ratio of peak SWE between disturbances and clearcut (F:O ratio) was less variable in 2007 than 2002 (Fig. 6.5). This trend was the same between years (increasing with extent under the least disturbed scenarios (MF and MPB)), although the WF scenario resulted in an increase in F:O at the highest extent in 2007, but a decrease in 2002. The F:O ratio was very similar between disturbance severities in 2007, although slightly higher under the WF scenario. The magnitude of difference in the F:O ratio between severity and extent of disturbance was larger in 2002 than 2007 (0.58-0.93 versus 0.79-0.87, respectively).

6.2.2.5 Date of 0 SWE

Overall, the date of complete snowpack removal between disturbance severities, extents, and years occurred earlier in 2002 by approximately 10 days, except for mid-high and high extents under the least severe scenarios (MF and MPB), where snow was

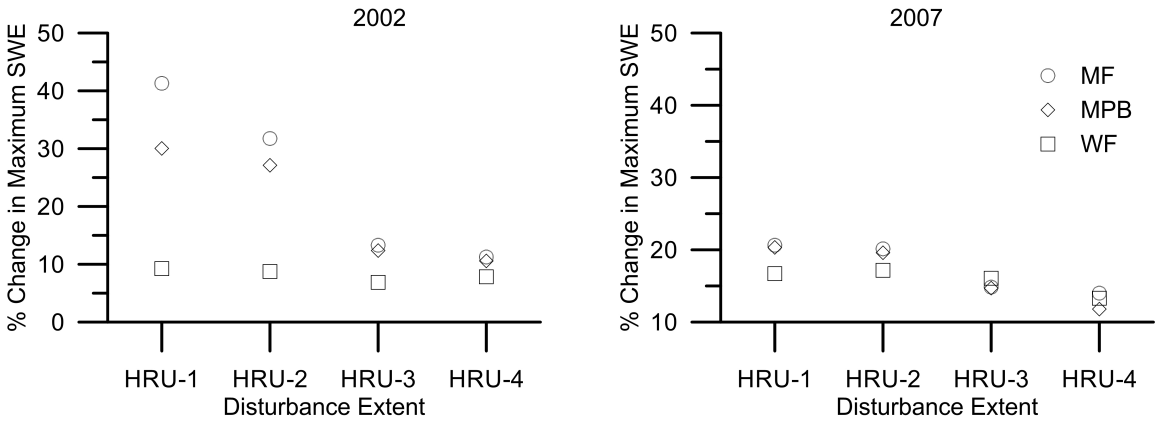

Figure 6.4: Percent change in simulated maximum snow water equivalent (SWE) for all disturbance scenarios (mature forest (MF), mountain pine beetle (MPB), wildfire (WF) relative to clearcut (CC) for all extents (lowest to highest elevation (HRU 1-4)) in 2002 (left) and 2007 (right).

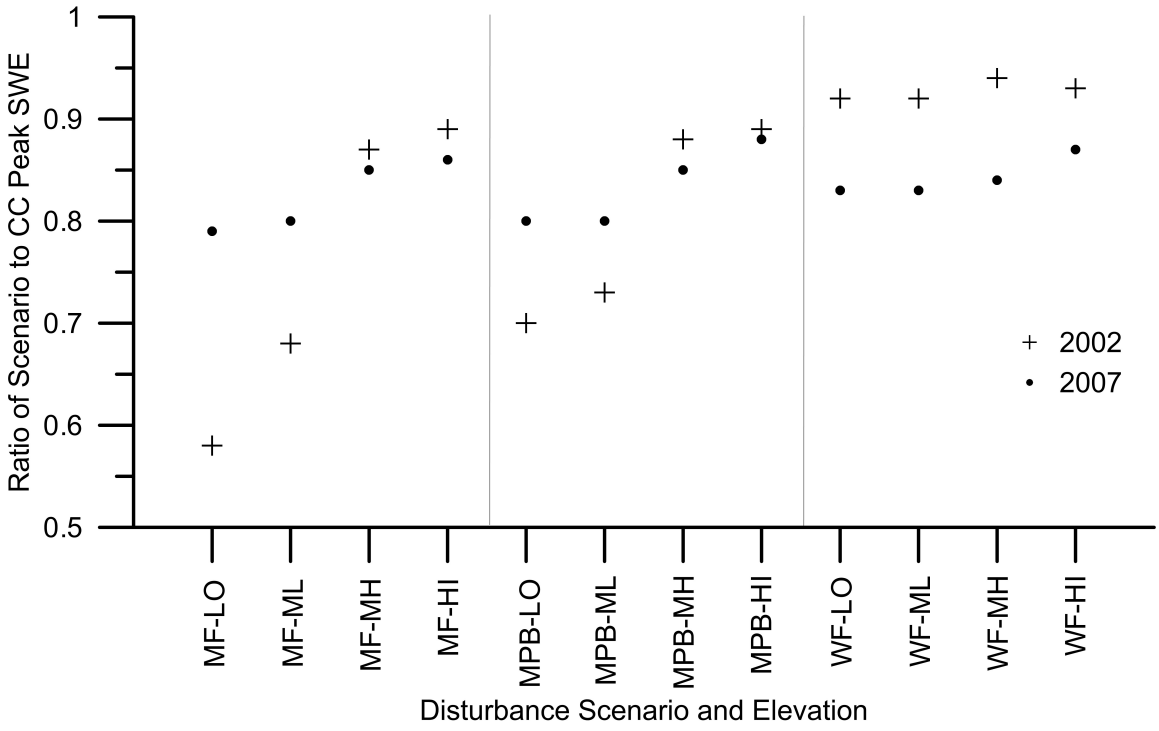

Figure 6.5: The ratio of simulated maximum snow water equivalent (SWE) under each forest disturbance scenario (mature forest (MF), mountain pine beetle (MPB), wildfire (WF)) relative to that under the clearcut (CC) scenario, for each elevational extent of disturbance (LO: low; ML: middle-low; MH: middle-high; H: high) in 2002 and 2007.

removed 3 to 7 days later in 2002 than 2007 (Fig. 6.3). Between scenarios in 2002, an increase in disturbance severity resulted in an earlier date of snowpack removal by up to 50 days, the earliest date occurring under the WF scenario. The greatest difference in date of snowpack removal between low and high elevation disturbance extents occurred in 2002 under both MF and MPB scenarios (27 days), with the smallest difference also occurring in 2002 under the CC scenario (4 days). In 2007, an increase in disturbance severity resulted in snowpack removal occurring up to 40 days earlier, and as observed in 2002 was earliest under the WF scenario. The date of snowpack removal between extents was generally later (∼5 days) at high versus low elevation extent.

6.2.2.6 Average Ablation Rate

The daily average ablation rate between severities and extents was lower in 2002 (3.0 mm d^{-1} to 7.1 mm d^{-1}) than in 2007 (4.0 mm d^{-1} to 8.6 mm d^{-1}) (Fig. 6.3). Overall, the ablation rate in 2002 increased with forest disturbance severity (3-6 mm d^{-1}), except for under the WF scenario where the rate was higher than all other scenarios (∼7.5 mm d^{-1}). Between disturbance extents in 2002, the largest differences in ablation rate occurred under the MPB scenario (∼1 mm d^{-1}). While the maximum ablation rate also generally increased with forest disturbance severity in 2007, the highest extent was almost 4 mm d^{-1} higher than the three lower extents under the WF scenario (Fig. 6.3). This occurred because the ablation rate was calculated from a later date at the highest extent than lower elevations, as the date of maximum SWE occurred on DOY 84, compared with lower disturbance extents where the date of maximum SWE occurred on DOY 65.

6.2.2.7 Duration of the Ablation Period

The duration of the ablation period overall was 15-20 days shorter in 2002 than 2007 (Fig. 6.3). The duration of the ablation period decreased with forest disturbance severity by an average of ∼20 days, except for the WF scenario which had the shortest duration at 30-36 days, and decreased with extent of disturbance (4-50 days). Overall, the duration of the ablation period also decreased with an increase in forest disturbance severity in 2007. However, the shortest ablation period occurred at the highest extents under the WF disturbance due to the same issue with double peak SWE noted in 6.2.2.2.

6.3 Incremental Forest Disturbance Impact on Total Basin SWE

As expected, total simulated basin SWE was lower in 2002 than 2007 for all scenarios (Fig. 6.6), which corresponds with measured SWE data. In 2002, disturbance severity and extent noticeably increased watershed-scale SWE. The most severe disturbances (WF, CC) not only increased total SWE more than less-disturbed scenarios (MF, MPB), but severe disturbance scenarios also increased total SWE with increasing elevational extent. The greatest increase in total SWE occurred when the full extent of 241Cr was disturbed. When the entire extent of 241Cr was simulated as MF, the total watershed-scale SWE was 187 mm; this increased with disturbance severity by 5% under the complete MPB scenario, 18% under the complete WF scenario, and with the greatest change under the complete CC scenario at 24%.

In 2007, forest disturbance extent and severity had a minimal effect on watershed-scale SWE, except under the CC scenario (Fig. 6.6). When the entirety of 241Cr was simulated as MF or MPB, the total basin SWE was 275 mm. This increased by less than 1% under complete WF disturbance, but increased by 17% under the most severe disturbance simulation (CC).

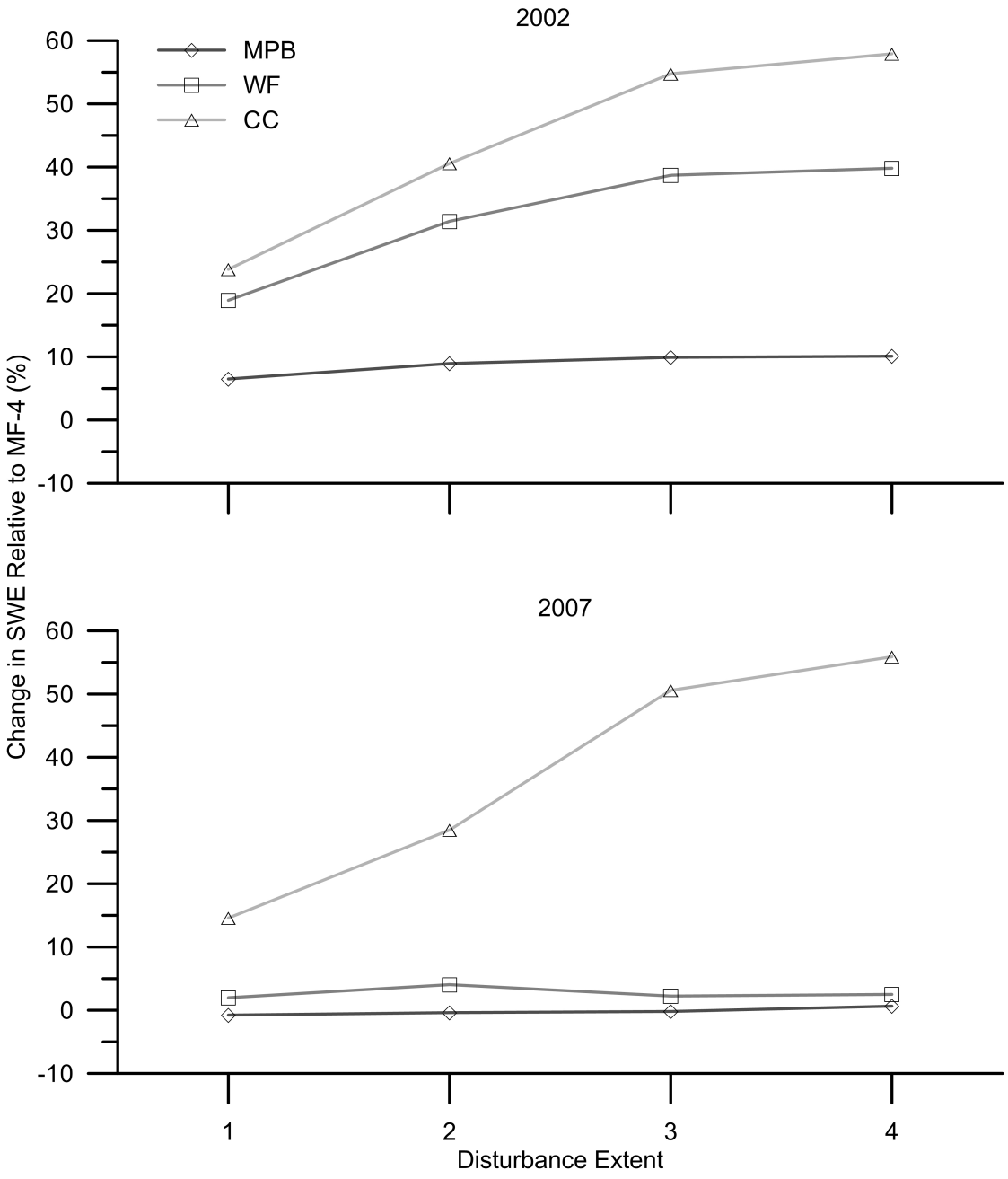

Figure 6.6: Change in simulated total basin snow water equivalent (SWE) for UPCr under each disturbance scenario (mountain pine beetle (MPB), wildfire (WF), clearcut (CC)) relative to the mature forest (MF) for 2002 and 2007. Disturbance extent is the number of HRUs disturbed, from the lowest to highest elevation. MF-4 indicates that all four HRUs represent mature forest.

6.4 Energy Balance Fluxes

Overall, increasing forest disturbance severity increased the total energy available for melt during both the accumulation and ablation periods in both years (Fig. 6.7). Dur-

ing the accumulation period for both years, total energy was more negative at the greatest extents of the least severe disturbances (MF and MPB), but more positive under greatest extents of the most severe disturbances (WF and CC), with the exception of a decreasing trend at the greatest extent under the WF and CC scenarios; negative total energy signifies a loss of energy from the snowpack to the atmosphere, while positive total energy is the opposite. Although the total energy was overall positive under the most severe disturbances (WF and CC) with the greatest increase near the melting point, the mean energy available (< 10 MJ m^{-2} h^{-1}) was insufficient to drive significant ablation during the accumulation season. Thus the remainder of this section focuses on the energy available for melt during the ablation period.

During the ablation period of 2002, positive net shortwave (K^*) drove the energy balance under the least severely disturbed scenarios (MF and MPB), but was largely offset by negative net longwave (L^*) under the scenarios with greatest severity (WF and CC) (Fig. 6.8). The turbulent fluxes contributed almost an order of magnitude less energy to the total energy available for melt relative to K^* and L^*. Positive contributions from net sensible heat (Q_H) offset negative latent heat (Q_E) under the MF and MPB scenarios, but with increasing disturbance severity (WF, CC), Q_H declined and increasingly negative Q_E dominated the turbulent fluxes (Fig. 6.9). Ground heat flux was considered zero.

Contributions of each component of the energy balance were similar between 2007 and 2002 (Fig. 6.8). In 2007, slightly more positive K^* also dominated the energy balance under the MF and MPB scenarios, but was offset more by negative L^* under the most severe disturbances (WF and CC) than in 2002. While the radiative fluxes were slightly larger in 2007, the total energy for melt was offset by smaller contributions from turbulent fluxes than in 2002, and the differences in between extents of disturbance was greater in 2002 than 2007. Total energy was notably higher under CC in mid-low and high elevational extents but occurred only in 2002. Similar to

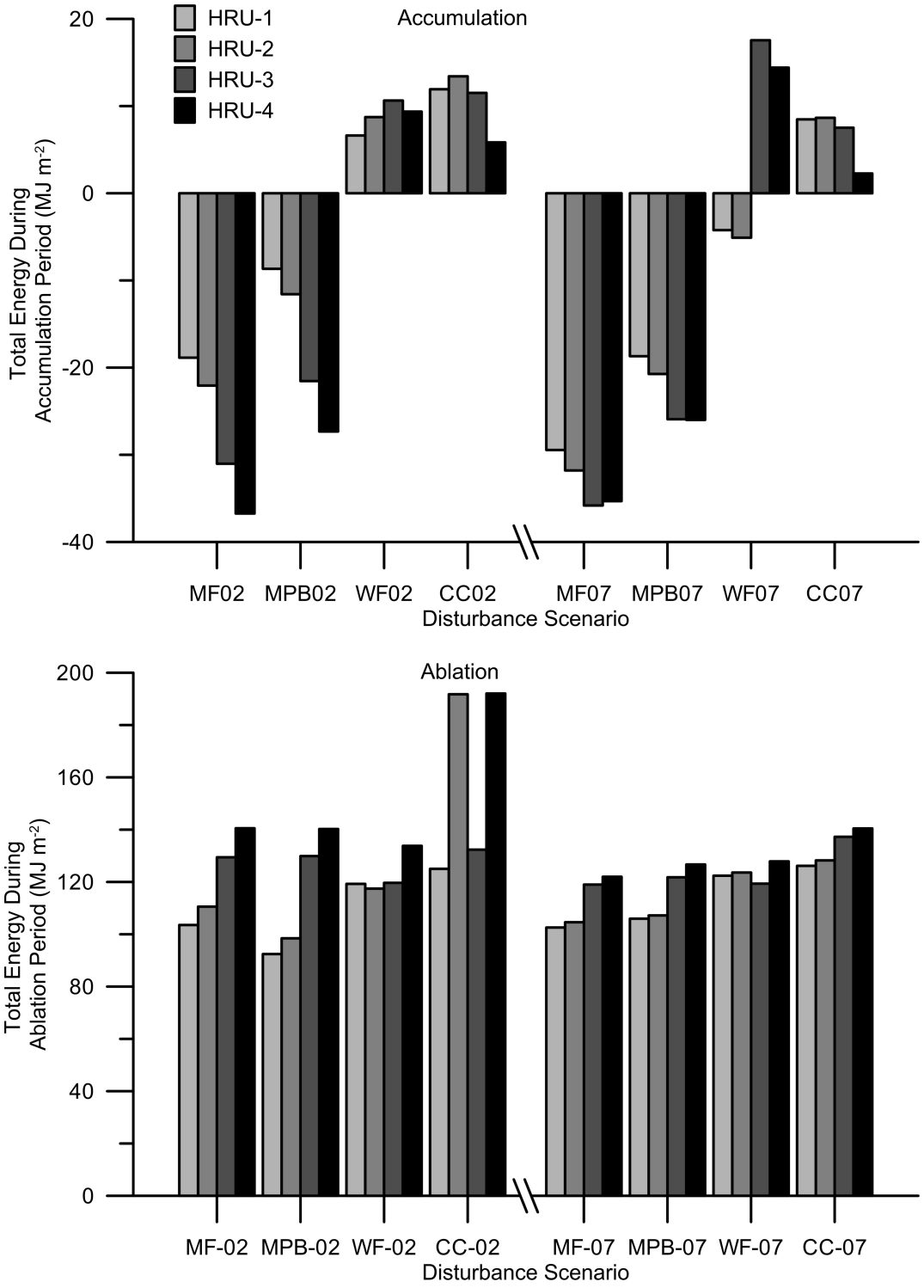

Figure 6.7: Total energy available for melt during the accumulation (date of first snow water equivalent (SWE) accumulation to date of maximum SWE) and ablation (date of maximum SWE to date of 0 SWE) periods of 2002 and 2007 for all disturbance scenarios (mature forest (MF), mountain pine beetle (MPB), wildfire (WF), clearcut (CC)) and extents. Positive and negative values represent the gain or loss of energy to snow, respectively.

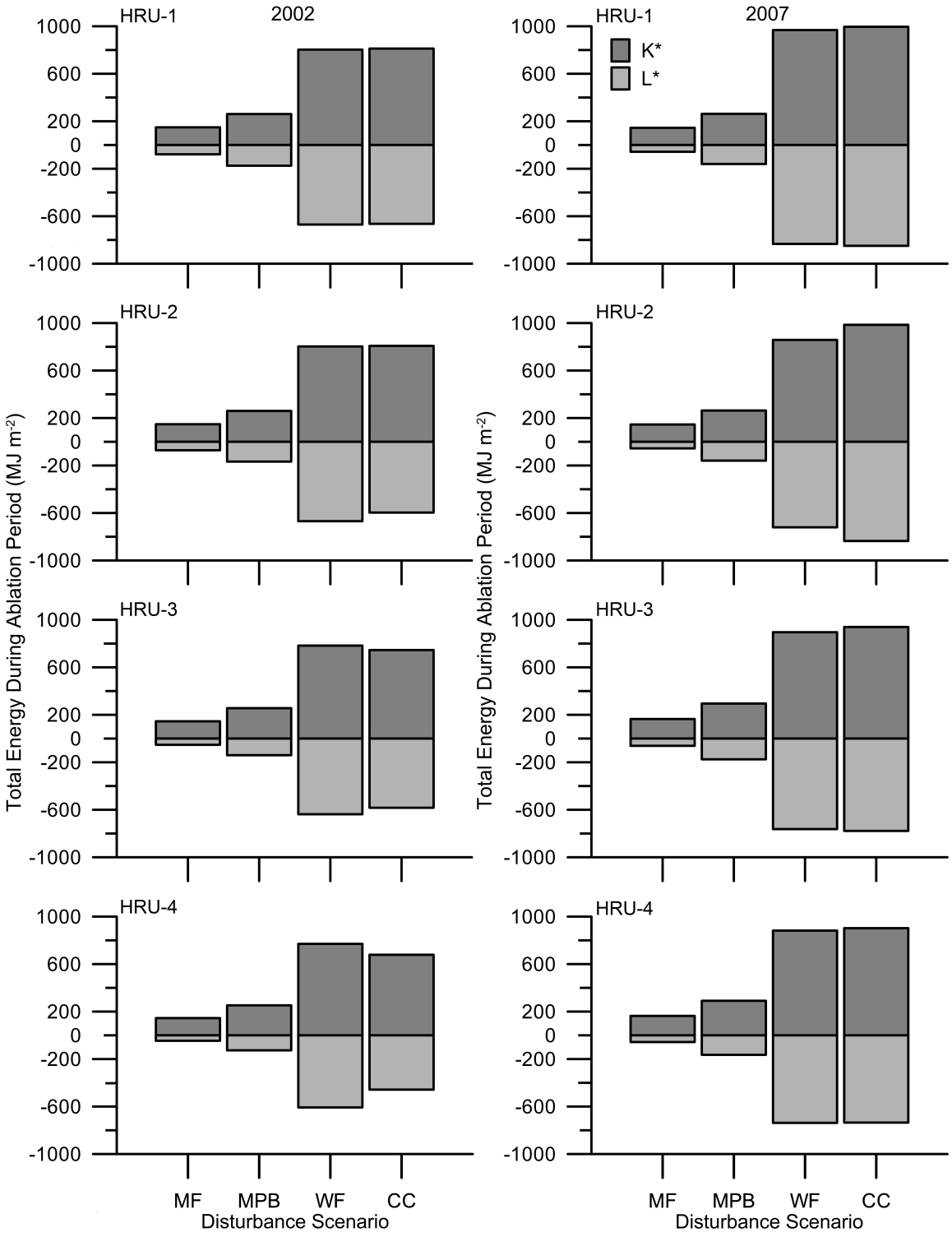

Figure 6.8: Total net shortwave (K^*) and net longwave (L^*) fluxes for the ablation period (date of maximum snow water equivalent (SWE) to date of 0 SWE) of 2002 (left) and 2007 (right) for all disturbance scenarios (mature forest (MF), mountain pine beetle (MPB), wildfire (WF), clearcut (CC)) and all extents of disturbance from the lowest (top) to highest (bottom) (HRU 1-4). Positive and negative values represent the gain or loss of energy to snow, respectively.

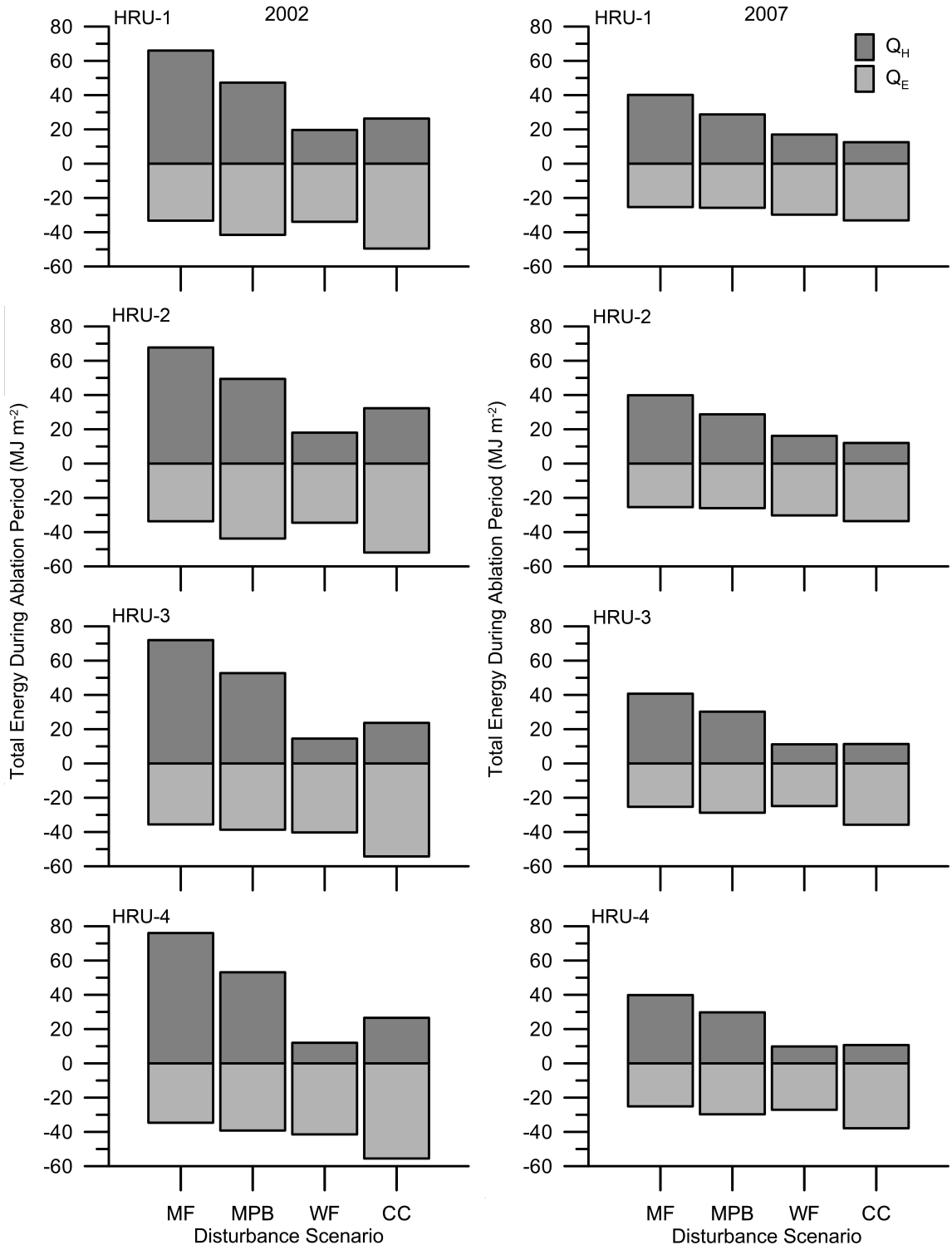

Figure 6.9: Total sensible (Q_H) and latent (Q_E) fluxes for the ablation period (date of maximum snow water equivalent (SWE) to date of 0 SWE) of 2002 (left) and 2007 (right) for all disturbance scenarios (mature forest (MF), mountain pine beetle (MPB), wildfire (WF), clearcut (CC)) and all elevations from the lowest (top) to highest (bottom) (HRU 1-4). Positive and negative values represent the gain or loss of energy to snow, respectively.

2002, turbulent fluxes contributed approximately an order of magnitude less energy to the total available for melt relative to K^* andL^* (Fig. 6.9). In both years, positive contributions from Q_H offset negative Q_E under the least severe disturbances (MF and MPB), but with increasing disturbance severity (WF and CC scenarios), Q_H declined and increasingly negative Q_E dominated the turbulent fluxes. Total energy was notably higher under CC in mid-low and high elevational extents but only occurred in 2002.

Contributions from K^* to the total energy available for melt decreased with disturbance extent by an average of 7% in 2002 but increased by an average of 1% in 2007. The largest decrease (16%) occurred under the CC scenario at the highest elevational extent in 2002. Contributions from L^* to total energy were increasingly negative with disturbance extent in 2002 (27%) than 2007 (5%), but the change was variable with increase in disturbance severity in 2002; MF scenario decreased with extent by 41% whereas more severely disturbed scenarios (MPB, WF and CC) decreased with extent of disturbance by 27%, 9% and 31%, respectively. Contributions from Q_H increased with extent under the the least severe disturbances (MF and MPB) (13% and 11%, respectively), but decreased with extent under the WF scenario by 39% (Fig. 6.9). Under the most severe disturbance (CC), Q_H increased in the mid-low extent (9%) but decreased in the highest elevational extent to a similar energy value as the lowest extent. Q_E remained relatively constant under the least severe distuebances (MF and MPB) for all extents, but increased with extent under the most severe disturbances (WF and CC) by 22% and 11%, respectively.

6.5 Conclusion

During the accumulation period, an increase in disturbance severity increased the rates of accumulation, and resulted in higher maximum SWE. An increase in the extent of disturbance did not change the rates of accumulation, but the difference in

maximum SWE between disturbance scenarios decreased with increasing extent. The difference in both maximum SWE and total basin-scale SWE between severities and extent was less pronounced in 2007, the year with more snow. The energy available for melt during the accumulation period decreased with extent of disturbance but increased with disturbance severity. However, the total energy available was insufficient to affect snow accumulation in either year.

During the ablation period, an increase in disturbance severity raised the rates of ablation, and decreased the duration of the ablation period, but the rate of ablation did not increase between elevational extents of disturbance. The differences in rate and duration of ablation between disturbance severities and extents were greater in the year with less snow (2002). In both years, the energy available for melt during the ablation period increased both with disturbance severity and extent. The contribution from individual fluxes varied with extent of disturbance, with the greatest percent change with extent occurring in the lower snow year (2002). Overall, net shortwave radiation decreased but was offset by more negative net longwave radiation loss, sensible heat flux increased under the two least disturbed forests (MF and MPB) while decreasing under the two most severely disturbed scenarios (WF and CC), and latent heat flux generally increased with extent of disturbance.

Chapter 7

Discussion

7.1 Introduction

This study examined snow accumulation and ablation response to increasing forest disturbance severity and disturbance extent at the watershed scale: the study basin was 241 Creek (241Cr). In general, the potential response from increases to both disturbance severity and extent resulted in an increase in the accumulation rate and in maximum snow water equivalent (SWE), and increased the energy available for ablation and subsequently increased the rate of ablation. More snow was able to accumulate under more severe disturbance scenarios because the loss of forest canopy reduced snow intercepted by the canopy and permitted greater sub-canopy accumulation. For two disturbance scenarios, dead canopy deposited debris on the snow surface which reduced snow surface albedo and further enhanced ablation.

7.2 Mature Forest

As expected, simulated accumulation rates of snow were lower under the least disturbed forest scenario (mature forest) compared to the two most severely disturbed scenarios (wildfire and clearcut) and maximum SWE was, on average, 11% lower than all other disturbance scenarios of greater severity. These results compare well with other studies that have found 0–40% lower maximum snow accumulation in mature forest stands relative to adjacent disturbed stands due to increased snowfall interception by the forest canopy (Golding and Swanson, 1986; Toews and Gluns, 1986; Spittlehouse and Winkler, 1996; Boon, 2007; Teti, 2008; Boon, 2011; Burles and Boon, 2011).

The rate of accumulation and SWE maximum were lowest under the least disturbed MF scenario because canopy interception resulted in substantial capture and

subsequent loss of canopy snow to the atmosphere. Comparison of the ratio of maximum SWE between the least and most disturbed scenarios (MF and CC) indicate that approximately 10–40% of total snowfall was intercepted by the canopy and likely sublimated to the atmosphere. These results are similar to other studies that found up to 45% of annual snowfall in western Canada is lost to forest canopy sublimation (Pomeroy et al., 1998b; MacDonald et al., 2010).

Model output of maximum SWE was most sensitive to elevational extent for the least disturbed scenario. Overall, the difference in maximum SWE between MF and other scenarios decreased with increasing extent, indicating the increased sensitivity of interception processes between extents of MF. This effect was greatest under the MF scenario where the magnitude of difference in maximum SWE from smallest to largest extent (lowest to highest elevation) was 90 mm and 52 mm in 2002 and 2007, respectively. The role of the canopy for interception processes decreased at higher elevations. Thus the canopy played less of a role in ground snow accumulation with increasing elevation, resulting in less difference between MF and the other scenarios at these elevational extents. Given that the elevational difference between extents is minimal, total accumulation differences were likely small, which suggests that model calculated interception processes are very sensitive. It is likely that the modelled canopy is more likely to unload snow to the ground at the higher elevational extents, which may be the result of slightly colder air temperature at this extent causing the model to unload more snow than lower elevations. The difference in maximum SWE between the least severely disturbed (MF) and increasingly severe disturbances (MPB, WF, CC) was smaller in 2007 (high snow year) than in 2002 (low snow year). This compares well with results from previous studies that show SWE differences between forested and disturbed stands are reduced in years with high snowfall (Storck et al., 2002; Stähli and Gustafsson, 2006; Boon, 2011). The higher maximum SWE and accumulation rate in 2007 was a function of more total precipitation which occurred

as more frequent and larger snowfall events.

Under the MF scenarios, the average ablation rate was lower than all increasingly severe disturbance scenarios, ranging from 20% lower than the moderately severe (MPB) scenario to 46% lower than both the most severe (WF and CC) scenarios. These values are at the low end of the 30-300% range determined in previous studies comparing mature forest ablation rates to adjacent disturbed stands (Storck et al., 1999; Spittlehouse and Winkler, 2004). The relatively low ablation rate resulted in an average ablation period duration 23 days longer than in the more severely disturbed scenarios. These results are on the high end of the range of ablation period duration observed in other studies between mature and disturbed forests (0-25 days) (Spittlehouse and Winkler, 2004; Boon, 2007; Teti, 2008; Boon, 2009; Seibert et al., 2010; Burles and Boon, 2011). Compared to previous studies, ablation rates under the MF scenario were not that much less than under disturbed scenarios but the duration of the ablation period was much different. This may be the result of a documented issue with the model which produces lag in simulated melt rates, resulting from an underestimation of energy available for melt which extends the snowmelt period later into the season when higher sun angles and warmer air temperatures can more rapidly ablate the sub-canopy snow (Ellis et al., 2010; Ellis, 2011).

As outlined in Chapter 2, ablation rates are inversely proportional to canopy density given canopy controls on shortwave radiation transmission to the snow surface (Molchanov, 1963; McKay and Adams, 1981). Relative to the disturbed scenarios, the total energy available for ablation in the MF scenario was overall an average of 12% lower due to this scenario having the greatest leaf area index (LAI). The energy balance under the MF scenario was driven largely by net shortwave radiation (K^*), which was an average of 80% lower in the MF scenario than in the increasingly severe disturbance scenarios. The rate of ablation did not differ with extent of MF which suggests that the elevation range ($\sim$400 m) was insufficient to significantly change

ablation processes. This was evident in both the small temperature lapse rate (see Chapter 4) and energy balance components between elevational extents. Because all elevational units have a similar aspect and slope, and the elevation range is small, incoming shortwave radiation and air temperature were similar across extents.

For all disturbance types, it appears that the radiation balance was only important near and above the melting point. Within approximately one week of the date of maximum SWE, differences in accumulation response were greatest in the lower elevational extents in 2002 and least in 2007. This suggests that the radiation balance was most important near the point of continuous melt. In the model, the cold content of the snowpack is gradually removed until remaining energy inputs drive melt rather than warming, which likely occurred soonest at low elevations because of higher air temperatures.

Furthermore, variability of energy balance fluxes for all disturbance types may be a function of the length of the ablation period in each extent of disturbance, and in each year.

7.3 Mountain Pine Beetle

Red-attack stage of mountain pine beetle disturbance represented the moderately severe disturbance in this study. Dead pine needles fall within 3-5 years following initial attack, which reduces the interception capacity of MPB-attacked forest relative to the mature forest (Mitchell and Preisler, 1998). Modelled output of rate of accumulation under the MPB scenario was relatively insensitive, as it was similar to that under the least severe (MF) scenario, but maximum SWE was 3% higher because the canopy needle drop reduced loss of intercepted snow to the atmosphere and allowed for more ground snow accumulation. The ratio of maximum SWE between CC and MPB was lower than under the most severe scenario (CC) which suggests that approximately 10-30% of the total snowfall was intercepted by the canopy, and was likely lost to

the atmosphere through sublimation. These results compare well with Winkler and Boon (2009), who compiled a synthesis of recent MPB research and found that, on average, red attack stands have a 25% reduction in maximum SWE. The difference in accumulation with elevation under MPB was similar to that under MF, thus the processes are similar to those described under the MF scenarios.

The small 3% increase in modelled maximum SWE compares well with recent studies, one of which found maximum SWE was similar under both mature forest and red-stage MPB, but was 15% higher under grey-stage MPB (Pugh and Small, 2011), while the other measured a 14% increase in maximum SWE relative to undisturbed forest in a mix of red and grey-attack stands (Biederman et al., 2011). My results also show that the effect was more pronounced in the year with smaller and less frequent storms, as evidenced by a 5% higher max SWE in the low versus the high snow year (2002 and 2007, respectively), and reflect results of similar studies between MPB and undisturbed forests that found enhanced differences in maximum SWE between high and low snow years (Biederman et al., 2011; Boon, 2011; Pugh and Small, 2011).

MPB disturbance opened the canopy, which resulted in an increased ablation rate, shortened ablation period, and thus an earlier date of 0 SWE. In this study, the average ablation rate was 20% higher under the MPB than the least disturbed scenario (MF), which is within the 15-25% range found in other studies (Boon, 2007; Teti, 2008; Pugh and Small, 2011; Winkler et al., in review). While slightly more snow accumulated under the MPB than the MF scenarios, the disturbed canopy resulted in enhanced ablation through both greater net short and longwave radiation, turbulent fluxes, and reduced snow surface albedo as a result of needle drop.

Several stand-scale studies have found an increase in the energy available for ablation post-MPB (Boon, 2007; Boon, 2009; Pugh and Small, 2011), and recent studies show that canopy needle loss in the red-attack stage reduces the surface albedo of the snowpack (Boon, 2007; Winkler and Boon, 2010; Pugh and Small, 2011; Boon

et al., in review; Winkler et al., in review). The canopy parameterization utilized a reduced leaf area index LAI for the MPB scenario to represent a slightly more open canopy relative to the MF scenario and allowed for increased incoming shortwave radiation. The albedo parameterization for the MPB scenario was also adjusted to represent higher litter concentration on snowpack than under the least severe MF scenario; this contributed to the increased ablation rate as K^* at the snow surface was higher. Despite these changes, the model simulated energy available for ablation under the moderately severe MPB scenario was virtually the same (1% lower) than under the least severely disturbed MF scenario. Increased K^* at the snow surface was offset by more negative net longwave radiation (L^*) as a consequence of the opened canopy; this loss of canopy increases emissivity, and results in greater outgoing longwave radiation. The increasingly negative latent heat (Q_E) was offset by more positive sensible heat (Q_H).

Interestingly, the MPB scenario had the greatest variability in ablation rate with extent of disturbance. All other scenarios had similar ablation rates across extents, except for the greatest extent under the most severely disturbed scenario (WF) which is described below. This variability in ablation rate under the MPB scenario is likely due to decreased uniformity or homogeneity of canopy structure, which permits enhanced ablation where canopy gaps have increased (Boon, 2011).

While the changes in K^*, L^*, and Q_E under the MPB scenario relative to the least severely disturbed MF scenario compare well with field observations from previous studies (Boon, 2009), the less positive Q_H is surprising. Disturbance generally reduces canopy and land surface roughness and typically results in higher wind speeds and enhanced turbulent fluxes relative to mature forests (Boon, 2009; Winkler et al., in review). One explanation could be that, while the ablation period was shorter under moderately severe disturbance than the least disturbed MF scenario, the greater variability of mean hourly Q_H under the MPB scenario cancelled any increase in

Q_H.

7.4 Wildfire

Moderately-severe wildfire represented an intermediate disturbance severity between the moderately severe MPB and most severe CC scenarios. As such, the sensitivity of modelled snow accumulation was as expected: the substantial loss of canopy associated with the more severely disturbed WF scenario decreased the interception capacity relative to less-disturbed MF and MPB scenarios to more closely represent the rate of accumulation and maximum SWE under the most severely disturbed CC scenario. The difference in maximum SWE between MF and WF decreased with extent of disturbance, because the forest canopy was more important for interception at lower elevations. The 9% average increase in maximum SWE relative to the least disturbed MF scenario was in the lower range of 9-58% values found in other studies (Skidmore et al., 1994; Seibert et al., 2010; Burles and Boon, 2011). Results from our study were much closer to those found in Skidmore *et al.* (1994) who found an increase of 9% in maximum SWE under both wildfire and clearcut relative to the nearby undisturbed mature forest, but the mean canopy coverage in the mature forest was low (42% cover) which suggests that differences in accumulation between disturbed and undisturbed stands may be lower when forest canopy is less dense. Our modelled results were lower than the other study sites and these differences likely stem from study site variations: Burles and Boon's (2011) study site was more severely burned and had a greater increase (50-58%) in maximum SWE relative to an undisturbed site, while Seibert *et al.* (2010) found an average of 50% greater maximum SWE in a more severely burned stand with greater area (486 km^2), much larger variability of slope (50% gradient) and elevation range (603-2164 m) than at 241Cr, suggesting that more severely burned forests and site-specific topographic conditions have greater accumulation response than forests with moderately severe wildfire.

The ratio of maximum SWE between WF and and the most severe disturbance (CC) suggests that approximately 6-17% of snow was intercepted by the canopy relative to the incoming total, and inferred to be lost to sublimation as the snow otherwise would have dropped off the canopy and increased sub-canopy snow accumulation. Currently, no published literature has quantified the sublimation loss of snow in post-wildfire stands, but Burles and Boon (2011) noted higher wind speeds and reduced stem density in burned stands which would affect sublimation, and should be included in future studies. As the post-wildfire canopy is characterized by standing dead stems and branches, model parameterization required low LAI and maximum canopy intercepted snow load ($Sbar$) values to represent this canopy, and thus allowed some snow to be retained and sublimated by the canopy. A limitation of this approach may be that more snow was captured by the canopy than would be in the field because the model is assuming that LAI is an interception platform with needles, stems, and branches, much of which is removed by fire, so the accumulation of sub-canopy snow would be reduced as interception processes are more important than real-world stands. As with the MPB scenario, there are currently no measured $Sbar$ values for WF; $Sbar$ was determined in this study for both MPB and WF as a percent change of literature derived values relative to LAI, but further work is required to determine appropriate forest canopy parameter values in both MPB and WF scenarios. The accumulation differences between disturbance extents were, like the less-severe disturbances (MPB and MF), smaller in the high snow year (2007).

Results indicate that the potential response of moderately-severe wildfire disturbance may alter the rate, timing and duration of ablation to more closely represent most severe clearcut than less severe MF and MPB scenarios. The increase in ablation rate and decreased the duration of the ablation period relative to the MF and MPB scenarios is not unexpected. Previous studies have shown that wildfire opens the canopy which permits greater sub-canopy radiation transmittance to more rapidly

ablate snowpack (Seibert et al., 2010; Burles and Boon, 2011). However, modelled ablation was sensitive under this disturbance scenario, as evidenced by the notably high ablation rate which is the result of increased incoming shortwave and outgoing longwave radiation which in turn enhanced the energy available for ablation coupled with low snow surface albedo. This was caused by soot falling from the remaining branches and trunks to the snow surface, resulting in greater absorption of shortwave radiation and greater availability of energy for ablation (Conway et al., 1996). This is the first study to examine post-wildfire snow processes, thus there is no previous work against which to compare these results. However, given the high model sensitivity to low albedo values (see Chapter 5), the model may be overly sensitive to the combination of soot deposition on the snow (low albedo values) and loss of canopy (reduced LAI), resulting in rapid ablation and large reduction in the duration of the ablation period. The ablation rate remained relatively constant with extent of disturbance, except for the highest elevational extent under WF in 2007 where a second SWE peak occurred later in the year at lower elevational extents, thus extending the snow season later in the year when sun angle is higher and air temperatures are increasing, and subsequent rapid ablation.

7.5 Clearcut

The CC scenarios were the most severe disturbance and consequently had the greatest impact on snow accumulation. Maximum SWE was greatest under this scenario, increasing by an average of 20% compared to the least severe disturbance (MF), which is in the low range of the 20-40% values noted in the literature (Golding and Swanson, 1986; Faria et al., 2000; Spittlehouse and Winkler, 2004). This variation is likely due to differences in both snowfall magnitude and timing, and mature forest canopy closure and density across sites. Similar to the other disturbances, interannual differences in total snowfall resulted in different percent change in maximum SWE relative to the

least severe MF scenario. In the lower snow year (2002), average maximum SWE was 25% higher under the most severe disturbance (CC) relative to the least severe MF scenario, but was only 17% higher in the higher snow year (2007). Between disturbance extents, the difference in maximum SWE relative to the least severely disturbed MF scenario decreased with increasing disturbance extent as the role of the canopy in interception decreased. These differences were also a function of the less frequent and smaller snow events of 2002 that were retained in the canopy at lower elevations. Given the lack of canopy in the CC scenario, accumulation here is assumed to be the maximum incoming SWE. This provided a baseline against which the maximum SWE under each remaining disturbance severity (MF, MPB and WF) was compared.

It is important to note, however, that clearcut forests often lose snow to sublimation. The removal of forest canopy decreases surface roughness, resulting in greater wind speeds, and subsequently increased turbulent fluxes with subsequent redistribution and loss of snow due to blowing snow and sublimation (Toews and Gluns, 1986; Spittlehouse and Winkler, 2004; Winkler et al., 2005). However, these processes have been observed to have minimal impact on CC stands at the UPCr study site (Winkler, unpub. data; Spittlehouse, pers. comm.). Although the blowing snow module was tested during the model simulations, loss of snow from this process was negligible and thus confirmed field observations.

As expected, the rate and timing of snow ablation was altered under the most severely disturbed scenario (CC). Ablation under the CC scenario was faster than under either of the least severe disturbances (MF and MPB), but the rate and timing of complete ablation fell between the MPB and WF scenarios. Ablation rates under the CC scenario were on average 86% greater than under the least disturbed MF scenario. These results are within the higher range of typical ablation rates (30% to $> 100\%$) found in the literature, but compare well with measured values at the study site (e.g., Toews and Gluns, 1986; Berris and Harr, 1987; Spittlehouse and Winkler,

2004; Winkler et al., 2005).

The complete removal of forest canopy under the CC scenario resulted in the greatest increase in average total energy available for ablation (26%) relative to least disturbed MF scenario. Differences in rate of ablation between extents of CC disturbance were minimal, with the date of complete snowpack removal occurring only 3-5 days later in greatest extent of disturbance. Since the change in energy available for ablation was minimal with elevational extent, more days were required to completely ablate the higher SWE at higher elevations.

7.6 Total Basin-Scale SWE

Greater forest disturbance severity increased total basin-scale SWE in both years, but the response was more notable in the lower snow year (2002). The greatest difference between disturbance severities was in 2002 was because the interception capacity of the forest is more important in a low than in a high snow year (Jost et al., 2007; Boon, 2011). In high-snowfall years such as 2007, differences between disturbances and between disturbance extent were reduced as heavy snowfalls exceeded the interception capacity of the canopy (Schmidt, 1991; Hedstrom and Pomeroy, 1998; López-Moreno and Latron, 2008). There was a noticeable increase in basin SWE with both disturbance extent and severity. Under all scenarios of disturbance severity, the greatest response in total basin SWE occurred when the disturbance extent spread from the mid-low to mid-high elevation, and the least response occurred when the disturbance moved into the highest elevational extent.

Under the MPB scenarios, total basin-scale SWE increased by 0-5% with increasing disturbance extent relative to the MF scenarios. These results agree well with Biederman *et al.* (2011) who observed no change in maximum SWE at the small catchment scale, but differs from the results of Bewley *et al.* (2010) who found a 12–19% increase in basin-scale SWE post grey-attack MPB disturbance, and Pomeroy

et al. (2012) who found that 15% of basin area disturbed by a mix of red and grey attack MPB resulted in approximately 5% increase in basin SWE.

These differences are likely a function of variations between study sites. The basin in Biederman *et al.* (2011) was of similar size to 241Cr, but received almost double the snowfall amount which may have led to the canopy being less important in driving SWE. Bewley *et al.* (2010) studied a large (>1251 km^2) basin with a greater elevation range (400-1600 m), where elevation likely played a larger role in basin-scale SWE than in 241Cr. Pomeroy *et al.* (2012) studied a basin with an 1100 m elevation range, while that in 241Cr is only 400 m. Additionally, their watershed contained a combination of southerly and northerly aspects, whereas 241Cr is largely south facing. While both Bewley *et al.* (2010) and Pomeroy *et al.* (2012) reduced LAI to represent disturbance, neither study incorporated changes in snow surface albedo due to needle drop.

Total basin-scale SWE was much more responsive to disturbance extent under increasingly severe WF disturbance than the less severe MPB scenario (0-5%), increasing by up to 21% relative to least severe MF disturbance scenario. Greater loss of forest canopy under the WF scenario relative to MPB scenario increased the rate of accumulation and the maximum SWE. Few studies have examined basin-scale SWE response to wildfire. Results from this study found an increase of 10–21% in total basin SWE under the WF scenario with 24–100% of the basin area disturbed, which was much smaller than results from Pomeroy *et al.* (2012) who found an increase of 18% and 47% in basin SWE with 35% and 60%, respectively, of the total basin area subject to wildfire. A moderately-severe wildfire was simulated in this study, whereas Pomeroy *et al.* (2012) selected parameters to represent a more severe disturbance with in some cases no canopy or trunk retained. When combined with a larger elevation range, this likely resulted in much higher SWE accumulation than in this study. As with MPB, the total basin-scale SWE did not increase with disturbance extent in the

higher snow year (2007) relative to that under least severely disturbed MF scenarios.

Basin-scale SWE response to disturbance extent was greatest under the most severely disturbed CC scenario, with an increase of 31% under complete basin extent of disturbance relative to the least severely disturbed MF scenario. When 24-46% of the basin was disturbed under the CC scenario, total basin SWE increased by 13–22%. This was lower than results from Pomeroy *et al.* (2012), who calculated an increase in basin SWE of 18–32% when 15-37% of the watershed was clearcut. The range of meteorological and topographic conditions between studies makes comparison of results difficult; however, results from this study fall within the lower range of post-CC maximum SWE percent change relative to MF (5–70%) from stand-scale studies in British Columbia (Toews and Gluns, 1986; Winkler and Moore, 2006; Jost et al., 2007; Teti, 2008; Winkler et al., in review).

Although runoff was not modelled in this study, results provide information based on process knowledge and hydrologic theory that form the basis for future studies. Understanding the response of total basin-scale SWE to forest disturbances of increasing severity and extent is required to quantify the amount of melt water available for runoff. Results from this study suggest that large changes in runoff volume post red-attack MPB may not occur at 241Cr as observed in other studies due to a slight increase in snow water equivalent (0–5 mm) relative to MF (Alila et al., 2009; Schnorbus and Bennett, 2010). The large increase in rate of ablation under the wildfire scenario suggests that runoff may occur soonest of all the disturbances examined in this study, which - when coupled with an increase in total basin-scale SWE relative to the least disturbed MF scenario - could result in substantial changes to spring snowmelt. Results from the most severely disturbed clearcut scenario indicate that extent of disturbance may increase the total amount of snow water equivalent in the basin regardless of snowfall events. Small difference in ablation rates between years or between extent of disturbance suggests that melt across the watershed may be

synchronized, and if the date of complete snowpack removal becomes similar across elevations, melt timing may also be synchronized across the watershed resulting in greater runoff response relative to desynchronized melt across the watershed. Between disturbance severity scenarios, the ablation rate under the moderately severe MPB scenario was similar to the least severely disturbed MF scenario, but under increasingly severe disturbances (WF and CC), higher ablation rates suggest a greater runoff response relative to those under the less disturbed scenarios (MF and MPB).

7.7 Conclusion

Results from this study indicate that total basin SWE increased with disturbance severity, as loss of forest canopy resulted in less loss of snow to interception and greater sub-canopy accumulation. Disturbance extent also increased the response of basin-scale SWE as more disturbed area permitted greater accumulation of snow. In the year with less snow, the response to both disturbance severity and extent was greater than the year with more snow, where only the most severely disturbed clearcut scenario resulted in more total basin-scale snow water equivalent. Disturbance severity also increased SWE ablation as the loss of canopy increased the amount of total energy available for ablation. The two disturbances with greatest severity resulted in more snow water equivalent and significantly increased rates of ablation which is likely to enhance the timing and magnitude of snowmelt runoff from 241Cr.

Chapter 8

Summary and Conclusions

The purpose of this thesis was to initialize and validate a hydrological model for a forested, snowmelt-dominated catchment in south central British Columbia, and to use field data from stand-scale studies to parameterize the model to represent forest disturbances in order to quantify the potential snow hydrology response to varying spatial extent of disturbance.

Forest disturbances can have severe and long term implications for water resources. For example, dramatic reduction in forest canopy closure and density as a result of disturbances may reduce water quality, increase flooding and potentially damage infrastructure, and alter fresh water availability for downstream users (Overpeck et al., 1990; Dale et al., 2001; Silins et al., 2009; Haughian et al., 2012). Water resource management often develops strategies for dealing with forest disturbance by either reducing vulnerability to disturbances, or enhancing subsequent recovery (Dale et al., 2001). Thus, greater understanding of post-disturbance hydrologic response can aid in developing risk assessments for water resource management. Vose (2011) identified several high-priority areas for future forest ecohydrological research, including understanding the impacts of accelerated natural disturbances, such as wildfire and mountain pine beetle (MPB), that have the potential to reduce the capacity of forested watersheds to provide abundant water (Buttle et al., 2000; Ellison et al., 2005; Lodge et al., 2006). The National Research Council of the United States (2012) also suggest that a greater understanding of the hydrologic response to abrupt landcover change is necessary for future water management. This understanding is critical for providing key information of hydrologic variability as a result of forest disturbances in order to predict its future range and response.

This study was conducted in 241 Creek, a sub-basin of the Upper Penticton Creek (UPCr) watershed located in the Okanagan Basin of British Columbia. UPCr was

established as a research watershed in the early 1980s to monitor the long-term effects of natural and anthropogenic forest disturbances on hydrological processes. Created as a paired watershed experiment, pre- and post-clearcut treatments were applied at UPCr in adjacent sub-basins with predominantly lodgepole pine forest cover. The 241 Creek sub-basin was clearcut in increments up to 50%, while 240 Creek was left as a control.

Modelling of current and disturbed forest scenarios was performed with the Cold Regions Hydrological Model (CRHM) (Pomeroy et al., 2007). CRHM was parameterized with UPCr data describing current forest cover (mature forest and clearcut) and with measured and literature-based forest disturbance (mountain pine beetle and wildfire) parameters, quantify the sensitivity of snow accumulation and ablation at the catchment scale to varying spatial extents of disturbance. CRHM was run with 9 years of input meteorological data from the UPCr experiment. This study is one of the first applications of this model in British Columbia, and one of the first to quantify watershed-scale snow response to wildfire and MPB.

Sensitivity tests were conducted to determine the effect of key model parameters on model output. Results suggested that, under mature forest conditions, the model tends to oversimulate accumulation and ablation, while under clearcut conditions the response is more variable. Model output was very sensitive to parameter values exclusive to the mature forest, particularly leaf area index (LAI) and maximum canopy intercepted snow load ($Sbar$). Output was also sensitive to albedo values under both forest conditions. Results were used to calibrate the model with parameter values within a reasonable range of field and literature values.

Results from the model validation baseline indicated that model performance was better in clearcut than mature forest conditions due to complex interactions between forest canopy and snow processes, and indicated that customization of parameters for individual years may increase model accuracy. Given that disturbance scenarios were

based on modified mature forest conditions, two years were selected for simulations that best represented observed snow conditions in both mature forest and clearcut.

To represent 241 Creek spatially, the watershed was divided into four homogeneous hydrologic response units (HRU). The four HRUs were incrementally disturbed from the lowest to the highest elevation HRU to represent varying spatial extent of disturbance through a continuum of increasing disturbance severity: mature forest, red-attack mountain pine beetle, moderately severe wildfire, and clearcut. Overall, results indicate that the response of snow accumulation and ablation increases with disturbance severity. Accumulation of snow increased with disturbance severity as greater loss of canopy reduced interception losses and permitted more snow to accumulate under the canopy. Ablation was enhanced by disturbance in general as the less dense canopy allowed for greater incoming solar radiation to reach the snowpack which enhanced the energy available for melt. These results compare well with recent stand-scale studies of forest disturbances that found canopy loss from disturbance increased the maximum amount of accumulation and enhanced ablation (Winkler et al., 2005; Boon, 2009, 2011; Burles and Boon, 2011; Pomeroy et al., 2011). However, results from this study were within the lower range of accumulation response as found in other studies (Golding and Swanson, 1986; Biederman et al., 2011; Burles and Boon, 2011), which suggests that disturbances may have relatively small impact in basins or sub-basins with similar topographic and meteorological conditions. Differences between accumulation/ablation response and disturbance types were reduced both by elevation, and large and more frequent snowfall events, indicating the greater importance of canopy both at lower elevations and years with smaller and less frequent snowfall events.

The total basin-scale accumulation of snow increased with forest disturbance severity and extent of disturbance. Loss of forest canopy from disturbance resulted in greater accumulation at the basin scale, which increased as disturbance extended

into higher elevations. In general, total accumulation in the watershed was increased with disturbance severity relative to the mature forest, but the difference between disturbance scenarios and extent decreased in the year with more frequent and larger snowfall events. This again indicates that the importance of canopy varies with snowfall regimes.

While basin-scale response to clearcutting is well documented (e.g.,Troendle and King, 1985; Jones, 2000; Jost et al., 2007), this study is one of the first to examine the response to mountain pine beetle and wildfire disturbances. When compared with the few studies that do exist, results are within the lower range of values (Bewley et al., 2010; Pomeroy et al., 2012); this difference is likely associated with differences in meteorological and topographic characteristics between study sites.

The results presented in this study provide water resource management with potential response to snow accumulation and ablation post forest disturbance. The mountain pine beetle-killed forest response was similar to that of the mature forest, with a small increase in snow water equivalent and the rate of snow ablation, which results in an earlier snow removal. The extent of pine beetle disturbance resulted in gradients in snow water equivalent, ablation rate, and date of snow removal. The wildfire response was similar to the clearcut, with a large increase in snow water equivalent and the highest rate of rate of ablation. The extent of wildfire disturbance had minimal to no extent gradient in snow water equivalent, ablation rate, and date of snow removal, which suggests that runoff response may be synchronized across the watershed. Given these results, water resource management should be more concerned with the potential for greater impact on runoff post wildfire, whereas the pine beetle killed impact may be less severe.

While the model applied in this thesis was able to simulate snow accumulation and ablation effectively, and presented fundamental information on the differences in snow response between forest disturbances at the watershed scale, the following

recommendations and considerations are presented to improve post-disturbance hydrological modelling at the watershed scale.

1. Data were quality assured and checked before application to the model, the study site was visited, and communication was maintained with those who collected the data. There was no personal involvement in data collection, and as a result, a knowledge gap exists between the collection and application of data.

2. As with all modelling studies, the methodology, parameter values, and model output have explanatory power but may always be limited in their interpretation of real world processes. However, we should expect that greater understanding of hydrological processes will improve the development and application of models.

    (a) The model applied in this study divided the watershed into lumped, homogeneous HRUs that assume uniform hydrological response and subsequently do not account for spatial distribution of input variables or parameters. Delineating lumped units for this study was generally simple given the relatively uniform topography and forest closure, but may have averaged processes that would have otherwise influenced model results. For example, the average aspect values were mostly south-facing, while small areas of the watershed were slightly west or north-facing and would not receive the same solar radiation as the averaged value. Increasing the number of HRUs to incorporate local processes driving snow accumulation and ablation may increase the accuracy of model output across space. Furthermore, sensitivity tests to determine relative sensitivity of HRU selection and parameterization on model output may improve the spatial representation of the watershed within the model.

    (b) The model was driven by parameter values from field studies and the literature that may vary between specific watersheds and at different loca-

tions within the watershed, and therefore may not be representative of site-specific conditions.

(c) Meteorological conditions give leaf area index, maximum intercepted snow load, and albedo differing importance between years, therefore annual parameterization of these values may improve model output.

3. Although the conclusions derived from results may be valid for similar snowmelt dominated and forested watersheds in the southern interior of British Columbia, transfer of results to other regions with dissimilar meteorological conditions, forest cover, and topographical characteristics augments uncertainty. Additional studies are required in different regions to evaluate the impact of forest disturbances on snow processes in a range of conditions.

4. While this study focused on post-disturbance snow processes and total basin-scale snow water equivalent, a link needs to be established with surface runoff and groundwater to increase the understanding of post-disturbance hydrology.

This thesis presented the application of a hydrological model to simulate forest disturbance effects on the watershed-scale accumulation and ablation of snow. Results from this study may help water resource management determine future risk assessments. The total basin-scale accumulation of snow water equivalent increased with disturbance severity and extent of disturbance, but differences between disturbance types were reduced in the year with greater snowfall. Therefore, when developing future risk assessments, it is important for water resource management to consider forest disturbance severity and extent, and to incorporate these considerations within a range of snowfall regimes to gain a greater understanding of potential basin-scale response.

References

Abbot, M., J. Bathurst, J. Cunge, P. O'Connel, and J. Rasmussen (1986), An introduction to the European Hydrological Systems-Systeme Hydrologique Europeen, 'SHE'. 1. History and philosophy of a physically based distributed modelling system, *Journal of Hydrology*, *84*, 45–59.

Adams, H., M. Guardiola-Claramonte, G. Barron-Gafford, J. Camilo Villegas, D. Breshears, C. Zou, P. Troch, and T. Huxman (2009), Temperature sensitivity of drought-induced tree mortality portends increased regional die-off under global-change-type drought, *PNAS*, *106*(17), 7063–7066.

Alila, Y., and J. Beckers (2001), Using numerical modelling to address hydrologic forest management issues in British Columbia, *Hydrological Processes*, *15*, 3371–3387.

Alila, Y., and Y. Luo (2007), Delineating the limits of peak flow and water yield responses to clearcut salvage logging in large watersheds, *Tech. rep.*, FORREX Forum for Research and Extension in Natural Resources, Kamloops, BC.

Alila, Y., D. Bewley, P. Kuras, P. Marren, M. Hassan, C. Luo, and T. Blair (2009), Effects of pine beetle infestations and treatments on hydrology and geomorphology: Integrating stand-level data and knowledge into mesoscale watershed functions, *Tech. rep.*, Natural Resources Canada, Canadian Forest Service, Pacific Forestry Center, Victoria, BC. Mountain Pine Beetle Working Paper 2006-2009. 69p.

Amman, G., and B. Baker (1972), Mountain pine beetle influence on lodgepole pine stand structure, *Journal of Forestry*, *70*(4), 904–909.

Anderson, A. (1968), Development and testing of snowpack energy balance equations, *Water Resources Research*, *4*(1), 19–37.

Andreasson, J., S. Bergstrom, B. Carlsson, L. Graham, and G. Lindstrom (2004), Hydrological change - climate change impact simulations for Sweden, *A Journal of the Human Environment*, *33*(4), 228–234.

Aukema, B., A. Carroll, Y. Zheng, J. Zhu, K. Raffa, R. Moore, K. Stahl, and S. Taylor (2008), Movement of outbreak populations of mountain pine beetle: influences of spatiotemporal patterns and climate, *Ecography*, *31*, 348–358.

Bailey, W., T. Oke, and W. Rouse (1997), *The Surface Climates of Canada*, p. 484, McGill-Queen's University Press, Montreal & Kingston.

Ballard, R., M. Walsh, and W. Cole (1984), The penetration an growth of blue-stain fungi in the sapwood of lodgepole pine attacked by mountain pine beetle, *Canadian Journal of Botany*, *62*, 1724–1729.

Barnett, T., J. Adams, and D. Lettenmaier (2005), Potential impacts of a warming climate on water availability in snow-dominated regions, *Nature*, *438*(17), 303–309.

Beckers, J., R. Pike, A. Werner, T. Redding, B. Smerdon, and A. Anderson (2009), Hydrologic models for forest management applications: Part 2: Incorporating the effects of climate change, *Streamline - Watershed Management Bulletin*, *13*(1), 45–54.

Bemrose, R., P. Meszaros, B. Quenneville, M. Henry, L. Kemp, and F. Soulard (2010), Using a trend-cycle approach to estimate changes in southern Canada's water yield from 1971 to 2004, *Tech. rep.*, Environment Canada, Ottawa, ON.

Beniston, M. (2003), Climatic change in mountain regions: a review of possible impacts, *Climatic Change*, *59*, 5–31.

Bentz, B., J. Logan, and G. Amman (1991), Temperature-dependent development of the Mountain Pine Beetle (Coleoptera: Scolytidae) and simulation of its phenology, *Canadian Entomologist*, *123*, 1083–1094.

Bergstrom, S. (1995), *The HBV model*, pp. 443–476, Water Resources Publications, Highlands Ranch, CO.

Berris, S., and R. Harr (1987), Comparative snow accumulation and melt during rainfall in forested and clear-cut plots in the Western Cascades of Oregon, *Water Resources Research*, *23*(1), 135–142.

Bethlalmy, N. (1974), Water supply as affected by micro- and macro-watershed management decisions on forest lands, *Northwest Science*, *48*(1), 1–8.

Beven, K. (1989), Changing ideas in hydrology - the case for physically-based models, *Journal of Hydrology*, *105*, 157–172.

Beven, K., and M. Kirkby (1979), A physically based, variable contributing area model of basin hydrology, *Hydrological Sciences*, *24*(1-3), 43–69.

Bewley, D., Y. Alila, and A. Varhola (2010), Variability of snow water equivalent and snow energetics across a large catchment subject to mountain pine beetle infestation and rapid salvage logging, *Journal of Hydrology*, *388*, 464–479.

Biederman, J., A. Adrian, E. Gutmann, D. Reed, D. Gochis, and P. Brooks (2011), The impacts of pine tree die-off on snow accumulation and distribution at plot to catchment scales, in *American Geophysical Union, Fall Meeting 2011, Abstract B33B-0461*.

Birkinshaw, S., J. Bathurst, A. Iroume, and H. Palacios (2010), The effect of forest cover on peak flow and sediment discharge - an integrated field and modelling study in central-southern Chile, *Hydrological Processes*.

Black, P. (1996), *Watershed hydrology: Second edition*, Ann Arbor Press, Inc, Chelsea, MI.

Black, T., J. Chen, X. Lee, and R. Sagar (1991), Characteristics of shortwave and longwave irradiances under a Douglas-fir forest stand, *Canadian Journal of Forest Research*, *21*, 1020–1028.

Blöschl, G., D. Gutknecht, and R. Kirnbauer (1991), Distributed snowmelt simulations in an alpine catchment 2. Parameter study and model predictions, *Water Resources Research*, *27*(12), 3181–3188.

Boon, S. (2007), Snow accumulation and ablation in a beetle-killed pine stand in northern interior British Columbia, *B.C. Journal of Ecosystems and Management*, *8*(3), 1–13.

Boon, S. (2009), Snow ablation energy balance in a dead forest stand, *Hydrological Processes*, *23*(18), 2600–2610.

Boon, S. (2011), Snow accumulation following forest disturbance, *Ecohydrology*, *5*(3).

Boon, S., R. Winkler, and B. Zimonick (in review), Effects of post-mountain pine beetle forest litter on snow surface reflectance, *Geophysical Research Letters*.

Brewer, R., S. Cohen, E. Embley, M. Julian, T. Kulkarni, B. Taylor, J. Tansey, R. VanWynsberghe, and P. Whitfield (2001), Water management and climate change in the Okanagan Basin, *Tech. rep.*, Environment Canada, Ottawa, ON.

Brown, S., P. Schroeder, and J. Kern (1999), Spatial distribution of biomass in forests of the eastern USA, *Forest Ecology and Management*, *123*(1), 81–90.

Brutsaert, W. (1982), *Evaporation into the atmosphere: Theory, history and applications*, p. 299, Springer.

Burles, K. (2010), Snowmelt energy balance in a burned forest stand, Crowsnest Pass, Alberta, Master's thesis.

Burles, K., and S. Boon (2011), Snowmelt energy balance in a burned forest plot, Crowsnest Pass, Alberta, Canada, *Hydrological Processes*, *25*(19), 3012–3029.

Buttle, J., I. Creed, and J. Pomeroy (2000), Advances in Canadian forest hydrology, 1995-1998, *Hydrological Processes*, *14*, 1551–1578.

Cameron, D., K. Beven, J. Tawn, S. Blazkova, and P. Naden (1999), Flood frequency estimation by continuous simulation for a gauged upland catchment (with uncertainty), *Journal of Hydrology*, *219*(3-4), 169–187.

Carpenter, T., and K. Georgakakos (2006), Intercomparison of lumped versus distributed hydrologic model ensemble simulations on operational forecast scales, *Journal of Hydrology*, *329*(1-2), 174–185.

Carroll, A., J. Regniere, J. Logan, S. Taylor, B. Bentz, and J. Powell (2006), Impacts of climate change on range expansion by the Mountain Pine Beetle, *Tech. rep.*, Natural Resources Canada, Canadian Forest Service, Pacific Forestry Centre, Information Report BC-X-39.

Carver, M., M. Weiler, C. Scheffler, and K. Rosin (2009), Development and application of a peak-flow hazard modelf or the Fraser basin (British Columbia), *Tech. rep.*, Natural Resources Canada, Canadian Forest Service, Pacific Forestry Centre, Victoria, BC.

Cayan, D. (2001), Changes in the onset of spring in the western United States, *Bulletin of the American Meteorological Society*, *82*, 399–415.

Chang, M. (2003), *Forest hydrology: an introduction to water and forests*, CRC Press, Boca Raton, Fla.

Chen, J., and T. Black (1992), Defining leaf area index for non flat leaves, *Plant Cell Environment*, *15*, 421–429.

Clark, M., D. Rupp, R. Woods, H. Tromp-van Meerveld, N. Peters, and J. Freer (2009), Consistency between hydrological models and field observations: linking processes at the hillslope scale to hydrological responses at the watershed scale, *Hydrological Processes*, *23*, 311–319.

Clarke, R. (1973), A review of some mathematical models used in hydrology, with observations on their calibration and use, *Journal of Hydrology*, *19*, 1–20.

Clow, D., C. Rhoades, J. Briggs, M. Claldwell, and W. Lewis Jr. (2011), Responses of soil and water chemistry to mountain pine beetle induced tree mortality in Grand County, Colorado, USA, *Applied Geochemistry*, *26*(Supplement), S174–S178.

Cohen, S., and T. Kulkarni (2001), Water management & climate change in the Okanagan Basin, *Tech. rep.*, Natural Resources Canada, Canadian Forest Service, Pacific Forestry Centre, Victoria, BC.

Colbeck, S. (1988), Snowmelt increase through albedo reduction, *Tech. rep.*, U.S. Army Cold Regions Research and Engineering Laboratory, Office of the Chief of Engineers, Washington, DC.

Committee on Challenges and Opportunities in the Hydrologic Sciences; National Research Council (2012), *Challenges and opportunities in the hydrologic sciences*, p. 161, The National Academies Press, Washington, DC.

Conway, H., A. Gades, and C. Raymond (1996), Albedo of dirty snow during conditions of melt, *Water Resources Research*, *32*(6), 1713–1718.

Coughlan, J., and S. Running (1997), Regional ecosystem simulation: A general model for simulating snow accumulation and melt in mountainous terrain, *Landscape Ecology*, *12*, 119–136.

Coulson, R., B. McFadden, P. Pulley, C. Lovelady, J. Fitzgerald, and S. Jack (1999), Heterogeneity of forest landscapes and the distribution and abundance of the southern pine beetle, *Forest Ecology and Management*, *114*(2-3), 471–485.

Dale, V., et al. (2001), Climate change and forest disturbance, *Bioscience*, *51*, 723–734.

de la Giroday, H. (2010), Spatial associations between infestations of Mountain Pine Beetle and landscape features in the Peace River region of British Columbia, Master's thesis.

DeBeer, C., and J. Pomeroy (2010), Simulation of the snowmelt runoff contributing area in a small alpine basin, *Hydrology and Earth System Sciences*, *14*, 1205–1219.

DeFries, R., and K. Eshleman (2004), Land-use change and hydrologic processes: a major focus for the future, *Hydrological Processes*, *18*(11), 2183–2186.

Demographics Analysis Section: BC Stats (2009), Sub-provincial population projections, *Tech. rep.*, Government of BC, Victoria, BC.

Dingman, S. L. (2002), *Physical Hydrology*, p. 600, 2nd ed., Prentice Hall, Upper Saddle River New Jersey.

Dunne, T. (2001), *Introduction to Section 2 - Problems in measuring and modeling the influence of forest management on hydrologic and geomorphic processes*, American Geophysical Union, Washington, DC.

Elder, K., W. Rosenthal, and R. E. Davis (1998), Estimating the spatial distribution of snow water equivalence in a montane watershed, *Hydrological Processes*, *12*, 1793–1808.

Ellis, C. (2011), Radiation and snowmelt dynamics in mountain forests, Ph.D. Thesis, University of Saskatchewan, Saskatoon, SK.

Ellis, C., J. Pomeroy, T. Brown, and J. MacDonald (2010), Simulation of snow accumulation and melt in needleleaf forest environments, *Hydrology and Earth System Sciences Discussions*, *7*, 1033–1072.

Ellison, A., et al. (2005), Loss of foundation species: consequences for the structure and dynamics of forested ecosystems, *Frontiers in Ecology and the Environment*, *3*, 479–486.

Essery, R., M. Best, and P. Cox (2001), MOSES 2.2 Technical Documentation, *Tech. rep.*, Hadley Centre, Met Office, UK. Hadley Center Technical Note 30.

Essery, R., J. Pomeroy, C. Ellis, and T. Link (2008), Modelling longwave radiation to snow beneath forest canopies using hemispherical photography or linear regression, *Hydrological Processes*, *22*(15), 2788–2800.

Faria, D., J. Pomeroy, and R. Essery (2000), Effect of covariance between ablation and snow water equivalent of snow-covered area in a forest, *Hydrological Processes*, *14*, 2683–2695.

Flannigan, M., B. Amiro, K. Logan, B. Stocks, and B. Wotton (2005), Forest fires and climate change in the 21st century, *Mitigation and Adaption Strategies for Global Change*, *11*, 847–859.

Gelfan, A., J. Pomeroy, and L. Kuchment (2004), Modelling forest cover influences on snow accumulation, sublimation, and melt, *Journal of Hydrometeorology*, *5*, 785–803.

Golding, D., and R. Swanson (1986), Snow distribution patterns in clearings and adjacent forest, *Water Resources Research*, *22*(13), 1931–1940.

Goodison, B., H. L. Ferguson, and G. A. McKay (1981), *Measurement and Data Analysis*, pp. 191–274, The Blackburn Press, Caldwell, New Jersey.

Government of British Columbia (2010), TRIM II, *Tech. rep.*, Government of BC, Victoria, BC.

Gower, S., and J. Norman (1991), Rapid estimation of leaf area index in conifer and broad-leaf plantations, *Ecology*, *72*(5), 1896–1900.

Granier, B., and A. Ohmura (1970), The evaluation of surface variations in solar radiation income, *Solar Energy*, *13*, 21–34.

Gray, D., and P. Landine (1988), An energy budget snowmelt model for the Canadian Prairies, *Canadian Journal of Environmental Science*, *25*, 1292–1303.

Grayson, R., I. Moore, and T. McMahon (1992), Physically based hydrologic modelling 2: Is the concept realistic, *Water Resources Research*, *28*, 2659–2666.

Groisman, P., and T. D. Davies (2001), *Snow Cover and the Climate System*, pp. 1–44.

Gubler, H., and J. Rychetnik (1991), *Effects of forests near the timberline avalanche formation*, pp. 19–38, IAHS Publication No. 205, IAHS Press, Wallingford, UK.

Gunter, A., S. Uhlenbrook, J. Seibert, and C. Leibundgut (1999), Multi-criterial validation of topmodel in a mountainous catchment, *Hydrological Processes*, *13*, 1603–1620.

Halpern, C., and T. Spies (1995), Plant species diversity in natural and managed forests of the Pacific Northwest, *Ecological Applications*, *5*(4), 913–934.

Haughian, S., P. Burton, S. Taylor, and C. Curry (2012), Expected effects of climate change on forest disturbance regimes in British Columbia, *BC Journal of Ecosystems and Management*, *13*(1), 1–24.

Hedstrom, N., and J. Pomeroy (1998), Measurements and modelling of snow interception in the boreal forest, *Hydrological Processes*, *12*, 1611–1625.

Hibbert, A. (1967), *Forest treatment effects on water yield*, pp. 527–543, Pergamon, New York, NY.

Hicke, J., and J. Jenkins (2008), Susceptibility of lodgepole pine to mountain pine beetle attack: Mapping stand structure across the western United States, *Forest Ecology and Management*, *255*, 1536–1547.

Hock, R. (2003), Temperature index melt modelling in mountain areas, *Journal of Hydrology*, *282*, 104–115.

Hood, E., M. Williams, and D. Cline (1999), Sublimation of a seasonal snowpack at a continental, mid-latitude alpine site, *Hydrological Processes*, *13*, 1781–1797.

IPCC (2007), *Climate Change 2007: The physical basis: Summary for policy makers*, pp. 1–18, Cambridge University Press, UK.

Jasper, K., P. Calanca, D. Gyalistras, and J. Fuhrer (2004), Differential impacts of climate change on the hydrology of two alpine river basins, *Climate Research*, *26*, 113–129.

Jeffrey, W. (1970), *Snow hydrology in the forest environment*, pp. 1–20, Canadian National Committee for the International Hydrological Decade, Queen's Printer for Canada, Ottawa.

Johnson, E., and C. Larsen (1991), Climatically induced change in fire frequency in the southern Canadian Rockies, *Ecology*, *72*, 194–201.

Jones, J., G. Achterman, L. Augustine, I. Creed, P. Folliot, L. MacDonald, and B. Wemple (2009), Hydrologic effects of a changing forested landscape - challenges for the hydrological sciences, *Hydrological Processes*, *23*, 2699–2704.

Jones, J. A. (2000), Hydrologic processes and peak discharge response to forest removal, regrowth, and roads in 10 small experimental basins, western Cascades, Oregon, *Water Resources Research*, *36*(9), 2621–2642.

Jost, G., M. Weiler, D. R. Gluns, and Y. Alila (2007), The influence of forest and topography on snow accumulation and melt at the watershed scale, *Journal of Hydrology*, *347*, 101–115.

Kampf, S., and S. Burges (2007), A framework for classifying and comparing distributed hillslope and catchment hydrologic models, *Water Resources Research*, *43*(W05423), 24 pp.

Kavvas, M., et al. (2004), Watershed Environmental Hydrology (WEHY) model based on upscaled conservation equations: hydrologic module, *Journal of Hydrologic Engineering*, *9*(6), 450–464.

Keeley, J. (2009), Fire intensity, fire severity and burn severity: a brief review and suggested usage, *International Journal of Wildland Fire*, *18*, 116–126.

Koivusalo, H., and T. Kokkonen (2002), Snow processes in a forest clearing and in a coniferous forest, *Journal of Hydrology*, *262*, 145–164.

Lamb, R., K. Beven, and S. Mayrabo (1998), Use of spatially distributed water table observations to constrain uncertainty in a rainfall-runoff model, *Advances in Water Resources*, *22*(4), 305–317.

Lawler, R., and T. Link (2011), Quantification of incoming all-wave radiation in discontinuous forest canopies with application to snowmelt prediction, *Hydrological Processes*, *25*, 3322–3331.

Legates, D., and G. McCabe Jr. (1999), Evaluating the "goodness-of-fit" measures in hydrologic and hydroclimatic mode validation, *Water Resources Research*, *35*(1), 233–241.

Leung, L. (2005), Effects of climate variability and change on mountain water resources in the Western U.S., *Advances in Global Change Research*, *23*(3), 355–364.

Liden, R., and J. Harlin (2000), Analysis of conceptual rainfall-runoff modelling performance in different climates, *Journal of Hydrology*, *237*(3-4), 231–247.

Lindstrom, G., M. Gardelin, B. Johansson, M. Persson, and S. Bergstrom (1997), Development and test of the distributed HBV-96 hydrological model, *Journal of Hydrology*, *201*, 272–288.

Link, T., and D. Marks (1999), Point simulation of seasonal snowcover dynamics beneath boreal forest canopies, *Journal of Geophysical Research*, *104*(D22), 27,841–27,857.

Littell, J., D. McKenzie, D. Peterson, and A. Westerling (2009), Climate and wildfire area burned in western U.S. ecoprovinces, 1916-2003, *Ecological Applications*, *19*(4), 1003–1021.

Lodge, D., et al. (2006), Biological invasions: Recommendations for US policy and management, *Ecological Applications*, *16*, 2035–2054.

López-Moreno, J., and J. Latron (2008), Influence of canopy density on snow distribution in a temperate mountain range, *Hydrological Processes*, *22*, 117–126.

López-Moreno, J., S. Goyette, M. Beniston, and B. Alvera (2008), Sensitivity of the snow energy balance to climatic changes: prediction of the snowpack in the Pyrenees in the 21st century, *Climate Research*, *36*, 203–217.

MacDonald, M., J. Pomeroy, and A. Pietroniro (2010), On the importance of sublimation to an alpine snow mass balance in the Canadian Rocky Mountains, *Hydrology and Earth System Sciences*, *14*, 1401–1415.

Male, D., and R. Granger (1981), Snow surface energy exchange, *Water Resources Research*, *17*(3), 609–627.

Marks, D., and J. Dozier (1992), Climate and energy exchange at the snow surface in the alpine region of the sierra nevada: 2. snow cover energy balance, *Water Resources Research*, *28*(11), 3043–3054.

Marks, D., and A. Winstral (2001), Comparison of snow deposition, the snow cover energy balance, and snowmelt at two sites in a semiarid mountain basin, *Journal of Hydrometeorology*, *2*(3), 213–227.

Marks, D., M. Reba, J. Pomeroy, T. Link, A. Winstral, G. Flerchinger, and K. Elder (2008), Comparing simulated and measured sensible and latent heat fluxes over snow under a pine canopy to improve an energy balance snowmelt model, *Journal of Hydrometeorology*, *9*(6), 1506–1522.

Mattson, W., and R. Haack (1987), The role of drought in outbreaks of plant-eating insects, *Bioscience*, *37*(2), 110–118.

McGaughey, J. (1984), A radiation and energy balance study of mature forest and clear-cut sites, *Boundary-Layer Meteorology*, *32*, 1–24.

McKay, G. A., and W. Adams (1981), *Snow and Living Things*, pp. 3–31, The Blackburn Press, Caldwell New Jersey.

Miller, D. (1964), Interception processes during snowstorms, *Tech. rep.*, Pacific Southwest Forest & Range Experiment Station, Portland, OR. Research Paper PSW-RP-18.

Mitchell, R., and H. Preisler (1998), Fall rate of lodgepole pine killed by mountain pine beetle in central Oregon, *Western Journal of Forestry*, *81*, 598–601.

Molchanov, A. (1963), The hydrologic role of forests, *Israel program for scientific translations*, *870*, pp. 407.

Mote, P. (2006), Climate-driven variability and trends in mountain snowpack in western North America, *Journal of Climate*, *19*(23), 6209–6220.

Murray, C., and J. Buttle (2003), Impacts of clearcut harvesting on snow accumulation and melt in a northern hardwood forest, *Journal of Hydrology*, *271*, 197–212.

Nagelkerke, N. (1991), A note on a general definition of the coefficient of determination, *Biometrika*, *78*(3), 691–692.

National Climate Data Information Archive (2011), Canadian Climate Normals 1971-2000, *Tech. rep.*, Government of Canada, Ottawa, ON.

Neilson-Welch, L., and D. Allen (2007), Groundwater and hydrogeological conditions in the Okanagan Basin, British Columbia: A state-of-the-basin report, *Tech. rep.*, Simon Fraser University, Burnaby, BC.

Nelson, T., B. Boots, and M. Wulder (2003), *Spatial-Temporal Analysis of Mountain Pine Beetle Infestations to Characterize Pattern, Risk, and Spread at the Landscape Level*, pp. 164–173, Natural Resources Canada, Canadian Forest Service, Pacific Forestry Centre, Victoria B.C.

Oke, T. (1987), *Boundary Layer Climates*, p. 435, 2nd ed., Routledge, London, England.

Overpeck, J., D. Rind, and R. Goldberg (1990), Climate-induced changes in forest disturbance and vegetation, *Nature*, *343*(6253), 51–53.

Parry, M., O. Canziana, and J. Palutikof (2008), Key IPCC conclusions on climate change impacts and adaptations, *WMO Bulletin*, *57*(1), 78–85.

Penna, D., H. Tromp-van Meerveld, A. Gobbi, M. Borga, and G. Dalla Fontana (2011), The influence of soil moisture on threshold runoff generation processes in an alpine headwater catchment, *Hydrology and Earth System Sciences*, *15*, 689–702.

Poff, N., and J. Ward (1989), Implications of streamflow variability and predictability for biotic community structure: A regional analysis of streamflow patterns, *Canadian Journal of Fisheries and Aquatic Sciences*, *46*, 1805–1818.

Pomeroy, J., and K. Dion (1996), Winter radiation extinction and reflection in a boreal pine canopy: measurements and modelling, *Hydrological Processes*, *10*, 1591–1608.

Pomeroy, J., and R. Essery (1999), Turbulent fluxes during blowing snow: field tests of model sublimation predictions, *Hydrological Processes*, *13*, 2963–2975.

Pomeroy, J., and R. Granger (1997), Sustainability of the western Canadian boreal forest under changing hydrological conditions - I - snow accumulation and ablation, *International Association of Hydrological Sciences*, *240*, 237–242.

Pomeroy, J., and D. Gray (1995), Snow accumulation, relocation and management, *Tech. rep.*, Environment Canada, National Research Institute Science Report No. 7.

Pomeroy, J., and R. Schmidt (1993), The use of fractal geometry in modelling intercepted snow accumulation and sublimation, *Proc. Eastern Snow Conference*, *50*, 1–10.

Pomeroy, J., J. Parviainen, N. Hedstrom, and D. Gray (1998a), Coupled modelling of forest snow interception and sublimation, *Hydrological Processes*, *12*, 2317–2337.

Pomeroy, J., D. Gray, K. Shook, B. Toth, R. Essery, A. Pietroniro, and N. Hedstrom (1998b), An evaluation of snow accumulation and ablation processes for land surface modelling, *Hydrological Processes*, *12*, 2339–2367.

Pomeroy, J., J. Parviainen, N. Hedstrom, and D. Gray (1998c), Coupled modelling of forest snow interception and sublimation, *Hydrological Processes*, *12*, 2317–2337.

Pomeroy, J., D. Gray, T. Brown, N. Hedstrom, W. Quinton, R. Granger, and S. Carey (2007), The cold regions hydrological model: a platform for basing process representation and model structure on physical evidence, *Hydrological Processes*, *21*, 2650–2667.

Pomeroy, J., D. Marks, D. Link, C. Ellis, D. Hardy, A. Rowlands, and R. Granger (2009), The impact of coniferous forest temperature on incoming longwave radiation to melting snow, *Hydrological Processes*, *23*(17), 2513–2525.

Pomeroy, J., X. Fang, C. Ellis, and M. Guan (2011), Sensitivity of snowmelt hydrology on mountain slopes to forest cover disturbance, *Tech. rep.*, University of Saskatchewan, Centre for Hydrology, Saskatoon, SK.

Pomeroy, J., X. Fang, and C. Ellis (2012), Sensitivity of snowmelt hydrology in Marmot Creek, Alberta, to forest cover disturbance, *Hydrological Processes*.

Postel, S., and S. Carpenter (1997), *Freshwater ecosystem services*, Island Press, Washington, DC.

Pugh, E., and E. Small (2011), The impact of pine beetle infestation on snow accumulation and melt in the headwaters of the Colorado River, *Ecohydrology*.

Quick, M., and A. Pipes (1977), UBC Watershed Model, *Hydrological Sciences Bulletin*, *221*, 153–161.

Refsgaard, J., and J. Knudsen (1996), Operational validation and intercomparison of different types of hydrological models, *Water Resources Research*, *32*(7), 2189–202.

Reid, L. (1993), Research and cumulative watershed effects, *Tech. rep.*, US Department of Agriculture, Forest Service, Pacific Southwest Research Station, Albany, CA. Gen. Tech. Rep. PSW-GTR-141.

Reifsnyder, W., and H. Lull (1965), Radiant energy in relation to forests, *Tech. Rep. 1344*, U.S. Department of Agriculture, Washington, DC. Technical Bulletin No. 1344.

Roed, M., and J. Greenough (2004), *Okanagan Geology, British Columbia*, Kelowna Geology Committee, Kelowna, BC.

Rouse, W. (2009), Microclimatic changes accompanying burning in subarctic lichen woodland, *Arctic and Alpine Research*, *8*(4), 18.

Rutter, N., et al. (2009), Evaluation of forest snow processes models (SnowMIP2), *Journal of Geophysical Research*, *114*, 18.

Safranyik, L. (1978), *Effects of climate and weather on Mountain Pine Beetle populations*, pp. 77–84, University of Idaho, Moscow, ID.

Safranyik, L., and A. Carroll (2006), *The biology and epidemiology of the mountain pine beetle in lodgepole pine forests*, pp. 3–66, Natural Resources Canada, Canadian Forest Service, Pacific Forestry Centre, Victoria, BC.

Satterlund, D. (1970), The disposition of snow caught by conifer crowns, *Water Resources Research*, *6*, 649–652.

Satterlund, D., and H. Haupt (1967), Snow catch by conifer crowns, *Water Resources Research*, *3*, 1035–1039.

Schmidt, R. (1972), Sublimation of wind-transported snow - a model, *Tech. rep.*, US Department of Agriculture, Forest Service, Rocky Mountain Forest and Range Experimental Station, Fort Collins, CO.

Schmidt, R. (1991), Sublimation of intercepted snow by an artificial conifer, *Agriculture and Forest Meteorology*, *54*, 1–27.

Schmidt, R., and J. Pomeroy (1990), Bending of a conifer branch at subfreezing temperatures: implications for snow interception, *Canadian Journal of Forest Research*, *20*, 1250–1253.

Schmidt, R., and C. Troendle (1989), Snowfall into a forest and clearing, *Journal of Hydrology*, *110*, 335–348.

Schnorbus, M. (2011), A synthesis of the hydrological consequences of large-scale mountain pine beetle disturbance, *Tech. rep.*, Natural Resources Canada, Canadian Forest Service, Pacific Forestry Centre, Victoria, BC. Mountain Pine Beetle Working Paper 2010-01.

Schnorbus, M., and A. W. Bennett, K. Werner (2010), Quantifying the water resource impacts of mountain pine beetle and associated salvage harvest operations across a range of watershed scales: Hydrologic modelling of the Fraser River Basin, *Tech. rep.*

Seibert, J., J. McDonnell, and R. Woodsmith (2010), Effects of wildfire on catchment runoff response: a modelling approach to detect changes in snow-dominated forested catchments, *Hydrology Research*, *41*(5), 378–390.

Seidl, R., et al. (2010), Modelling natural disturbances in forest ecosystems: a review, *Ecological Modelling*, *222*(4), 903–924.

Shakesby, R., and S. Doerr (2006), Wildfire as a hydrological and geomorphological agent, *Earth-Science Reviews*, *74*, 269–307.

Shiklomanov, I. (2000), Appraisal and assessment of world water resources, *Water International*, *25*(1), 11–32.

Shore, T., and L. Safranyik (1992), Susceptibility and risk rating systems for the mountain pine beetle in lodgepole pine stands, *Forestry Canada Information Report*, pp. BCX–336.

Sicart, J., J. Pomeroy, R. Essery, J. Hardy, T. Link, and D. Marks (2004), A sensitivity study of daytime net radiation during snowmelt to forest canopy and atmospheric correction, *Journal of Hydrometeorology*, *5*, 744–784.

Sidle, R. (2006), Field observations and process understanding in hydrology: essential components in scaling, *Hydrological Processes*, *20*, 1439–1445.

Silins, U., K. Bladon, M. Stone, M. Emelko, S. Boon, C. Williams, M. Wagner, and J. Howery (2009), Southern Rockies Watershed Project: Impact of natural disturbance by wildfire on hydrology, water quality, and aquatic ecology of Rocky Mountain Watersheds Phase 1 (2004-2008), *Tech. rep.*

Singh, V. (1989), *Hydrologic systems: rainfall-runoff modeling*, p. 960, Prentice Hall.

Singh, V., and D. Woolhiser (2002), Mathematical modeling of watershed hydrology, *Journal of Hydrologic Engineering*, *7*(4).

Skidmore, P., K. Hansen, and W. Quimby (1994), Snow accumulation and ablation under fire-altered lodgepole pine forest canopies, in *62nd Western Snow Conference*, pp. 43–52.

Smerdon, B., and T. Redding (2007), Groundwater: more than water below the ground, *Streamline*, *10*(2), 1–6.

Soja, A., et al. (2007), Climate-induced boreal forest change: Predictions versus current observations, *Global and Planetary Change*, *56*, 274–296.

Spittlehouse, D. (2006), ClimateBC: Your access to Interpolated Climate Data for BC, *Streamline - Watershed Management Bulletin*, *9*(2), 16–21.

Spittlehouse, D., and R. Winkler (1996), Forest canopy effects on sample size requirements in snow accumulation and melt comparisons, in *Proceedings of the 64th Annual Meeting of the Western Snow Conference*, pp. 39–46.

Spittlehouse, D., and R. Winkler (2004), Snowmelt in a forest and clearcut, in *72nd Western Snow Conference*, pp. 33–43, B.C. Ministry of Forests and Range.

Stähli, M., and D. Gustafsson (2006), Long-term investigations of the snow cover in a subalpine semi-forested catchment, *Hydrological Processes*, *20*, 411–428.

Stanton, C. (1966), Preliminary investigations of snow accumulation and melting in forested and cut-over areas of the Crowsnest Forest, in *Proceedings of the 34th Annual Meeting of the Western Snow Conference*, pp. 7–12.

Stednick, J., and C. Troendle (2004), *Water yield and timber harvesting practices in the subalpine forests of the central Rocky Mountains*, pp. 165–182, Society of American Foresters. Elsevier Pub, Washington DC.

Steppuhn, H. (1981), *Snow and Agriculture*, pp. 60–126, The Blackburn Press, Caldwell, New Jersey.

Stern, N. (2007), *The Economics of Climate Change: The Stern Review*, p. 692, Cambridge University Press, Cambridge, U.K.

Stewart, I., D. Cayan, and M. Dettinger (2005), Changes towards earlier streamflow timing across Western North America, *Journal of Climate*, *18*, 1136–1155.

Stonesifer, C. (2007), Modeling the cumulative effects of forest fire on watershed hydrology: A post-fire application of the distributed hydrology-soil-vegetation model (DHSVM), M.sc. thesis, the university of montana, missoula, mt.

Storck, P., L. Bowling, P. Wetherbee, and D. Lettenmaier (1998), Application of a GIS-based distributed hydrology model for prediction of forest harvest effects on peak stream flow in the Pacific Northwest, *Hydrological Processes*, *12*(6), 889–904.

Storck, P., T. Kern, and S. Bolton (1999), Measurement of differences in snow accumulation, melt, and micrometeorology due to forest harvesting, *Northwest Science*, *73*(Special Issue), 87–101.

Storck, P., D. Lettenmaier, and S. Bolton (2002), Measurement of snow interception and canopy effects on snow accumulation and melt in a mountainous maritime climate, oregon, united states, *Water Resources Research*, *38*(11), 1223–1238.

Strasser, U., M. Bernhardt, M. Weber, G. Liston, and W. Mauser (2007), Is snow sublimation important in the alpine water balance?, *The Cryosphere Discussions*, *1*(2), 303–350.

Summit Environmental Consultants Ltd (2005), Okanagan Basin water supply and demand study: Phase 1, *Tech. rep.*, Summit Environmental Consultants Ltd, Vernon, BC. Report prepared for Land and Water BC Inc.

Swanson, R. (2004), The complete wrenss hydrologic model, in *Proceedings of the 72nd Western Snow Conference*, pp. 99–104.

Tague, C., and L. Band (2001), Simulating the impact of road construction and forest harvesting on hydrological response, *Earth Surface Processes and Landforms*, *26*, 135–151.

Tague, C., and L. Band (2004), RHESSyS: Regional Hydro-Ecological Simulation System: An object-oriented approach to spatially distibuted modeling of carbon, water and nutrient cycling, *Earth Interactions*, *8*(19), 1–42.

Taylor, B., and M. Barton (2003), *Climate analysis and scenarios*, pp. 16–26, Environment Canada, Agriculture & Agri-Food Canada and University of British Columbia, Ottawa, ON.

Teti, P. (2008), Effects of overstory mortality on snow accumulation and ablation, *Tech. rep.*, Natural Resources Canada, Canadian Forest Service, Pacific Forestry Centre, Victoria, BC. Mountain Pine Beetle Working Paper 2008-34.

Toews, D., and D. R. Gluns (1986), Snow accumulation and ablation on adjacent forested and clearcut sites in southeastern British Columbia, in *Proceedings of the 54th Annual Meeting of the Western Snow Conference*, pp. 101–111.

Toews, M., and D. Allen (2007), Aquifer characterization, recharge modelling and groundwater flow modelling for well capture zone analysis in the Oliver Area of the Southern Okanagan, BC., *Tech. rep.*, Department of Earth Sciences, Simon Fraser University, Burnaby BC.

Troendle, C., and J. King (1985), The effect of timber harvest on the Fool Creek watershed, 30 years later, *Water Resources Research*, *21*(12), 1915–1922.

US Army Corps of Engineers (1956), Snow Hydrology: Summary Report of the Snow Investigations, *Tech. rep.*, US Army Corps of Engineers, North Pacific Division, Portland OR.

Uunila, L., B. Guy, and R. Pike (2006), Hydrologic effects of mountain pine beetle in interior pine forests of British Columbia: Key questions and current knowledge, *Streamline - Watershed Management Bulletin*, *9*(2).

van de Vosse, H. (2008), Mountain Pine Beetle Infestation: Hydrological Impacts, *Tech. rep.*, Ministry of Environment, Victoria, BC.

Varhola, A., N. Coops, M. Weiler, and R. Moore (2010), Forest canopy effects on snow accumulation and ablation: An integrative review of empirical results, *Journal of Hydrology*, *392*(3-4), 219–233.

Veatch, W., P. Brooks, J. Gustafson, and N. Molotch (2009), Quantifying the effects of forest canopy cover on net snow accumulation at a continental, mid-latitude site, *Ecohydrology*, *2*, 115–128.

Vose, J. (2011), Forest ecohydrological research in the 21st century: What are the critical needs?, *Ecohydrology*, *4*(2), 146–158.

Walther, G., P. E., P. Convey, A. Menzel, C. Parmesan, T. Beebee, J. Fromentin, O. Hoegh-Guldberg, and F. Bairlein (2002), Ecological responses to climate change, *Nature*, *416*, 381–395.

Westerling, A., H. Hidalgo, D. Cayan, and T. Swetnam (2006), Warming and earlier spring increase western U.S. forest wildfire activity, *Science*, *313*(5789), 940–943.

Westerling, A., M. Turner, E. Smithwick, W. Romme, and M. Ryan (2011), Continued warming cound transform Greater Yellowstone fire regimes by mid-21st century, *Proceedings of the National Academy of Sciences*, *108*, 13,165–13,170.

Wheeler, K. (1987), Interception and redistribution of snow in a subalpine forest on a storm-by-storm basis, in *Proceedings of the 55th Annual Meeting of the Western Snow Conference*, pp. 70–77.

Whitaker, A., Y. Alila, J. Beckers, and D. Toews (2003), Application of the distributed hydrology soil vegetation model to Redfish Creek, British Columbia: Model evaluation using internal catchment data, *Hydrological Processes*, *17*, 199–224.

Wigmosta, M., and S. Burges (2001), *Land use and watersheds: human influence on hydrology and geomorphology in urban and forest areas*, American Geophysical Union, Washington, D.C.

Wigmosta, M., L. Vail, and D. Lettenmaier (1994), A distributed hydrology-vegetation model for complex terrain, *Water Resources Research*, *30*(6), 1665–1679.

Winkler, R. (2001), The Effects of Forest Structure on Snow Accumulation and Melt in South-Central British Columbia, Ph.D. Thesis, University of British Columbia, Vancouver, BC.

Winkler, R. (2011), Changes in snow accumulation and ablation after a fire in South-central British Columbia, *Streamline - Watershed Management Bulletin*, *14*(2), 1–7.

Winkler, R., and S. Boon (2010), The effects of mountain pine beetle attack on snow accumulation and ablation: A synthesis of ongoing research in British Columbia, *Streamline - Watershed Management Bulletin*, *13*(2), 25–31.

Winkler, R., and R. Moore (2006), Variability in snow accumulation patterns within forest stands on the interior plateau of British Columbia, Canada, *Hydrological Processes*, *20*, 3683–3695.

Winkler, R., D. Spittlehouse, T. Giles, B. Heise, G. Hope, and M. Schnorbus (2004), Upper Penticton Creek: How forest harvesting affects water quantity and quality, *Streamline - Watershed Management Bulletin*, *8*(1), 18–20.

Winkler, R., D. Spittlehouse, and D. Golding (2005), Measured differences in snow accumulation and melt among clearcut, juvenile, and mature forests in southern British Columbia, *Hydrological Processes*, *19*, 51–62.

Winkler, R., D. Spittlehouse, D. Allen, T. Redding, T. Giles, G. Hope, B. Heise, Y. Alila, and H. Voeckler (2008), The Upper Penticton Creek Watershed Experiment: Integrated water resource research on the Okanagan Plateau, in *One Watershed - One Water Conference Proceedings*, Canadian Water Resources Association.

Winkler, R., R. Moore, T. Redding, D. Spittlehouse, B. Smerdon, and D. Carlyle-Moses (2009), Chapter 7: The effects of forest disturbance on hydrologic processes and watershed response, *Tech. rep.*, BC Ministry of Forests and Range Research Branch and FORREX Forum for Research and Extension in Natural Resources Society, Victoria, BC and Kamloops, BC.

Winkler, R., S. Boon, B. Zimonick, and K. Baleshta (2010), Assessing the effects of post-pine beetle forest litter on snow albedo, *Hydrological Processes*, *24*, 803–812.

Winkler, R., S. Boon, B. Zimonick, and D. Spittlehouse (in review), Snow accumulation and ablation response to changes in forest structure and snow surface albedo after attack by mountain pine beetle, *Hydrological Processes*.

Wiscombe, W., and S. Warren (1980), The spectral albedo of snow: Effects of age, depth, cloud cover, sun angle, and impurities, *A model for the spectral albedo of snow, 1, Pure snow*, *37*, 2712–2733.

Zar, J. (1999), *Biostatistical analysis*, 4th edition ed., Prentice-Hall, Upper Saddle River, New Jersey.

Ziemer, R., J. Lewis, R. Rice, and T. Lisle (1991), Modeling the cumulative watershed effects of forest management strategies, *Journal of Environmental Quality*, *20*, 36–42.